

Sarah Abelen

**Signals of Weather Extremes
in Soil Moisture and Terrestrial Water Storage
from Multi-Sensor Earth Observations
and Hydrological Modelingmissions**

München 2016

**Verlag der Bayerischen Akademie der Wissenschaften
in Kommission beim Verlag C. H. Beck**



Signals of Weather Extremes
in Soil Moisture and Terrestrial Water Storage
from Multi-Sensor Earth Observations
and Hydrological Modelings

Vollständiger Abdruck
der von der Ingenieur fakultät Bau Geo Umwelt
der Technischen Universität München
zur Erlangung des akademischen Grades eines
Doktor-Ingenieurs (Dr.-Ing.)
genehmigten Dissertation

von

Sarah Abelen

München 2016

Verlag der Bayerischen Akademie der Wissenschaften
in Kommission beim Verlag C. H. Beck

Adresse der Deutschen Geodätischen Kommission:



Deutsche Geodätische Kommission

Alfons-Goppel-Straße 11 • D – 80 539 München

Telefon +49 – 89 – 23 031 1113 • Telefax +49 – 89 – 23 031 -1283 / - 1100

e-mail post@dgk.badw.de • <http://www.dgk.badw.de>

Prüfungskommission

Vorsitzender: Univ.-Prof. Dr.rer.nat. E. Rank

Prüfer der Dissertation: 1. Univ.-Prof. Dr.-Ing. F. Seitz
2. Univ.-Prof. Dr.-Ing. U. Stilla
3. Univ.Prof. Dr.techn. W. Wagner,
Technische Universität Wien, Österreich

Die Dissertation wurde am 16.03.2016 bei der Technischen Universität München eingereicht
und durch die Ingenieur fakultät Bau Geo Umwelt am 15.06.2016 angenommen.

Diese Dissertation ist auf dem Server der Deutschen Geodätischen Kommission unter <http://dgk.badw.de/>
sowie auf dem Server der Technischen Universität München unter
https://mediatum.ub.tum.de/670323?show_id=1295206&style=full_text elektronisch publiziert

© 2016 Deutsche Geodätische Kommission, München

Alle Rechte vorbehalten. Ohne Genehmigung der Herausgeber ist es auch nicht gestattet,
die Veröffentlichung oder Teile daraus auf photomechanischem Wege (Photokopie, Mikrokopie) zu vervielfältigen.

Abstract

Soil moisture and terrestrial water storage (TWS) are of vital importance for water supply and agricultural production, and play a key role in the climate system. In this study interrelations between these two important hydrological parameters are analyzed. The analysis targets a better understanding of the dynamics of TWS, which in prior studies have primarily been related to changes in groundwater and surface water. Another objective is to gain insight about the drivers of soil moisture on global scale, and to find out whether the combined analysis of both parameters creates added value for their application in the field of natural disaster monitoring.

The global mapping of soil moisture and TWS is a relatively new field of research because operational satellite products, which provide information on both parameters on large scales, have just emerged in the past 15 years. This study makes use of TWS data from the satellite gravity mission GRACE (Gravity Recovery And Climate Experiment) and two surface soil moisture satellite products, which originate from the active microwave sensor ASCAT (Advanced SCATterometer) and the passive microwave sensor AMSR-E (Advanced Microwave Scanning Radiometer for Earth Observing System). Additionally, global outputs for root zone soil moisture from the WGHM (WaterGAP Global Hydrology Model) and other ancillary data sets as for example for precipitation are integrated into the study.

Following a three step approach first the question is posed whether it is at all feasible to relate data sets for soil moisture and TWS because especially GRACE data differ significantly in data structure and processing from the global soil moisture products. In order to achieve comparable formats, all data sets are harmoniously processed. Main steps include the conversion into spherical harmonics, Gauss filtering and the projection of all data onto a $1^\circ \times 1^\circ$ grid in monthly time intervals. A least-squares filter is additionally applied to the GRACE data. Results show that the main impact of the harmonious processing is homogeneous spatial smoothing of the data in most parts of the world. Exceptions are mainly deserts. In these regions variations in soil moisture are artificially amplified and altered through the conversion into spherical harmonics and spatial leakage from Gauss filtering. Therefore, these areas are excluded from the analyses. Furthermore, regions of low data quality are identified individually for each data set via correlation and time shift analysis. The information on the data quality is also integrated in the analysis.

Second, interrelations between soil moisture and TWS; and soil moisture and other water storage components are analyzed. Therefore, each hydrological signal is split into a seasonal signal and its anomaly. Both parts of the signal are then correlated separately and in sum for different pairs of water storage components. Furthermore, time shifts between different hydrological parameters are calculated. The analysis shows that the seasonal signal of soil moisture dominates the seasonal signal of other storage components over large areas, especially in the southern hemisphere. However, in some of these areas the seasonal amplitude of soil moisture is very low (<40 mm). In regions where soil moisture and TWS are in high agreement (e.g., southern China and India), variations in soil moisture are strongly related to those of other dominating storage components such as groundwater or surface water. A special case is the Sahel zone. In this region variations of soil moisture correlate strongly with changes in TWS (≥ 0.6), because the seasonal signal of soil moisture is dominant and has a large

amplitude (ranging between 40 and 140 mm according to WGHM). Therefore, soil moisture plays a key role for TWS in the Sahel zone.

Third, variations in soil moisture and TWS are compared to gain insight into weather extremes in the La Plata Basin in South America. Specifically those events are brought into focus that had a severe impact on society, and therefore have been registered as natural disasters in the International Disaster Database EM-DAT. Results show that in the La Plata Basin extreme weather events accumulate in El Niño and La Niña years. While most variations in soil moisture can be assigned to single natural disasters, changes in TWS mainly correspond to spatially extended and long-duration drought and flood periods. For two events, namely the La Plata drought of 2009 and the flooding period during the El Niño event in the boreal winter of 2009/2010, changes in soil moisture serve as indicator for upcoming lack or surplus in TWS. Although there is generally a high correspondence between natural disasters and weather extremes, there are also some discrepancies between both data sets. For example, Bolivia was only moderately hit by the 2009 La Plata drought but still more than one hundred thousand people were affected. In contrast the southeastern part of the basin was struck at a similar level but no social impacts have been registered for this region. A possible reason for this discrepancy is the fact that the destructiveness of a disaster does not only depend on the severity of the weather extreme but also on social factors such as population density and the preparedness of the population. Furthermore, information provided within EM-DAT might be incomplete or faulty as the collection of these critical data is challenging on an international level.

In summary this study showed that soil moisture and TWS are interrelated over large parts of the world, either because soil moisture contributes significantly to seasonal changes in TWS or because soil moisture changes proportionally with other dominant storage components. In the La Plata Basin this information could be used for the analysis of extreme weather events and associated natural disasters, which had a high impact on society. By the integration of additional information on the absolute amount of soil moisture in the entire root zone, future studies could investigate the concrete share of soil moisture in TWS.

Zusammenfassung

Sowohl der terrestrische Wasserspeicher als auch die Bodenfeuchtigkeit sind für die Wasserversorgung und die landwirtschaftliche Produktion von lebenswichtiger Bedeutung und haben Schlüsselfunktionen im Klimasystem der Erde. In dieser Studie wird untersucht welche Wechselwirkungen und Zusammenhänge zwischen diesen beiden wichtigen hydrologischen Parametern bestehen. Ziel der Analyse ist es ein besseres Verständnis über die Veränderungen des terrestrischen Wasserspeichers zu erlangen, die bislang meistens auf Variationen des Grundwassers und der Oberflächengewässer zurückgeführt wurden. Außerdem sollen die Ergebnisse Aufschluss darüber geben, welche Faktoren die Bodenfeuchtigkeit auf globaler Ebene beeinflussen, und ob die Verknüpfung beider Parameter einen Mehrwert für ihre Verwendung beim Monitoring von Naturkatastrophen darstellt.

Die globale Beobachtung der Bodenfeuchtigkeit und des terrestrischen Wasserspeichers ist ein relativ neues Forschungsfeld, da Satellitendaten, die globale Informationen über beide Parameter liefern, erst seit ca. 15 Jahren operationell verfügbar sind. Diese Studie basiert auf Daten der Gravitationsfeldmission GRACE (Gravity Recovery And Climate Experiment), die unter anderem Veränderungen des terrestrischen Wasserspeichers widerspiegeln, und auf den Daten zweier Satellitenmissionen zum Beobachten der Oberflächenfeuchtigkeit: dem aktiven Mikrowellensensor ASCAT (Advanced SCATterometer) und dem passiven Mikrowellensensor AMSR-E (Advanced Microwave Scanning Radiometer for Earth Observing System). Diese Daten werden ergänzt durch die globalen Bodenfeuchtigkeitswerte des hydrologischen Modells WGHM (WaterGAP Global Hydrology Model) in der Wurzelzone und durch zusätzliche Datensätze zum Beispiel über den Niederschlag.

Diese Studie ist in drei Teile gegliedert. Als erster Schritt geht sie der Frage nach, ob es überhaupt möglich ist Datensätze über Bodenfeuchtigkeit und den terrestrischen Wasserspeicher in Verbindung zu bringen, da insbesondere GRACE-Daten sich erheblich in ihrer Struktur und Prozessierung von den globalen Bodenfeuchtigkeitsdaten unterscheiden. Um die Formate der verschiedenen Datensätze aneinander anzugleichen, wird die Prozessierung aller Datensätze vereinheitlicht. Dies beinhaltet, dass alle Daten zunächst in Kugelflächenfunktionen dargestellt werden und mit einem Gauß-Filter geglättet werden. Dann werden die monatlichen Mittelwerte wieder auf ein $1^\circ \times 1^\circ$ Gitter projiziert. Die GRACE-Daten werden zusätzlich mit einem Kleinste-Quadrat-Filter geglättet. Die Ergebnisse zeigen, dass die vereinheitlichte Prozessierung in den meisten Gebieten der Erde vor allem eine gleichförmige räumliche Glättung zur Folge hat. Ausnahmen sind vor allem Wüstengebiete. In diesen Regionen werden aufgrund der Umrechnung in Kugelflächenfunktionen und aufgrund von scheinbaren räumlichen Verlagerungen, die unter Anwendung des Gauß-Filters entstehen, Veränderungen der Bodenfeuchtigkeit verstärkt und abgewandelt. Deshalb werden diese Gebiete in den folgenden Analysen nicht berücksichtigt. Zusätzlich wird die Qualität aller Datensätze durch die Berechnung von Korrelationskoeffizienten und zeitlichen Verschiebungen zwischen den Datensätzen überprüft. Auch die Ergebnisse zur Datenqualität werden in den weiteren Analysen berücksichtigt.

Als zweiter Schritt werden hydrologische Zusammenhänge zwischen der Bodenfeuchtigkeit und dem terrestrischen Wasserspeicher sowie zwischen der Bodenfeuchtigkeit und anderen Wasserspeichern analysiert. Hierfür wird jedes hydrologische Signal in eine saisonale Komponente und dessen Abweichung aufgeteilt. Anschließend werden beide Komponenten separat und in der Summe für verschie-

dene Wasserspeicherkombinationen korreliert. Außerdem werden zeitliche Verschiebungen zwischen verschiedenen hydrologischen Parametern ermittelt. Die Analyse zeigt, dass das saisonale Signal der Bodenfeuchtigkeit insbesondere in weiten Teilen der südlichen Hemisphäre das saisonale Signal anderer Wasserspeicher dominiert. Allerdings ist die Amplitude des saisonalen Signals in einigen dieser Regionen sehr gering (<40 mm). In Gebieten, in denen die Variationen der Bodenfeuchtigkeit mit denen des terrestrischen Wasserspeichers übereinstimmen (wie zum Beispiel in Süd-China und Indien), sind Variationen der Bodenfeuchtigkeit an die der anderen dominierenden Wasserspeicher, wie Grundwasser oder Oberflächenwasser, gekoppelt. Eine Ausnahme ist die Sahel-Zone. In dieser Region gibt es höhere Korrelationswerte (≥ 0.6) zwischen den Veränderungen der Bodenfeuchtigkeit und des terrestrischen Wasserspeichers, weil das saisonale Signal der Bodenfeuchtigkeit dominant ist und eine hohe Amplitude (variierend zwischen 40 und 140 mm basierend auf dem WGHM) aufweist. Dies bedeutet, dass die Bodenfeuchtigkeit in der Sahel-Zone eine Schlüsselfunktion für den terrestrischen Wasserspeicher einnimmt.

Als dritter Schritt werden Variationen der Bodenfeuchtigkeit und des terrestrischen Wasserspeichers verglichen, um Aufschluss über Extremwetterereignisse im La Plata Einzugsgebiet in Südamerika zu erlangen. Dabei stehen insbesondere Ereignisse im Vordergrund, die schwerwiegende Auswirkungen auf die Gesellschaft hatten und deshalb als Naturkatastrophen in die internationale Katastrophendatenbank EM-DAT aufgenommen wurden. Die Ergebnisse zeigen, dass im La Plata Einzugsgebiet Extremwetterereignisse mit El Niño und La Niña Jahren zusammenfallen. Während Veränderungen der Bodenfeuchtigkeit zum größten Teil einzelnen Naturkatastrophen zugeordnet werden können, zeigen Variationen des kontinentalen Wasserspeichers Übereinstimmung mit länger anhaltenden Hochwasser- und Trockenperioden. Bei zwei Ereignissen, nämlich der La Plata Dürre 2009 und der Überschwemmungsperiode während des El Niño Winters 2009/2010, weisen Veränderungen der Bodenfeuchtigkeit auf eine folgende Knappheit oder einen Überschuss im terrestrischen Wasserspeicher hin. Obwohl Naturkatastrophen und Wetterextrema weitestgehend übereinstimmen, gibt es auch Unstimmigkeiten zwischen beiden Datensätzen. Zum Beispiel war die La Plata Dürre in Bolivien von moderater Stärke und mehr als einhunderttausend Menschen waren von der Dürre betroffen. Der südöstliche Teil des Einzugsgebiets wurde hingegen in vergleichbarer Stärke von der Dürre getroffen, aber in dieser Region gab es keine Einträge über soziale Auswirkungen. Ein möglicher Grund für diese Unstimmigkeit ist die Tatsache, dass die Zerstörungskraft eines Ereignisses nicht nur von der Schwere des Wetterextrems abhängt sondern auch von sozialen Faktoren wie der Bevölkerungsdichte und der Katastrophenvorsorge. Außerdem ist es auch möglich, dass die Informationen der Datenbank EM-DAT unvollständig oder fehlerhaft sind, da das Sammeln dieser kritischen Daten auf internationaler Ebene eine Herausforderung darstellt.

Zusammengefasst hat diese Studie gezeigt, dass die Bodenfeuchtigkeit und der terrestrische Wasserspeicher in weiten Teilen der Erde im Zusammenhang stehen, weil entweder die Bodenfeuchtigkeit die saisonale Veränderung des terrestrischen Wasserspeichers signifikant beeinflusst oder weil sich die Bodenfeuchtigkeit zeitgleich mit anderen dominanten Wasserspeichern verändert. Im La Plata Einzugsgebiet konnten diese Informationen für die Analyse von Extremwetterereignissen und den damit verbundenen Naturkatastrophen, die schwerwiegende Auswirkungen auf die Gesellschaft hatten, genutzt werden. Durch die Einbindung von weiteren Informationen über den Absolutbetrag der Bodenfeuchtigkeit in der Wurzelzone, könnte in zukünftigen Studien der exakte Anteil der Bodenfeuchtigkeit am kontinentalen Wasserspeicher berechnet werden.

Preface

In this PhD thesis the results of three peer-reviewed publications are integrated. Those publications are listed in the following:

Abelen S, Seitz F, Schmidt M, Güntner A (2011) Analysis of regional variations in soil moisture by means of remote sensing, satellite gravimetry and hydrological modelling. In: GRACE, Remote Sensing and Ground-Based Methods in Multi-Scale Hydrology, IAHS Red Book Series, Nr. 343, International Association of Hydrological Sciences, pp 9–15

Abelen S, Seitz F (2013) Relating satellite gravimetry data to global soil moisture products via data harmonization and correlation analysis. *Remote Sensing of Environment* 136:89–98, DOI 10.1016/j.rse.2013.04.012

Abelen S, Seitz F, Abarca-del Rio R, Güntner A (2015) Droughts and Floods in the La Plata Basin in Soil Moisture Data and GRACE. *Remote Sensing* 7(6):7324–7349, DOI 10.3390/rs70607324

Whenever a passage of one of those publications is used in this thesis it is marked as following:

◁ ... ▷ (Abelen et al, 2011)

◁ ... ▷ (Abelen and Seitz, 2013)

◁ ... ▷ (Abelen et al, 2015)

This marking does not mean that the text is copied word by word. The highlighted passage might contain slight modifications, which do not alter the content and meaning of the text. For example more recent publications might be added to the references, phrases like “we used the method”, might be rephrased to “the method was used”, references to previous chapters might be added, or explanatory notes might be provided.

Contents

Abstract	5
Zusammenfassung	7
Preface	9
Abbreviations	13
1 Introduction	15
1.1 Motivation	15
1.2 Target of Research	16
1.3 Structure of the Dissertation	17
2 Large-Scale Mapping of Soil Moisture	21
2.1 Introduction to Soil Moisture	21
2.2 Soil Moisture from Microwave Remote Sensing	23
2.3 Soil Moisture from Hydrological Models	28
2.4 Validation	29
2.5 Application	33
2.6 Contribution of the Study	36
3 Large-Scale Mapping of Terrestrial Water Storage	39
3.1 Introduction to Terrestrial Water Storage	39
3.2 Terrestrial Water Storage from Satellite Gravimetry	41
3.3 Terrestrial Water Storage from Hydrological Models	44
3.4 Validation	45
3.5 Application	48
3.6 Contribution of the Study	50
4 Data and Preprocessing	53
4.1 Surface Soil Moisture from ASCAT	53
4.2 Surface Soil Moisture from AMSR-E	54
4.3 Terrestrial Water Storage from GRACE	55
4.4 Water Storage Components from WGHM	57
4.5 Precipitation from GPCC	57
4.6 Oceanic Niño Index	59
4.7 The International Disaster Database EM-DAT	59
5 Linking Soil Moisture to Terrestrial Water Storage	61
5.1 Theoretical Background	61
5.2 Data Harmonization	62
5.3 Scaling	68

5.4	Correlation Analysis and Fisher's z Transformation	69
5.5	Time Shift Analysis	69
5.6	Principal Component Analysis	70
5.7	Analysis of Hydrological Extremes	70
6	Comparability of Data Sets	73
6.1	Impacts of Data Harmonization	73
6.2	Comparison of Soil Moisture Products	79
6.3	Comparison of Terrestrial Water Storage Products	81
6.4	Summary	84
7	Hydrological Interdependencies	85
7.1	Analysis of Seasonal Amplitudes	85
7.2	Interdependency of Soil Moisture and Terrestrial Water Storage	88
7.3	Interdependencies with other Hydrological Parameters	93
7.4	Summary	96
8	Hydrological Extremes in Soil Moisture and Terrestrial Water Storage	99
8.1	Study Area: La Plata Basin	99
8.2	Regional Comparison of Soil Moisture Products	102
8.3	Regional Interdependency of Soil Moisture and TWS	105
8.4	Hydrological Extremes and Natural Disasters	106
8.5	Summary	113
9	Conclusion	115
10	Outlook	119
	Bibliography	123

Abbreviations

AMSR-E	Advanced Microwave Scanning Radiometer for Earth Observing System
ASCAT	Advanced SCATterometer
CSR	Center for Space Research at University of Texas at Austin
DLR	German Aerospace Center
ECMWF	European Centre for Medium-Range Weather Forecasts
EGSIEM	European Gravity Service for Improved Emergency Management
EM-DAT	The International Disaster Database
EOF	Empirical Orthogonal Function
EPOS	Earth Parameter and Orbit System
GFZ	German Research Centre for Geosciences
GPCP	Global Precipitation Climatology Center
GRACE	Gravity Recovery And Climate Experiment
GW	Groundwater
ISMIN	International Soil Moisture Network
JPL	Jet Propulsion Laboratory
LEO	Low Earth Orbit
LPB	La Plata Basin
LSM	Land-Surface Model
MIRAS	Microwave Imaging Radiometer using Aperture Synthesis
NASA	National Aeronautics and Space Administration
NOAA	National Oceanic and Atmospheric Administration
NRCS	Natural Resource Conservation Service
ONI	Oceanic Niño Index
PC	Principal Component
PCA	Principal Component Analysis
PGR	Post-Glacial Rebound
RQ	Research Question

SAR	Synthetic Aperture Radar
SGG	Satellite Gravity Gradiometry
SH	Spherical Harmonics
SMAP	Soil Moisture Active Passive
SMN	Argentinean National Meteorological Service
SMOS	Soil Moisture and Ocean Salinity
SST	Satellite-to-Satellite Tracking
SST-hl	high-low Satellite-to-Satellite Tracking
SST-ll	low-low Satellite-to-Satellite Tracking
SUR	Surface Water
SWI	Soil Water Index
TRMM	Tropical Rainfall Measuring Mission
TUM	Technische Universität München
TWS	Terrestrial Water Storage
UNISDR	United Nations Office for Disaster Risk Reduction
UNEP	United Nations Environmental Programme
USDA	United States Department of Agriculture
USGS	United States Geological Survey
WaterGAP	WaterGlobal Assessment and Prognosis
WGHM	WaterGAP Global Hydrology Model

1 Introduction

1.1 Motivation

The Food and Agricultural Organization declared the year 2015 as the International Year of Soils. Soil moisture plays a crucial role in food security and is a key variable in the climate system (Section 2.1). It is a storage component for precipitation and a source of water for the atmosphere by influencing plant transpiration and bare soil evaporation (Seneviratne et al, 2010). In 2009 soil moisture has been recognized as an Essential Climate Variable within the Intergovernmental Panel on Climate Change and the United Nations Framework Convention on Climate Change. Terrestrial water storage (TWS) refers to all water which is stored over the continents (Section 3.1). It is an important part of the hydrological cycle as it entails the fraction of precipitation, which reaches the Earth's surface and is neither evaporated nor drained through runoff to the ocean (Schmidt et al, 2006c).

◁ Soil moisture and TWS are closely linked, as soil moisture is an essential component of TWS in addition to surface water, snow, ice, and groundwater. Furthermore, both parameters strongly depend on the difference between inflow (precipitation) and outflow (percolation, drainage, and evapotranspiration) of the soil and its water-holding capacity (as a function of, e.g., soil physical properties). ▷ (Abelen et al, 2015)

In the past both parameters, TWS and soil moisture, were not mapped over extensive areas, because adequate large-scale monitoring systems (referring to spatial extents $> 100^2 \text{ km}^2$, herein as defined by Ochsner et al, 2013) were not operationally available (see Section 2.1 and Section 3.1). This changed significantly in the last 15 years. In 2003 the satellite gravity mission GRACE (Gravity Recovery And Climate Experiment) was launched enabling for the first time in history the global mapping of changes in TWS. From 2002 onwards the operational availability of global soil moisture products was made possible with the launch of at least five major satellite missions (AMSR-E, ASCAT, SMOS, SMAP and Sentinel-1).

Recent data sets from satellites (see Section 2.2 and Section 3.2), in combination with outputs of global hydrological models (see Section 2.3 and Section 3.3), have opened up new possibilities for the analysis of soil moisture and TWS on global scale. At the same time there is a growing need for hydrological and climatological studies because of increasing pressure on agriculture due to population growth, and changing weather and climate (Overgaard et al, 2005), which is coupled with more intense and frequent weather extremes.

The validation and application of those newly available data sets has caught the interest of many scientists (see Section 2.4 and Section 2.5 for soil moisture and Section 3.4 and Section 3.5 for TWS). Key challenges which still remain have been described as the following:

“Two main issues with GRACE estimates are, however:

1. the necessary disaggregation of the data in separate estimates of the individual terrestrial water storage components (e.g. soil moisture, groundwater, snow);

2. the still coarse resolution of the estimates” (Seneviratne et al, 2010)

“In closing, we again note the growing need to develop the science necessary to make effective use of the rising number of large-scale soil moisture data sets.” (Ochsner et al, 2013)

Previous studies have analyzed large-scale soil moisture and TWS products individually or in combination with other data sets (e.g., on precipitation, river runoff). However, studies which primarily connect global soil moisture data sets with TWS estimates from GRACE were lacking. The focus of this thesis is on the combined analysis of recent large-scale soil moisture and TWS products to address the above mentioned open challenges (more detailed information on the contribution of this study is given in Section 2.6 and Section 3.6). The motivation is to find out which role soil moisture plays within TWS and how the dynamics of soil moisture and TWS are linked on global scale. A further objective is to find out if the combination of both data sets adds value to their application in the field of natural disaster monitoring.

1.2 Target of Research

The main target of this research is to give answer to the question whether it is feasible to compare large-scale soil moisture products with TWS from GRACE to tackle the above mentioned challenges and those which are listed in more detail in Section 2.6 and Section 3.6. More specifically this thesis addresses three main research questions (RQ 1 to RQ 3):

1. Is it feasible to compare the various soil moisture products with TWS from GRACE with respect to the different characteristics of the data sets, considering in specific:
 - a) Their varying data structures (e.g. in terms of spatial and temporal resolution and required preprocessing), and
 - b) Their heterogeneous data quality?
2. Which hydrological interdependencies exist between soil moisture and TWS, considering in specific:
 - a) The relative share of soil moisture in the seasonal signal of TWS,
 - b) Correlations and time shifts between variations in soil moisture and TWS,
 - c) Interdependencies between soil moisture and other hydrological parameters such as ground-water and surface water?
3. What can we learn with the help of soil moisture and TWS from GRACE about hydrological extremes and associated natural disasters?

This three step approach is also reflected in the title of this thesis as shown in Figure 1.1. First, this study focusses on data-related issues as multi-sensor Earth observations and outputs of one hydrological model have to be brought into comparable formats. This establishes the basis for the following investigations. Second, the two hydrological variables, soil moisture and TWS, and their interrelations are brought into focus. It is investigated in which parts of the world variations of both data sets are in agreement and why hydrologic interrelations exist. Third, it is analyzed exemplarily for the La Plata Basin in South America if the knowledge on links between soil moisture and TWS can be used for the monitoring of weather extremes, which have high impact on society.

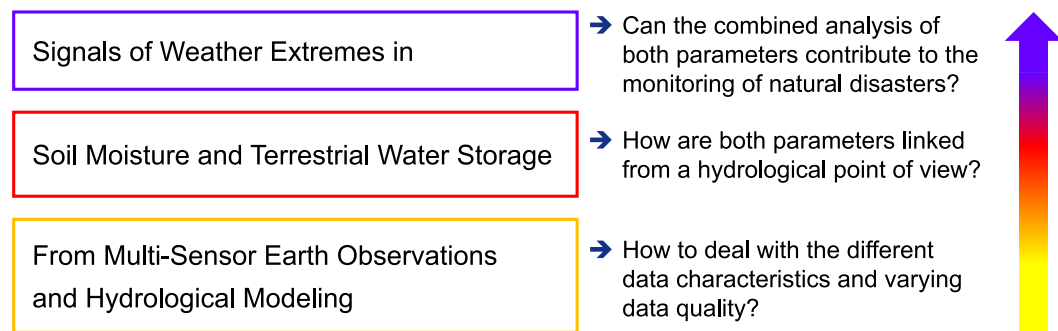


Figure 1.1: Title of the thesis and the followed three step approach.

1.3 Structure of the Dissertation

The structure of the thesis is shown in Figure 1.2. This introduction is followed by a state of the art on the large-scale mapping of soil moisture (Chapter 2) and the large-scale mapping of TWS (Chapter 3). After an introduction to the hydrological parameters soil moisture (Section 2.1) and TWS (Section 3.1), recent large-scale mapping techniques by satellites and models are described (see Section 2.2 and Section 2.3 for soil moisture, and Section 3.2 and Section 3.3 for TWS, respectively). Furthermore, an overview is given on studies which were dedicated to the validation and application of those data sets (see Section 2.4 and Section 2.5 for soil moisture, and Section 3.4 and Section 3.5 for TWS, respectively). At the end of both state of the art chapters the contribution of this study is described in detail (see Section 2.6 for soil moisture, and Section 3.6 for TWS).

Next, the various data sets used in this study are described (Chapter 4). They include two surface soil moisture products from the satellite sensors ASCAT and AMSR-E (see Section 4.1 and Section 4.2, respectively), information on TWS variation from the satellite mission GRACE (Section 4.3), and outputs for various storage components, which sum up to TWS (including root zone soil moisture), from WGHM (Section 4.4). Further ancillary data sets comprise precipitation data from GPCC (Section 4.5), information on El Niño and La Niña years based on the Oceanic Niño Index (Section 4.6), and a list of natural disasters provided by the International Disaster Database EM-DAT (Section 4.7).

Chapter 5 describes the methods which are used to align the formats of all data sets and to compare them in spatial and temporal terms. First, interrelations between variations in soil moisture and variations in TWS from GRACE are theoretically discussed and several assumptions for the following analysis are formulated (Section 5.1). Afterwards the approach for harmonizing soil moisture data and data from satellite gravimetry is described (Section 5.2). The harmonious processing is particularly adjusted to the special characteristics of GRACE data, which is why the data sets are introduced previous to the method, herein. As satellites only provide information on the surface soil moisture, they are scaled with respect to the root zone soil moisture which is provided by WGHM (Section 5.3). Interrelations among the data sets are calculated via correlation (Section 5.4), time shift (Section 5.5), and principal component analysis (Section 5.6). As last step hydrological extremes in soil moisture and TWS are linked to natural disasters, which had destructive impact on society (Section 5.7).

Results, which concern the comparability of data sets, are presented in Chapter 6. They reflect the impact of the harmonious data processing (Section 6.1) and provide spatial information on the data quality of the global soil moisture and TWS products (see Section 6.2 and Section 6.3, respectively). The results of Chapter 6 provide the basis for the analysis of hydrological interrelations. They are summarized in terms of RQ 1a and 1b in the last section of this chapter (Section 6.4).

Chapter 7 shows results, which emphasize how soil moisture and TWS are linked over large areas. The results provide information about the seasonal amplitude of soil moisture and how it relates to the seasonal amplitudes of other storage components (see Section 7.1). Furthermore, they show in which regions of the world soil moisture and TWS are strongly interconnected (Section 7.2) and how these findings are related to interdependencies between soil moisture and other storage components (Section 7.3). In the final summary of this chapter RQ 2a, 2b, and 2c are addressed (Section 7.4).

The focus of Chapter 8 is on the application of soil moisture and TWS data for the monitoring of hydrological extremes in the La Plata Basin in South America (Section 8.1). Therefore, the quality of the used soil moisture data (Section 8.2) and the interdependency of soil moisture and TWS (Section 8.3) are analyzed more in detail for this region. Then, time series of soil moisture and TWS data are matched with impacts of weather extremes, which have been registered within the International Disaster Database EM-DAT (Section 8.4). Also connections to El Niño and La Niña years are emphasized. The summary of this chapter is devoted to RQ 3 (Section 8.5).

In Chapter 9 final conclusions from all findings of this thesis (which are summarized in Section 6.4, Section 7.4, and Section 8.5) are drawn with respect to the comparability of the used data sets, interrelations of soil moisture and TWS on global scale, and potential benefits of integrating both data sets into the analysis of weather extremes. The outlook in Chapter 10 describes new potential approaches to gain deeper insight about interdependencies between soil moisture and TWS on large scale.

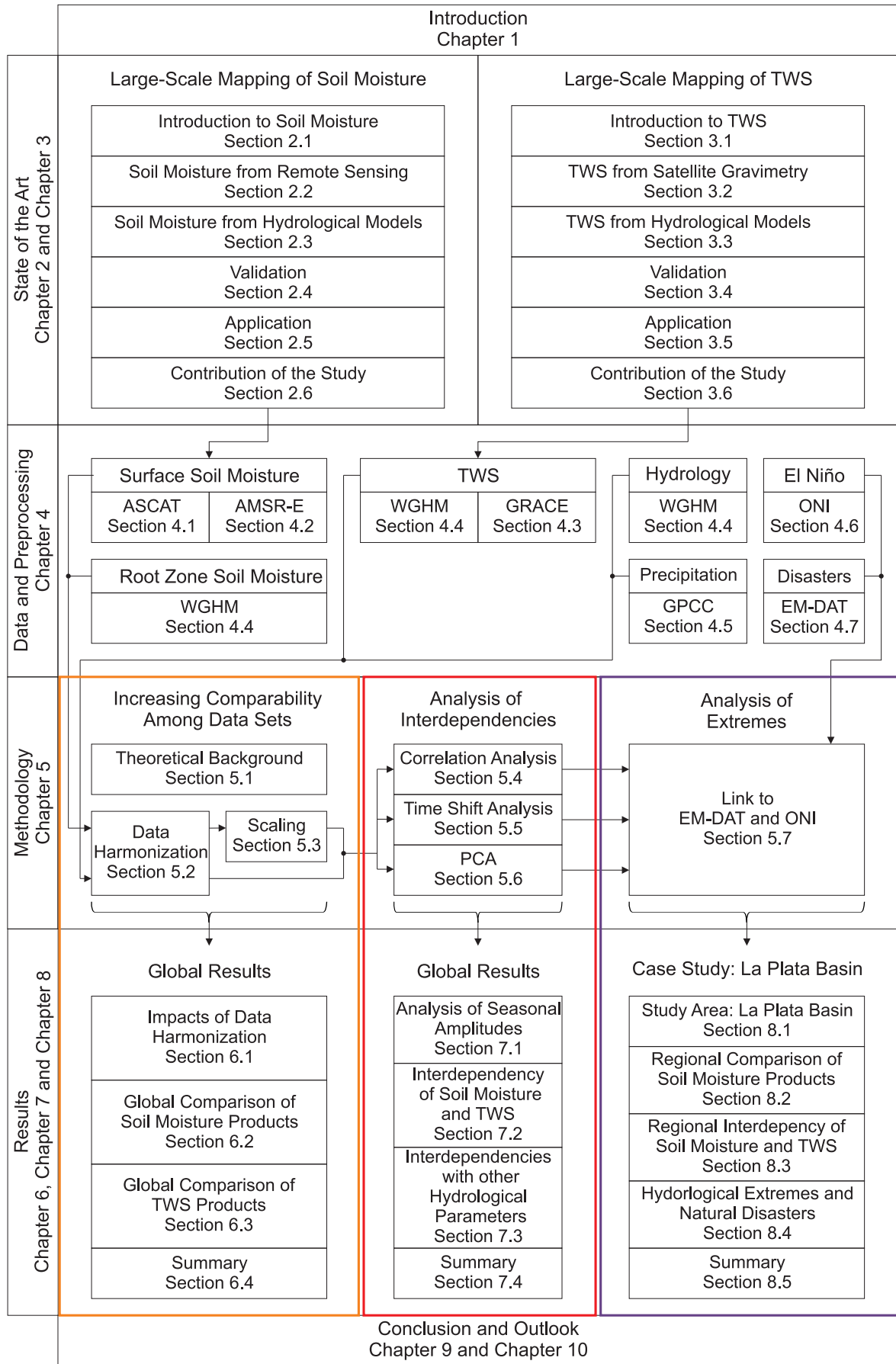


Figure 1.2: Structure of the thesis.

2 Large-Scale Mapping of Soil Moisture

2.1 Introduction to Soil Moisture

Soil moisture is usually defined as the water contained in the unsaturated soil zone at the surface of the Earth (Petropoulos, 2014; Hillel, 1998). In the unsaturated and saturated soil zone one distinguishes between three main types of water (Figure 2.1). The water which is surrounding the soil in the first molecular layers is strongly held by the soil matrix. It is unavailable to plants and also called bound water (Wagner, 1998). The highest possible amount of bound water is defined by the so called permanent wilting point. Also inaccessible to plants is gravitational water. Gravitational water cannot be held by the soil matrix against gravitational forces and drains to the saturated soil zone. It is formed above the so called field capacity (Seneviratne et al, 2010).

Water accessible to plants in the unsaturated soil zone is neither tightly bound to the soil water (as in the case of bound water) nor subject to gravitational drainage (as in the case of gravitational water) (Seneviratne et al, 2010; Hillel, 1998). Its lower limit is defined by the permanent wilting point and its upper limit is defined by the field capacity. The field capacity and the permanent wilting point (and with it also the amount of bound, available and gravitational water) vary geographically as they depend on the properties of the soil (e.g. the texture of the soil). The permanent wilting point (and with it also the amount of bound water) additionally depends on the vegetation type (Seneviratne et al, 2010; Sperry et al, 2002).

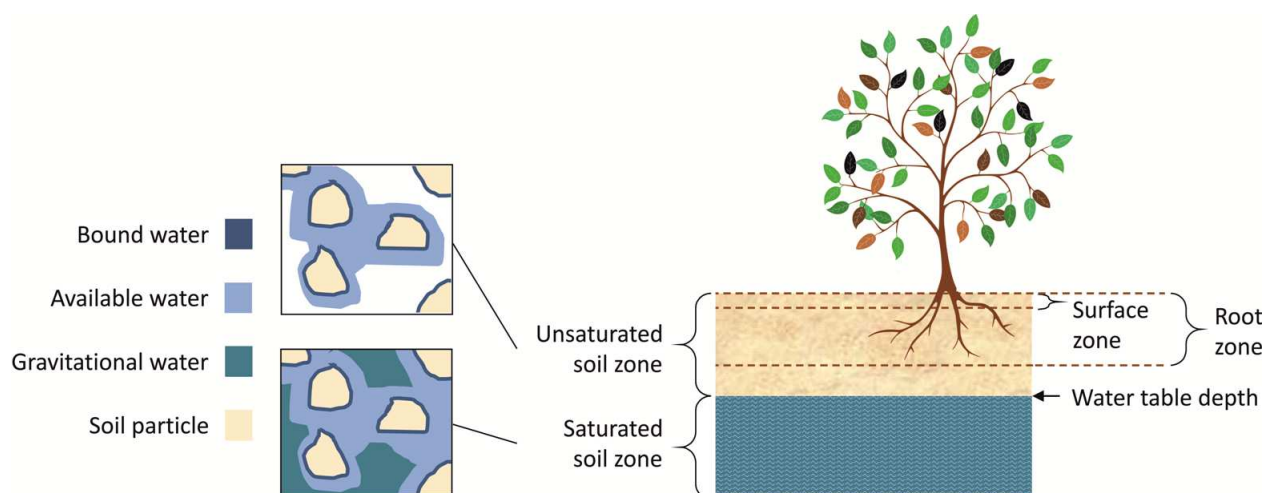


Figure 2.1: Schematic on the presence of bound, available and gravitational water in the unsaturated and saturated soil zone (left), and the location of the surface zone (as captured by microwave satellite remote sensing) and the root zone (being specifically relevant to agro-ecological studies) in the unsaturated soil zone (right).

The targeted fraction of soil moisture which is measured or estimated differs significantly among various techniques (Dorigo et al, 2010). Microwaves sensors on satellite platforms capture the moisture in the surface zone of the soil (Figure 2.1, right). For bare soil this zone is approximately up to 2 cm deep (Escorihuela et al, 2010; Schneeberger et al, 2004), mainly depending on the operating wavelength of the satellite sensor and the soil moisture content (see Section 2.2). For models the depth of the considered soil zone is usually deeper. Depending on the model the moisture of one or more discrete soil layers are simulated (see Section 3.3).

Often the targeted fraction of the soil is the root zone (Figure 2.1, right) because the available water in this zone is of specific interest to the agricultural sector (Wang et al, 2007) and a key parameter for investigations of soil moisture-climate interactions (Seneviratne et al, 2010). As the rooting depth of vegetation (defining the root zone) and the water table depth (defining the unsaturated soil zone) vary over space and time, the targeted soil fraction may not be constant but change as function of space and time. When comparing different soil moisture products possible differences in the observed fraction of soil moisture (e.g. surface soil moisture vs. root zone soil moisture) have to be taken into account (Dorigo et al, 2010).

Soil moisture is vertically (at different soil depth) and horizontally (at different locations) heterogeneously distributed and shows strong fluctuation over time (e.g. at the soil surface within hours). This large variability is on the one hand based on geographic factors such as varying soil types and topography. On the other hand it is driven by manifold complex processes, such as soil moisture-precipitation coupling, soil moisture-temperature coupling and soil moisture-evapotranspiration coupling (Seneviratne et al, 2010).

When analyzing variations of soil moisture at different scales two main components can be distinguished. The first small-scale component (acting in the range of centimeters to hundreds of meters) refers to changes in soil moisture which originate from the heterogeneity in vegetation, soil type and topography. The second large-scale component (acting in the range of hundreds of kilometers) includes variability in soil moisture which is induced by large patterns of precipitation and evapotranspiration, resulting from meteorological and climate events (Scipal et al, 2005).

Comprehensive and continuous measurements of soil moisture from in-situ or proximal sensing techniques are currently not available on large scales, as existing networks are worldwide unevenly distributed. Especially in dry areas, at high latitudes, and in the tropics the number of stations is limited (Ochsner et al, 2013). Recently, efforts have been made to establish large in-situ networks with spatial extends $> 100^2 \text{ km}^2$. A list of large scale in-situ soil moisture monitoring networks is provided by Ochsner et al (2013).

Furthermore, the International Soil Moisture Network (ISMIN; <https://ismn.geo.tuwien.ac.at/>) has been founded in 2009 (Dorigo et al, 2011a,b). It is a joint initiative from the Global Energy and Water Cycle Experiment, the Group of Earth Observations and the Committee on Earth Observations Satellites, funded by the European Space Agency. ISMIN harmonizes and collects in-situ soil moisture data from different networks and makes them accessible through a centralized data portal. Many data from operational soil moisture networks are downloaded automatically and are available in near real time. Those data are essential for sensor calibration and the validation of soil moisture products from remote sensing (Ochsner et al, 2013, see Section 2.4).

2.2 Soil Moisture from Microwave Remote Sensing

Remote sensing techniques, estimating soil moisture indirectly from tower, aircraft or satellite platforms, have been used since the early 1960s (Ulaby and Long, 2014). The history and technological development of those measurements (and also of in-situ measurements) are described in detail by Ochsner et al (2013) and Ulaby and Long (2014). The use of satellite platforms for the remote sensing of soil moisture made the consistent and frequent global mapping of soil moisture possible (Kumar and Reshmidevi, 2013). Specifically microwave sensors with wavelength from 1 m to 1 mm (corresponding to frequencies of 0.3 to 300 GHz respectively) are suitable to provide quantitative measurements of soil moisture. Most important bands are X-band (wavelength = 2.5-3.8 cm, frequency = 12-8 GHz), C-band (wavelength 3.8-7.6, frequencies 8-4 GHz), and L-band (wavelength = 15-30 cm, frequency = 2-1 GHz).

Unfortunately all bands may be affected by radio frequency interference (RFI). This is also true for in principle protected bands, which are reserved for passive sensors only such as the L-band (Wagner et al, 2007). Impacts on the satellite signal through cloud coverage, rain, and vegetation decrease with increasing wavelength. For wavelengths larger than 4 cm cloud coverage and rain are negligible. With increasing wavelength the signal penetrates more deeply into the soil, whereby the penetration depth additionally depends on the dielectric properties of the ground and is deeper for surfaces with low vegetation cover and low soil moisture (Ulaby and Long, 2014).

Microwave sensors are able to sense soil moisture as they are sensitive to the dielectric constant of the ground, which increases with increasing amount of water in the soil (Ulaby et al, 1982). The real part of the dielectric constant determines the propagation characteristics of the signal through the soil, while the imaginary part determines the energy losses (de Jeu et al, 2008). Dielectric properties of common materials at the Earth's surface are provided in Table 2.1 as summary of the dielectric values presented by Wagner (1998). The table shows the large differences in the dielectric properties of dry soil and water. For example, the real part of the dielectric constant has a value of about 3 for dry soil and a value of about 70 and for water (Jackson, 2005). Furthermore, the table highlights that the dielectric constants of liquid and frozen water as well as of bound and free (available and gravitational) water differ significantly. The dielectric constant of vegetation increases with increasing moisture content. Challenges for soil moisture retrieval which arise from the mixture of different dielectric properties of various materials on the ground are highlighted in Table 2.3 in Section 2.4.

Table 2.1: Dielectric properties at C-band of common materials at the Earth's surface, summarized from Wagner (1998).

Natural Media	ϵ' real part of the dielectric constant		ϵ'' imaginary part of the dielectric constant	
	Pure Water	66.9 (0°)	73.3 (20°)	36.2 (0°)
Dry Soil	2 (small grain size, more bound water)	4 (large grain size, less bound water)	< 0.05	
Vegetation	1.5-2 (dry)	> 40 (high moisture content)	< 0.1 (dry)	> 2 (high moisture content)
Snow	< 1.7 (dry)	> 4 (15% volumetric fraction of water)	< 0.1 (dry)	> 1 (15% volumetric fraction of water)
Ice	3.17±0.03		< 10 ⁻³	

The link between the dielectric constant and the sensed microwave signal at the satellite is given by the reflectivity of the ground, expressed by the Fresnel reflection equation:

$$r_{surf\ fp} = \left| \frac{\cos \theta - \sqrt{k - \sin^2 \theta}}{\cos \theta + \sqrt{k - \sin^2 \theta}} \right|^2. \quad (2.1)$$

The Fresnel reflection equation tells that the reflectivity of the surface (r_{surf}) for a certain frequency band (f), and polarization (p), depends on the viewing angle of the sensor (θ) and the dielectric constant (k) of the ground. This simplified equation can be applied, assuming that the Earth has a plane surface and that the interface between the surface soil layer and the air (approximated as vacuum) have uniform dielectric properties (Jackson, 2005).

For the remote sensing of soil moisture two main techniques exist: active and passive microwave remote sensing. Passive sensors (radiometers) measure the natural thermal radio emission from the Earth, which is expressed as brightness temperature (T_B) for a particular frequency band (f), and polarization (p) (Njoku and Li, 1999):

$$T_{B\ fp} = e_{surf\ fp} T_{surf} e^{-\tau_f} + T_{up} + (1 - e_{surf\ fp}) T_{down} e^{-\tau_f} + (1 - e_{surf\ fp}) T_{space} e^{-2\tau_f}. \quad (2.2)$$

The brightness temperature is provided in degree Celsius or Kelvin and refers to the temperature a black body (for which emissivity = absorptivity = 1) would be in order to emit the recorded radiance at a given frequency and polarization (Liang et al, 2012).

The first term on the left side of the equation accounts for the emitted radiation from the surface. It is the product of the emissivity of the surface ($e_{surf\ fp}$), the physical temperature of the surface (T_{surf}) and the attenuation of the radiation by the atmospheric opacity (τ_f), also referred to as optical depth. The second term (T_{up}) is atmospheric upwelling radiation. The third term is the atmospheric downwelling radiation (T_{down}), which has been reflected at the surface ($1 - e_{surf\ fp} = r_{surf\ fp}$) and is also attenuated by the atmosphere. The last term accounts for the cosmic background radiation (T_{space} is the cosmic background temperature), which has been travelling twice through the atmosphere (once by reaching the surface and once after reflection at the surface). Taking into account that the reflectivity is equal to one minus the emissivity (Kirchhoff's law; Schanda, 1986) the formula can be directly linked to the reflectivity of the surface, which is again linked to the dielectric constant of the ground (see Equation 2.1).

Equation 2.2 highlights the main components influencing the brightness temperature which is measured by the satellite. The last term on the cosmic background radiation is about 2.7 K (Ulaby et al, 1982) and the upwelling and downwelling atmospheric radiation can be expressed as products of the weighted average atmospheric temperature and the atmospheric emissivity (Bevis et al, 1992). Therefore, the main remaining term in the equation is the first one, which mainly depends on the emissivity and temperature of the surface.

The physical temperature of the Earth can be estimated through model predictions, satellite measurements or air temperature observations, whereby the quality of those estimates is crucial for the quality of the soil moisture products (Parinussa et al, 2011). With information on the land surface temperature, the emissivity of the ground and with it also the dielectric constant and finally the soil moisture can be computed from the brightness temperature measured at the satellite. The emissivity of the ground and with it also the brightness temperature decreases with increasing soil moisture.

The second remote sensing technique for the measurement of soil moisture is based on active sensors, which are also called radars (radio detection and ranging). Those send an energy pulse actively to the Earth and measure the energy which is scattered back from the Earth's surface to the sensor. The received power at the satellite of a transmitted signal, which has been scattered back to the sensor by one specific target, has been described by Ulaby et al (1982) with the widely used monostatic (radar transmitter and receiver are co-located) radar equation (Joseph, 2005; Rees, 2013; Wagner, 1998):

$$P_r = \frac{P_t G}{4\pi R^2} \sigma \frac{1}{4\pi R^2} \frac{\lambda^2 G}{4\pi} = \frac{\lambda^2}{(4\pi)^3} \frac{P_t G^2}{R^4} \sigma, \quad (2.3)$$

where:

- P_r received power
- P_t transmitted power
- G gain of the antenna
- λ wavelength of the radar signal
- R distance (range) between radar and target
- σ radar cross-section of the target

The equation tells that the received Power (P_r) is equal to the power density that the transmitter produces at the target (first term on right hand side of the equation), times the radar cross-section of the target (second term on right hand side of the equation), times the isotropic spread of the intercepted power from the target back to the radar (third term on right hand side of the equation), times the effective area of the antenna that collects the returning power density (fourth term on right hand side of the equation). All parameters, except the radar cross-section of the target, are constant during an observation as they refer to the technical characteristics of the radar (P_t , G , λ) or its distance to the observed target (R). Consequently, the strength of the reflected radar signal is mainly dependent on the radar cross-section of the target (σ), which describes the ability of the observed target to reflect the transmitted radar signal in the direction of the radar receiver (Joseph, 2005).

In the case of remote sensing a large surface area is observed, that includes various point scattering targets. Therefore, the characteristic backscattering of the observed surface is expressed as differential scattering coefficient or normalized radar cross-section, which is commonly called backscattering coefficient (Schanda, 1986; Rees, 2013):

$$\sigma^0 = \frac{d\sigma}{dA}, \quad (2.4)$$

where:

- σ^0 backscattering coefficient, expressed in decibel ($\sigma^0 [\text{dB}] = 10 \log_{10} 10\sigma^0 [\text{m}^2/\text{m}^2]$)
- $d\sigma$ differential radar cross-section of the illuminated area
- dA differential unit area, which is illuminated by the sensor

Hence, in the context of radar remote sensing Equation 2.3 is rewritten as:

$$P_r = \frac{\lambda^2}{(4\pi)^3} \int_{\text{illuminated area}} \frac{P_t G^2}{R^4} \sigma^0 dA. \quad (2.5)$$

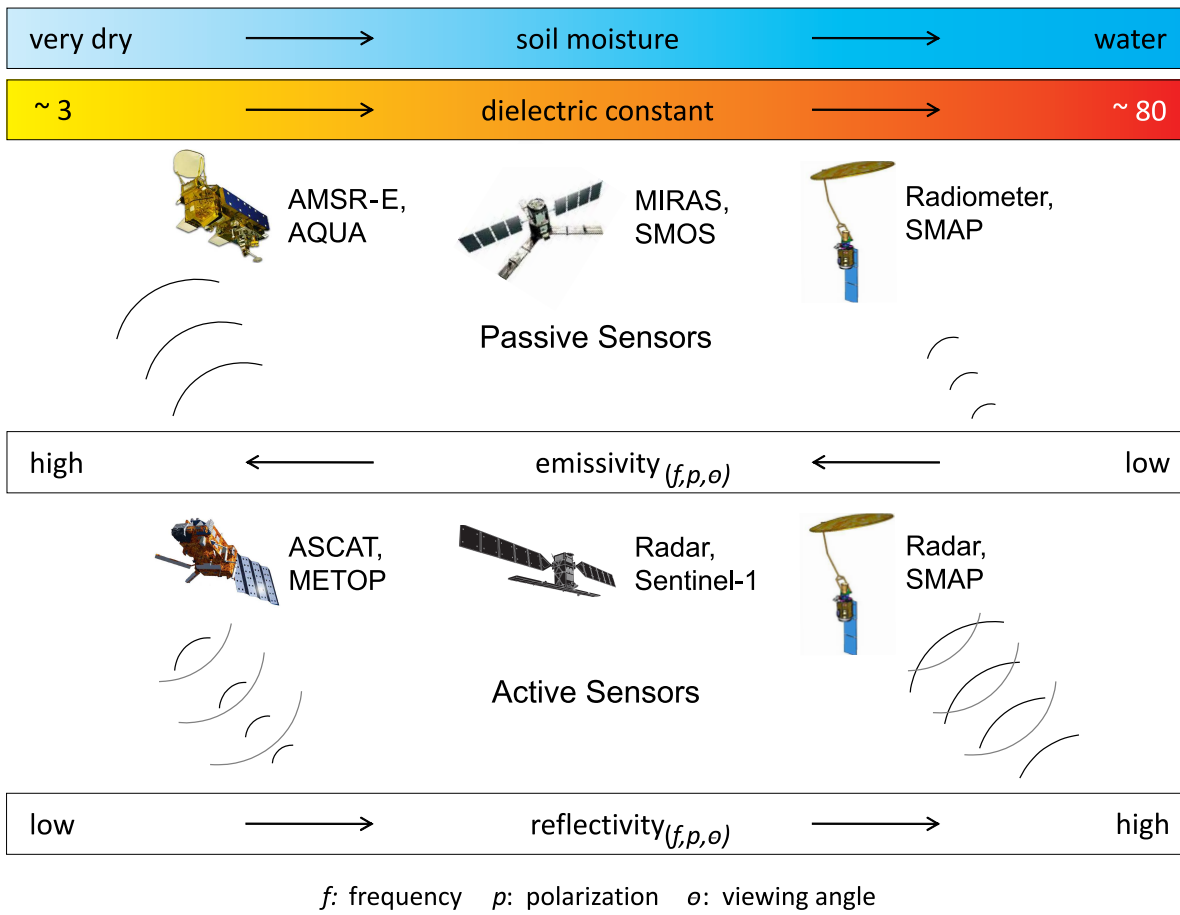


Figure 2.2: Interdependence of soil moisture, dielectric constant, emissivity, and reflectivity for a bare soil surface and examples for recent active and passive microwave sensors and their satellite platforms.

As the backscattering coefficient depends on the reflectivity of the ground (which again depends on the dielectric properties of the soil surface), it is the key parameter for soil moisture retrieval from radars.

Figure 2.2 summarizes the two main principles of microwave remote sensing and shows recent satellite missions, which carry active or passive sensors and deliver operational soil moisture products (for SMAP launched in January 2015, and for Sentinel-1A launched in April 2014 operational soil moisture products are under preparation). Some technical details of the shown sensors are listed in Table 2.2. More detailed information on operational soil moisture products and various active and passive sensors are provided by Dorigo et al (2010) and Ulaby and Long (2014), respectively.

Table 2.2 shows that the spatial resolution of the listed satellite sensors ranges from 1 km to 60 km. The temporal resolution lies between 2 to 6 days. For many applications an increase in spatial and temporal resolution, as well as the use of larger wavelength for more precise measurements of soil moisture would be beneficial. However, several limitations exist, as for example:

- with increasing spatial resolution (implying lower spatial coverage; e.g. in the case of SAR) the temporal resolution decreases (Kerr et al, 2010),
- with decreasing wavelength the spatial resolution increases but the sensitivity to soil moisture decreases (Ochsner et al, 2013),

- with increasing wavelength the antenna size of the sensor needs to be larger, which leads to higher costs and significant technical challenges (Kerr et al, 2010),
- with increasing spatial resolution as in the case of SAR sensors (spatial resolution < 1 km), the complexity of the sensor and the retrieval algorithms increase (Wagner et al, 2007; Kerr et al, 2010).

Due to these tradeoffs the most recent mission SMAP combines two different sensor systems (non-imaging L-Band SAR with high spatial resolution but low sensitivity to soil moisture and an L-Band radiometer with high sensitivity to soil moisture but low spatial resolution) to generate a soil moisture product with both, high spatial resolution (10 km) and high sensitivity to soil moisture (with an error of no greater than $0.04 \text{ m}^3/\text{m}^3$). After the launch of SMAP both sensors went successfully into operations, but SMAP radar failed for unknown reasons after a few months. Another strategy is to launch several satellites in short time intervals to operate various satellites in parallel, which increases the temporal resolution of the delivered soil moisture products. This is planned for the Sentinel-1 satellites (the first one, Sentinel-1A is already in orbit since April, 2014).

Table 2.2: Examples of satellite sensors, delivering data for operational soil moisture products (for SMAP and Sentinel-1A operational soil moisture products are under preparation).

Sensor	Satellite Platform	Type	Spatial Resolution	Temporal Resolution (near the equator)	Operation Time	Reference
AMSR-E (Advanced Microwave Scanning Radiometer for Earth Observing System)	AQUA	Radiometer (X-band and C-band)	40 km (X-band) 60 km (C-band)	~2 days	2002-2011	Njoku et al, 2003
ASCAT (Advanced SCATterometer)	MetOp (Meteorological Operational Satellite)	Scatterometer (C-Band)	25-50 km	~2 days	2006-present	Klaes et al, 2007; Wagner et al, 2007
MIRAS (Microwave Imaging Radiometer using Aperture Synthesis)	SMOS (Soil Moisture and Ocean Salinity)	Radiometer (L-band)	35-50 km	~3 days	2010-present	Kerr et al, 2010
Non-imaging synthetic aperture radar / Digital radiometer	SMAP (Soil Moisture Active Passive)	Radar (L-band) / Radiometer (L-band)	3 km (Radar) 40 km (Radiometer) 10 km (Radar and Radiometer)	~2-3 days	2015-present	O'Neill et al, 2010
Synthetic Aperture Radar (SAR)	Sentinel-1A	Radar (C-band)	1 km	6 days	2014-present	Hornacek et al, 2012

2.3 Soil Moisture from Hydrological Models

Hydrological models are simplified representations of the hydrologic system or its major parts (Lundin et al, 2000) and describe based on temporal and spatial features relationships between climate, water, soil and land-use (Jajarmizadeh et al, 2012). By simulating hydrological processes, known hydrometeorological variables such as rainfall and surface temperature can be used to derive unknown hydrological variables such as evapotranspiration or soil moisture (Musy et al, 2015). As various sectors are involved in the development and application of hydrological models, dealing for example with agricultural production, water supply, water withdrawal, erosion and sediment control, carbon fluxes, and climate change, it is an interdisciplinary research field, including many disciplines such as hydrology, geodesy, eco-climatology, and civil engineering. Central components of hydrological models include (Lundin et al, 2000; Vrugt et al, 2005):

- input data (e.g. available climate data on precipitation, solar radiation etc.), which drive the
- model equations, describing the complex hydrological system in a conceptualized and simplified way e.g. through water fluxes and storage processes
- model parameters, which control (as a volume knob in the radio) for example soil, land, climate, and river properties
- output data, which results from the processing and is finally used for certain applications.

In the context of hydrological modeling, model calibration refers to the process, during which indeterminable model parameters are adjusted in a way that the behavior of the model outputs are as closely and consistent as possible with observed hydrological responses over some historical time period (Vrugt et al, 2005). The match between modeled and observed parameters can also simply be done by tuning, using an adjustment factor (Sood and Smakhtin, 2015). Validation refers to the final testing of the calibrated and/or tuned model in terms of its capability to simulate realistic output data for an independent period of time (Lundin et al, 2000). As the hydrologic system is extremely complex and heterogenic, there is a large variety of types of models to describe hydrologic processes (Musy et al, 2015).

Hydrological models can be classified according to the concepts and mathematical methods, which are used in the model equations to define relationships between input and output variables. For example one can distinguish between physical modeling (hydrological processes are described by detailed physical equations), empirical modeling (hydrological processes are described based on observed relationships between input and output variables), and conceptual modeling (hydrological processes are described by a simplified representation of the hydrological system, conceptualizing important processes and transferring relationships between different hydrological components; Musy et al, 2015). Manifold further classification schemes exist as shown in “A Review on Theoretical Consideration and Types of Models in Hydrology” by Jajarmizadeh et al (2012). In this thesis the focus is on the practical purpose of hydrological models as their simulated output variables (specifically soil moisture and TWS) are of highest interest.

Spatial and temporal information on global soil moisture is generated by land surface models (LSMs, also named “Soil Vegetation Atmosphere Transfer schemes”) and by water balance models. Land surface models focus on interactions at the land surface and therefore simulate processes at the border between land and atmosphere and provide a link between hydrology and meteorology (Overgaard et al, 2005). The output parameters are related to the soil surface and include soil moisture, snow water, and canopy storage. Two examples of land surface models are the Global Land Data Assimilation

System (GLDAS; Rodell et al, 2004b), delivering information on soil moisture, canopy storage, and snow from 1979 to present, and the Land Dynamics World Model (LaD; Milly and Shmakin, 2002) accounting for snow, soil moisture and groundwater from 1989 until present.

Water balance models are based on the short-term water balance equation (Lundin et al, 2000), which tells that the runoff (R) is equal to precipitation (P) minus evapotranspiration (E) minus the change in TWS (ΔS):

$$R = P - E - \Delta S. \quad (2.6)$$

Thereby, the change in TWS is the sum of all changes in the hydrologic sub-components, including soil moisture, canopy storage, groundwater, surface waters in lakes, rivers and reservoirs, and snow and ice:

$$\Delta S = \Delta_{soil\ moisture} + \Delta_{canopy\ storage} + \Delta_{ground\ water} + \Delta_{surface\ water} + \Delta_{snow/ice} \quad (2.7)$$

The different water storage components are mostly estimated by calibrating them with respect to observed hydrological data as for example rainfall or streamflow data (Xu and Singh, 1998). As water balance models rely on the short-term water balance equation, they simulate in contrast to land surface models not only changes in specific storage components (which are related to the soil surface) but changes in TWS (which entail changes from all water storage components). For example, the WaterGAP Global Hydrology Model (WGHM; see Section 4.4) accounts for TWS by simulating soil moisture, groundwater, snow, canopy storage, and surface waters in lakes, rivers, wetlands, and reservoirs (Döll et al, 2003). The simulation of TWS is specifically valuable for this study as it is, besides soil moisture, the main parameter of interest.

Water balance models differ significantly among each other with respect to the amount of input data they require, their representation of hydrological processes (e.g. if parameters such as interception or deep percolation are considered) and their treatment of soil moisture and aquifer recharge. The described variety and heterogeneity in water balance models is discussed in more detail by Xu and Singh (1998). A detailed overview on recent global hydrological models is provided by Sood and Smakhtin (2015).

2.4 Validation

Soil moisture products from models or satellite remote sensing may contain errors due to problems in the retrieval or modeling algorithms, erroneous input data, limitations of the measurement device (e.g. decreasing sensitivity to soil moisture with increasing vegetation density) or external factors (e.g. RFI). The validation of soil moisture products is essential for the identification of error sources and impacting factors on the data quality. Results can inform users about the quality of a specific data set at their region of interest and about the performance of one specific soil moisture product in comparison to other soil moisture products (Leroux et al, 2013). This knowledge is also valuable for the generation of merged, superior multi-mission soil moisture data sets (Dorigo et al, 2010; Liu et al, 2011). Furthermore, information on error structures is important for the interpretation of variations and trends (Dorigo et al, 2010) and for the correct application of soil moisture data. Knowledge on data quality is also essential when assimilating soil moisture data into weather prediction (Drusch, 2007; Mahfouf, 2010) or runoff (Brocca et al, 2010, 2012) models.

Most commonly soil moisture products are validated with respect to in-situ measurements, which are point measurements at the location of interest and give information on soil moisture changes in absolute terms for local sites. The lessons learnt from one or more local study sites are then projected to larger regions. Traditional and emerging techniques for in-situ measurements of soil moisture are provided by Wagner (1998) and Ochsner et al (2013), respectively. Major in-situ validation sites in the USA include the Little Washita watershed in Oklahoma, Walnut Gulch in Arizona, Reynolds Creek in Idaho, and Little River in Georgia (Jackson et al, 2010). Those sites have been intensively used for the validation of AMSR-E data (Cosh, 2004; Cosh et al, 2006; Jackson et al, 2010) and also for the validation of SMOS data (Jackson et al, 2012). In Europe an extensive study has been made by Brocca et al (2011), who compared ASCAT and AMSR-E measurements with data of 17 in-situ stations in Italy, Spain, France, and Luxembourg. An intercontinental study was done by Albergel et al (2012), who evaluated soil moisture data from ASCAT and SMOS with respect to in-situ measurements from 200 stations, located in Africa, Australia, Europe, and the United States. A comparative study for soil moisture from models has been done by Kato et al (2007) who compared the soilwater content of the three GLDAS land surface models NOAH, MOSAIC and CLM with globally distributed in-situ data from the Global Energy and Water Cycle Experiment (GEWEX) at thirty field measurement stations.

Challenges associated with in-situ measurements are for example the high costs and efforts for maintenance and continuity of measurement stations, the need for standards to enhance consistency among sites, and the implementation of best practices for sensor calibration, installation, in-situ validation, data quality control, and data archiving (Ochsner et al, 2013). Furthermore, the heterogeneity of the landscape is often not reflected by the measurement sites (Ochsner et al, 2013) and there is a large difference in spatial scale when comparing several point measurements with one large satellite footprint (Miralles et al, 2010; Jackson et al, 2010) or a large modeled grid-cell area (Koster et al, 2009). Those challenges can partly be overcome by using harmonized data from well-equipped and continuously operating soil moisture networks. One of the main challenges remaining is the limited number of in-situ data in large parts of the world (see Section 2.1). There is specifically a lack of stations in the tropics, in dry areas and at high latitudes (Ochsner et al, 2013). In regions where there is no in-situ data the problem is a twofold: on the one hand in these regions data from models or satellites is specifically needed, on the other hand the quality of those data is often unknown as there is no ground truth for validation.

Specifically due to the limitation in spatial coverage of in-situ data, comprehensive global validation studies have mainly been done by the mutual comparison of different global soil moisture products from satellite sensors and hydrological models. This can be done for example by mathematical approaches such as statistical analysis (Dirmeyer et al, 2004), by triple collocation method (Scipal et al, 2008; Dorigo et al, 2010; Leroux et al, 2013) or by correlation analysis (de Jeu et al, 2008; Reichle et al, 2004; Liu et al, 2011, 2012; Al-Yaari et al, 2014).

Some essential results from these studies, comparing soil moisture data from various active and passive remote sensing products, are shown in Table 2.3. The table makes clear that the quality of satellite based soil moisture products largely depends on the land cover. The mix of different dielectric properties from manifold objects (as shown in Table 2.1) including trees and water surfaces is reflected in the microwave signal and makes the retrieval of soil moisture more difficult or even impossible. In the case of microwave remote sensing it is not possible to retrieve soil moisture over very dense forest, as the vegetation will absorb or scatter the radiation of the soil and at the same time emit radiation by itself (Jackson and Schmugge, 1991). This problem is very well known also from theory.

In other cases the reason of mismatch between data sets may remain unclear. For example it is often unknown to what degree deviating results from different satellite sensors are ascribed to the observation

principle (active versus passive) or to the applied retrieval algorithm (Dorigo et al, 2010). Also there is often no explanation for dispersed error patterns, which cannot be clearly linked to land cover or climate zones. The statistical analysis of satellite based soil moisture products might additionally be hampered as satellite missions and with it also their produced time series of soil moisture are short. Therefore, efforts have been made to merge different satellite products to receive long-term soil moisture records (Liu et al, 2012; Dorigo et al, 2012).

For soil moisture products from models main sources of errors include uncertainties in model structure, model parameters and input data (e.g. climate forcing, water use, land cover), and the lack of knowledge and understanding of relevant processes. Some of these sources of error can hardly be identified especially when fundamentally different models are compared (Müller Schmied et al, 2014). In the following some exemplary findings from validation studies of hydrological models, which are also partly integrating soil moisture data from satellites, are listed:

- Biemans et al (2009) showed that if the average uncertainty of precipitation inputs per river basin is about 30% (which was found when comparing seven global precipitation products), discharge uncertainties can reach about 90%.
- Guo and Dirmeyer (2006) analyzed the soil moisture outputs from eleven land surface models with respect to their sensitivity to different climate forcing data sets (especially to precipitation and radiation) and concluded that the uncertainty in knowledge of the drivers of the land surface climate might be as large as uncertainties which result from the use of different land surface models.
- Major differences among models, which were forced with the same set of climate data, were also identified in the study of Haddeland et al (2011).
- Gudmundsson et al (2012) analyzed nine large-scale hydrological models and identified a systematic decrease in performance from wet to dry runoff percentiles. They argue that this effect might be based on the fact that the relative magnitude of an absolute error value is higher for low river runoff values than for high river runoff values. Also they mention that incoming precipitation might be too quickly released, leading to underestimation of the lowest flow. Finally they conclude that the problem of worse and less consistent simulations of low flow is still not well understood.
- Dirmeyer et al (2004) compared eight global soil moisture products (three from global atmospheric reanalysis, three from land surface model calculations and two from microwave remote sensing) and found that in regions which are dominated by a strong seasonal cycle there is a better skill for simulating the mean annual cycle than for simulating soil moisture anomalies and that for regions with relatively weak annual cycle there is better skill for the simulation of soil moisture anomalies.
- Furthermore, the results of Dirmeyer et al (2004) show that the quality of soil moisture estimation decreases with poor or absent snow-melt modeling.

Reflecting on these results one can conclude that the global inter-comparison of various large-scale global soil moisture products has been helpful to identify error structures in soil moisture products from remote sensing and modeling. It provides in addition to validation studies with in-situ data valuable information for quality control. However, further studies are needed to understand dispersed error structures on regional scales and to investigate more deeply the underlying reasons for mismatches between different data sets.

Table 2.3: Challenges and limitations of active and passive microwave remote sensing of soil moisture.

Challenges	Passive Microwave Sensing	Active Microwave Sensing
Sparse to dense vegetation	From Jackson (2005): <ul style="list-style-type: none"> - Lower sensitivity to soil moisture - Observed emission from soil moisture decreases - Recorded emission from vegetation increases - Effects increase with increasing vegetation density / water content and decrease with increasing wavelength 	From Wagner (1998): <ul style="list-style-type: none"> - With increasing vegetation density or vegetation optical depth scattering effects from vegetation increase - Those include volume scattering within the canopy, attenuation of the send and backscattered signal by vegetation and multiple scattering by vegetation and soil surface
Very dense vegetation	- Soil moisture retrieval is not possible as the observed emissivity or backscattering is mainly due to vegetation (Owe et al, 2001)	
Intercepted moisture	- Dew or intercepted precipitation may decrease or increase the brightness temperature of the observed soil surface (Hornbuckle et al, 2007)	
Deserts	- There is reduced sensitivity to soil moisture as the variability of soil moisture is low (Dorigo et al, 2010) and the dielectric constant of bound water is extremely low (Jeu et al, 2008)	
		- Volume scattering effects of very dry sand and systematic surface roughness effects (Dorigo et al, 2010; Jeu et al, 2008; Scipal et al, 2008)
Surface roughness		- Significant at scales comparable to the wavelength as for example in sand deserts where winds form the shape and micro-relief of sand dunes (Stephen and Long, 2005; Bartalis et al, 2006)
Topographic complexity		- Low quality of soil moisture data (Draper et al, 2012; Dharssi et al, 2011) due to calibration errors and highly variable surface conditions, which are often coupled with snow, ice or dense forest (Bartalis et al, 2008)
Soil texture	- Fine clay (large surface area, much bound water) has generally a lower dielectric constant than coarse sand (small surface area, little bound water) (Jeu et al, 2008)	
Snow cover and frozen ground	- Affected regions have to be masked out, as the dielectric properties of snow and frozen water differ significantly from the ones of water (Wagner, 1998)	
RFI	- Causes signal contamination; soil moisture values artificially appear to be lower (Jeu et al, 2008; Oliva et al, 2012)	

2.5 Application

Large-scale soil moisture data have manifold applications in various disciplines. Table 2.4 describes potential fields of application, including agriculture, natural disaster monitoring and climate studies, and lists selected examples of scientific investigations in those fields. The different disciplines are interlinked as for example improved weather forecast is also beneficial for natural disaster monitoring, which is again of interest to the agricultural sector. It has been widely recognized that application possibilities of soil moisture products are not yet fully exploited and that further research is needed in this field. For example the “State of the Art in Large-Scale Soil Moisture Monitoring” of Ochsner et al (2013) states that there is a

“growing need to develop the science necessary to make effective use of the rising number of large-scale soil moisture data sets”.

They stress specifically the lack of research on the use of soil moisture data in ecological models (e.g. crop models) and in socioeconomic modeling and forecasting. Further potential fields of application for soil moisture products, which have hardly been explored, include famine early warning, wildfire forecast, and phenology.

The example of drought monitoring explains why the application of soil moisture products can be complex and an interdisciplinary challenge. Droughts can be divided in four classes: meteorological drought (reduction of precipitation), agricultural drought (shortage of available water for plant growth), hydrological drought (deficiency of surface and subsurface water supply), and socioeconomic and political drought (insufficient supply of water to meet the demand of economy and society; Wilhite and Buchanan-Smith, 2005; Zhang and Jia, 2013). Meteorological drought occurs more frequently and is together with hydrological drought most often assessed in studies, which focus on the analysis of hydrometeorological variables such as precipitation, soil moisture, and runoff. Meteorological drought normally triggers the other drought types (Wilhite and Buchanan-Smith, 2005). The analysis of agricultural and socioeconomic drought requires besides hydrometeorological data additional information from other disciplines. Social consequences depend for example on demographic factors and the preparedness of the population and are reflected by the number of people which are affected or killed by a drought. Economic consequences are influenced by the impact of the drought on trade and the supply of goods. The forecasting and monitoring of droughts with high impact on society through agricultural and economical loss or famine is therefore an interdisciplinary challenge, which requires the linking of manifold information sources from various disciplines. In case of transboundary events additional effort is required for the cooperation and coordination between governments and scientists (Lawrimore et al, 2002).

For satellite soil moisture products further open problems include the coarse spatial resolution (around 25 km, see Table 2.2), the lack of data continuity due to the short duration of satellite missions (which is planned to be overcome by the Sentinel-1 missions), and the lack of money and reward for keeping developed systems in operation (Ochsner et al, 2013). Furthermore, there is limited information on soil moisture at high latitude due to snow cover and frozen soil conditions (Loew et al, 2013) and no or limited information of soil moisture for densely vegetated regions (see Section 2.4). An advantage is the short data latency, ranging between a few hours for Level 1 products to about three days for Level 3 products (Wagner et al, 2014; O’Neill et al, 2010)

Also widely discussed (Ochsner et al, 2013; Seneviratne et al, 2010; Wagner et al, 2007) is the problem that satellites only deliver information on soil moisture in the thin near-surface layer rather than the entire profile, which is the targeted soil moisture zone for many fields of application (e.g. global

crop yield forecasts; Bolten et al, 2010). Several studies have demonstrated that the soil moisture at greater depth can be retrieved when assimilating surface soil moisture from satellites into land surface models (Walker and Houser, 2004; Heathman et al, 2003). Furthermore, simple algorithms exist which derive from surface soil moisture estimates of root zone soil moisture. One example is the so called soil water index (SWI; Albergel et al, 2008a; Wagner et al, 1999), which is based on an exponential filter and requires typically in-situ data for calibration (see Section 5.3).

For the application of large-scale soil moisture products from global hydrological models the coarse spatial resolution (about 0.5° to 2° ; Sood and Smakhtin, 2015) is also critical. Furthermore, hydrological models often have specifically in regions where modeled data is most valuable (due to lack of ground truth) low data quality to do missing input or reference data for validation or tuning. Also various models show large differences in their output parameters especially when it comes to the forecast of hydrological or climate variables (Dirmeyer et al, 2004; Haddeland et al, 2011; Gudmundsson et al, 2012). Large-scale soil moisture products serve as valuable input data to models as soil moisture contains in contrast to precipitation “memory” (wetness is retained in the soil) and is therefore temporally more persistent than information on rainfall events (Koster and Suarez, 2001).

Table 2.4: *Potential fields of application for large-scale soil moisture products and selected examples of scientific investigations in those fields.*

	Potential Fields of Application	Selected Examples of Scientific Investigations
Agriculture	<ul style="list-style-type: none"> - Irrigation and crop planting management, crop yield estimates, and crop insurance (Leese et al, 2001) 	<ul style="list-style-type: none"> - Assimilation of satellite surface soil moisture data from AMSR-E into a two-layer modified Palmer soil moisture model to estimate and forecast crop growth stage and condition for the global monitoring of agricultural yields (Bolten et al, 2010)
Natural Disaster Monitoring	<ul style="list-style-type: none"> - Operational drought monitoring, soil moisture indices (Ochsner et al, 2013) - Prediction of the location and temporal development of hydrologic extreme events and identification of their triggers in retrospect (Lundin et al, 2000) - Flood monitoring and forecasting, landslide and fire risk (Leese et al, 2001) - Initialization of models for the simulation or forecast of hydrology, sediment transport, and erosion (Leese et al, 2001) 	<p>Droughts:</p> <ul style="list-style-type: none"> - Characterization of the 2010–2011 Horn of Africa drought based on a merged soil moisture data set from microwave and thermal remote sensing, and physically based land surface modeling (Anderson et al, 2012) - Development of indicators for soil moisture extremes over agricultural regions in Canada based on AMSR-E data (Champagne et al, 2011) - Development of a new multi-sensor microwave remote sensing drought index over semi-arid regions based on TRMM, AMSR-E soil moisture, and AMSR-E surface temperature measurements (Zhang and Jia, 2013) - Development of the North American Drought Monitor (NADM) delivering monthly maps on short-term and long-term drought intensities based on five drought classes (Lawrimore et al, 2002) <p>Floods:</p> <ul style="list-style-type: none"> - Comparison of ERS scatterometer derived soil moisture with runoff data from the Zambezi River in Africa to assess the feasibility of assimilating soil moisture data into hydrological models (Scipal et al, 2005) - Development of a Soil Wetness Variation Index for the monitoring of soil moisture during flooding events (Lacava et al, 2005) - Assimilation of the root-zone or surface soil moisture product from ASCAT into a rainfall–runoff model and analysis of the model performance on flood estimation (Brocca et al, 2010; Brocca et al, 2012)
Climate	<ul style="list-style-type: none"> - Better understanding, identification, and validation of relevant processes related to soil moisture-climate interactions and feedbacks, also in the context of climate change (Seneviratne et al, 2010) - Initialization of models for the simulation or forecast of weather and climate (Leese et al, 2001) 	<ul style="list-style-type: none"> - Analysis of the role of soil moisture and vegetation state for the forecasting of weather over the central Great Plains and Rocky Mountain region, showing strong influence of initial soil moisture conditions on the seasonal evolution of weather (Pielke et al, 1999) - Use of soil moisture data from the Global Soil Wetness Project to specify boundary conditions in a land–atmosphere climate model, leading to improvement in the simulation of seasonal climate (Dirmeyer, 2000) - The multi-decadal satellite soil moisture data product is compared with soil moisture outputs from the Max Planck Institute for Meteorology Earth System Model and analyzed in terms of potential applications and limitations for climate model evaluation (Loew et al, 2013) - A review on the role of soil moisture for the climate system based on modeled and observed soil moisture data, focusing on soil moisture-temperature and soil moisture-precipitation feedbacks and their possible impact on climate change (Seneviratne et al, 2010)

2.6 Contribution of the Study

Figure 2.3 summarizes the challenges associated with the large-scale mapping of soil moisture, which have been mentioned in the previous sections. The figure is meant to give an overview on the large diversity of challenges at different levels (including e.g. the characteristics of soil moisture, limitations of available large-scale products, and the application and validation of those products), rather than to give a complete picture. Challenges associated with the development of hydrological models or soil moisture retrieval algorithms for different satellite sensors are not considered here. Out of the listed challenges this thesis addresses specifically the following issues:

Complex coupling with temperature, precipitation and evapotranspiration / Lack of knowledge and understanding of relevant hydrological processes / Lack of knowledge on the drivers of the land surface climate:

In contrast to other studies which focus for example on the link between soil moisture and precipitation, or soil moisture and evapotranspiration, this thesis links soil moisture to TWS (Section 7.2). In addition interdependencies with other hydrological parameters are analysed (Section 7.3). The aim is to better understand the interaction between soil moisture and TWS and their driving forces on large scales.

Difficulty to determine the reason of mismatch between different data sets (mapping technique vs. used retrieval or modeling algorithm):

In this thesis independent data sets from remote sensing, hydrological modeling and satellite gravimetry are compared (see Section 6.2 and see Section 6.3). The use of independent mapping techniques is of advantage for the interpretation of matches and mismatches among data sets as each mapping technique has different sources of error (e.g. hydrological models: input data; microwave remote sensing: mix of dielectric properties at the satellite footprint; satellite gravimetry: integral effect of various mass changes).

High spatial and temporal variability of soil moisture due to changes in land cover and soil texture / Dispersed error patterns are not well understood:

In this thesis the spatial resolution of all data sets is brought to a $1^\circ \times 1^\circ$ grid. Additionally, spatial patterns are smoothed by conversion into spherical harmonics and filtering (see Section 5.2). As a result of these processing steps the final spatial resolution of all data sets is much coarser than the original spatial resolution of the soil moisture data. The decrease in spatial resolution implies that the observed patterns map the large-scale component of soil moisture which refer to meteorological and climatic events. Those are for example related to precipitation and evapotranspiration patterns. The small-scale component of soil moisture is not mapped, which includes influences of vegetation, soil type and topography in the range of centimeters to hundreds of meters (Scipal et al, 2005). Therefore, dispersed small-scale patterns are differentiated from large-scale phenomena. This procedure is the converse of a widely used approach, which aims at an increase in spatial resolution to receive more detailed information on soil moisture patterns (Zhao and Li, 2013; Piles et al, 2011; Kim and Barros, 2002; Wu et al, 2014).

Spatial scales differ among mapping techniques:

In this study a procedure to harmonize the representations of different data sets on soil moisture and TWS is introduced. Throughout this procedure the spatial resolution of all data sets is unified and all data sets are processed and filtered in a harmonized way to achieve a comparable level of detail for all data sets (see Section 5.2).

Root zone varies over space and time / Mapped fraction of soil moisture differs among techniques / Remote sensing only provides surface soil moisture:

In this thesis only variations (and not absolute values) of soil moisture are analyzed. Furthermore, the temporal resolution is brought down to one month (see Section 5.2). By this means differences among soil moisture products, which are based on the varying characteristics of the sensed soil moisture volume (e.g. root zone vs. surface zone) are less prominent (Dirmeyer et al, 2004).

Coarse spatial and temporal resolution makes the application of soil moisture products difficult:

Due to their coarse spatial and temporal resolution, large-scale soil moisture products can hardly be used for e.g. small-scale agricultural monitoring or landslide and flashflood warning (as also mentioned in Section 5.7). Therefore, in this thesis large-scale soil moisture data are used to understand major drought and flood events, which had severe impact on society and are triggered by large-scale meteorological and climatic events such as the El Niño and La Niña phenomena (see Section 8.4).

Lack of interdisciplinary research, going beyond hydrometeorological analysis:

In this thesis not only hydrometeorological data is analyzed to assess extreme weather conditions. Additionally data from the International Disaster Database EM-DAT is integrated into the study which gives information on the socioeconomic impacts of natural disasters (see Section 4.7). Therefore, two totally independent data sets from different disciplines are linked (see Section 5.7).

Manifold fields of application are not yet exploited:

It has been clearly stated that specifically in the field of drought monitoring and socioeconomic modeling the use of satellite soil moisture products has not been fully exploited yet (Ochsner et al, 2013). By analyzing hydrological extreme events, such as floods, droughts and severe storms based on various soil moisture data sets and TWS from GRACE and by integrating information on the destructiveness of associated natural disasters (see Section 8.4) this study aims to contribute to a better understanding of soil moisture dynamics under extreme weather conditions and resulting social impacts.

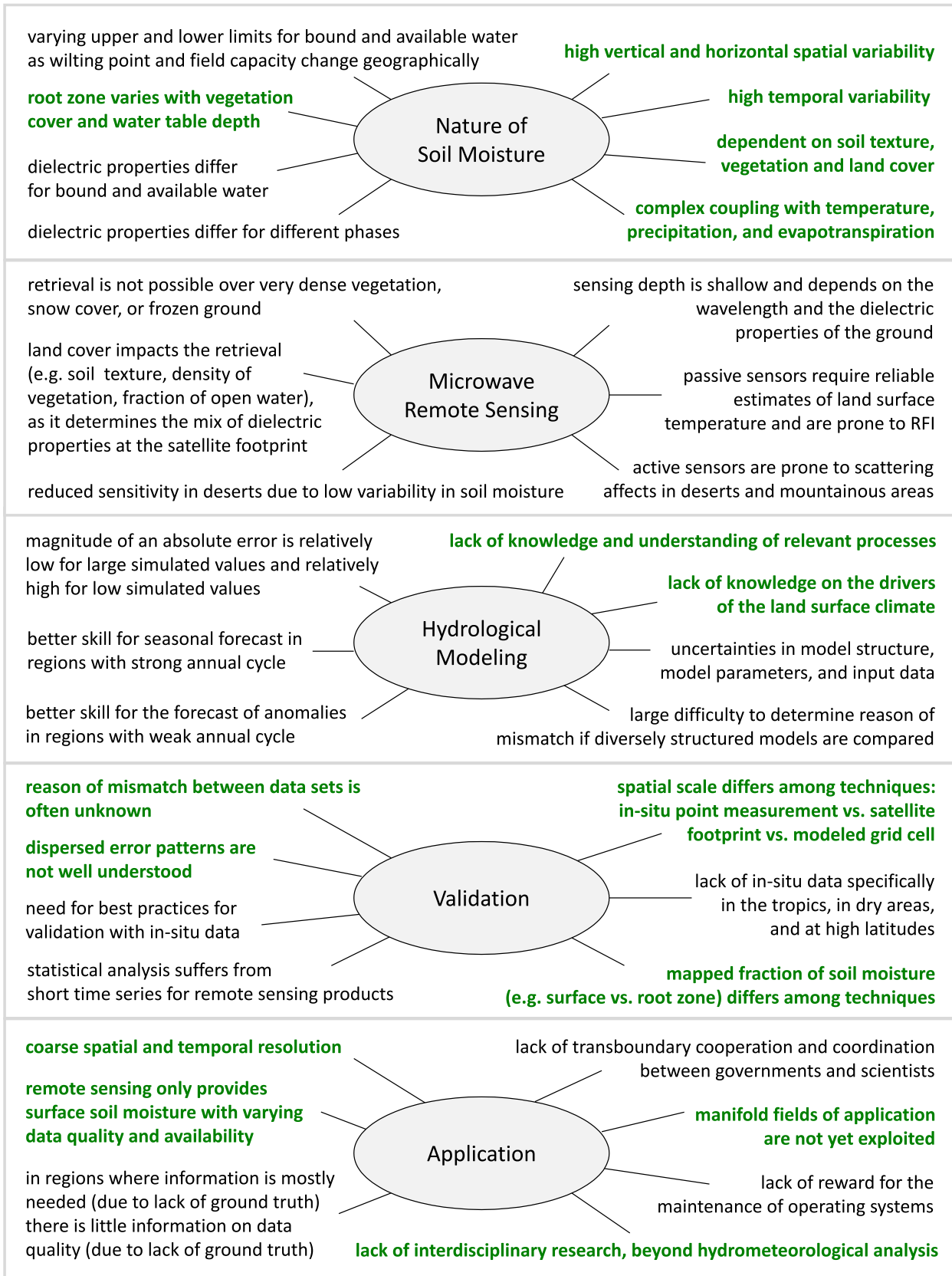


Figure 2.3: Examples of open challenges for the large-scale mapping of soil moisture with respect to the nature of soil moisture, the used retrieval technique (microwave remote sensing vs. hydrological modeling), and its validation and application; challenges which are mainly addressed in this thesis are highlighted in green.

3 Large-Scale Mapping of Terrestrial Water Storage

3.1 Introduction to Terrestrial Water Storage

Terrestrial water storage (TWS) refers to all water which is stored on and underneath the surface of the Earth (Syed et al, 2008). Main components of water storage encompass soil moisture, surface water (in rivers, wetlands, natural lakes, and man-made reservoirs), groundwater, snow, ice, and permafrost (Güntner et al, 2007). Further smaller components are biological water (water included in plants and animals; Shiklomanov, 1993) and canopy water storage (water which is stored on the surface of vegetation such as dew and intercepted precipitation; Syed et al, 2008). For studies focusing on water supply for irrigation, livestock or domestic use specifically the freshwater component is of interest, which makes up approximately 2.5% of the Earth's water masses (including oceans) and roughly 73% of continental water masses (percentages are derived from Shiklomanov, 1993). Figure 3.1 provides estimates of the volume of various components of TWS (here fresh and saline waters are not distinguished). Groundwater and frozen water in form of glaciers, ice and permafrost make up 50.8% and 48.8% of TWS, respectively. The remaining part (around 0.4%) originates by 85% from lakes, by 8% from soil moisture, by 5.5% from wetlands, by 1% from rivers and by 0.5% from biological water. Canopy storage is neglected here.

Although TWS is according to quantity dominated by groundwater and frozen water (specifically from glaciers and ice caps), smaller components also play a major role when changes in storage are considered. This is due to the fact that soil moisture and river runoff show higher fluctuations over a short period of time than groundwater or water captured in ice caps and glaciers. For example the residence time of groundwater and of ice caps, glaciers and permafrost is estimated to reach thousand years or more, which is much longer than the renewal period for soil moisture, which takes

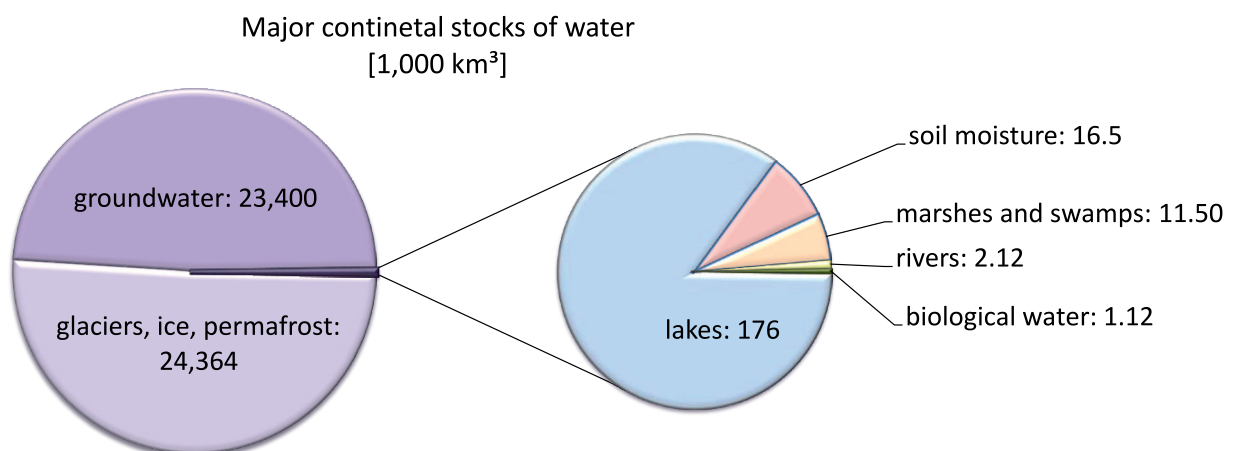


Figure 3.1: Major continental stocks of fresh and saline water with the unit 1,000 km³.

approximately 2 weeks to 1 year or the renewal period of water in river channels, which happens within a couple of weeks (UNEP, 2008).

The change in TWS is a key parameter in the continental water balance (as mentioned in Section 2.3 and expressed in Equation 2.6). It entails the fraction of precipitation, which reaches the Earth's surface and is neither evaporated nor drained through runoff to the ocean (Schmidt et al, 2006c). The change in TWS affects weather and climate and accounts for geophysical phenomena through the redistribution of water masses on Earth, causing changes in the Earth's gravity field (Wahr et al, 1998), the Earth's rotation (Fernández et al, 2007) and the elastic deformation of the Earth's surface (Bevis et al, 2005). By playing a part in the Earth's water, energy, and biogeochemical cycles, TWS affects our climate, contributes to sea level variation, and influences carbon, nutrient, and sediment cycles (Harding et al, 2011).

The contribution of various water storage components to the change in TWS is specific to the site. For example groundwater shows naturally low variation in large regions with recharge lower or equal to $\leq 5 \text{ mm yr}^{-1}$ (e.g. in the High Plain aquifer in the United States, the Nubian sandstone aquifer system in southern Africa, and the Great Artesian basin in Australia; Taylor et al, 2013). Human induced changes through water extraction and irrigation may cause much larger changes in groundwater storage. For example during a major drought in the Central Californian Valley extraction rates exceeded replenishment rates, leading to a decline in the water table from the beginning of October 2006 to the end of March 2010 by roughly 57 mm yr^{-1} (Scanlon et al, 2012). This illustrates that the components which dominate the water balance have to be identified specific to the region of interest. Also the temporal scale plays a role as for example fractions of snow and ice cover as part of TWS vary with the season.

Despite its fundamental role in the Earth system, until the early 2000s observations on TWS were deficient (Rodell and Famiglietti, 2001; Seneviratne et al, 2004). Changes in TWS can be estimated from gravimetric in-situ measurements. For example superconducting gravimeters have been used to map changes in TWS over Central Europe (Crossley et al, 2012). However, as in-situ measurement sites are sparse and unevenly distributed, they are not suitable to map changes in TWS on global scale with a spatial resolution of a few hundred kilometers (Crossley et al, 2012). Further problems include impacts from vertical ground motion (Van Camp et al, 2005) and complex gravity responses from stations below the ground surface (Crossley et al, 2012).

In addition to the possibility of measuring TWS in the aggregate, it is also possible to calculate TWS from the sum of all relevant storage components. This implies that all components need to be mapped individually to finally compute their total sum. In-situ measurements of the various storage components are up to date not available on global scale, specifically for groundwater (Seneviratne et al, 2004; Famiglietti et al, 2015). Furthermore, several problems are associated with the use of in-situ data for large-scale studies (as described in Section 2.4 for in-situ measurements of soil moisture). Those include high costs and high time consumption for the maintenance of in-situ stations. Also there is the need to bring point observations into spatially continuous data, resulting in high errors from statistical interpolation specifically in regions far away from observation sites (Jiang et al, 2014) or in heterogeneous environments.

An alternative to in-situ measurements is the gathering of information from various remote sensing products for example for soil moisture (Wagner et al, 2013; Njoku et al, 2003; Kerr et al, 2010), snow cover (Gao et al, 2010; Nolin, 2010), surface waters (Calmant et al, 2008; Singh et al, 2012), and vegetation water content (Gao, 1996; Yilmaz et al, 2008). However, several products do not map the total water mass of each component (Tang et al, 2009). Up to the present for soil moisture only the surface zone (Escorihuela et al, 2010; Schneeberger et al, 2004) and for surface waters only the spatial

extent (Kravtsova and Tarasenko, 2010; Sawaya, 2003) or variations of the water level (Calmant et al, 2008; Schwatke et al, 2015) can be captured. Furthermore, data quality is an issue because for some data products it is not homogeneous in space. For example data quality may decrease with increasing vegetation cover as it is the case for products of snow cover (Nolin, 2010) and soil moisture (see Section 2.4) from microwave sensors. The assessment of various spatially and temporally distributed error sources from different storage components is therefore challenging. Most critically is the lack of comprehensive information of groundwater, which can up to the present not be mapped individually from space (Jiang et al, 2014).

Two other widely used sources, providing information on TWS, are hydrological models and gravimetric measurements from satellites. Both approaches will be described in detail in the two following sections.

3.2 Terrestrial Water Storage from Satellite Gravimetry

The mapping of the Earth's gravity field via satellites is referred to as satellite gravimetry. Changes in the Earth's gravity field arise from the redistribution or exchange of mass in the Earth's system (Rummel, 2005). They reflect for example density anomalies in the lithosphere and the mantle, the dynamic ocean topography (in combination with satellite altimetry data), and hydrological mass changes over the continents (Rummel, 2005; Ramillien et al, 2008).

The Earth's gravity field is commonly expressed by the gravity potential which is the sum of the normal gravity potential (being the potential of a rotating ellipsoid approximating the Earth's shape, mass and rotation) and a disturbing potential (Xu et al, 2007). As the normal gravity potential can be derived analytically, satellite gravimetry missions mainly aim to provide information on the disturbing potential T , which is most commonly represented by a series of spherical harmonic coefficients (Heiskanen and Moritz, 1967; Rummel et al, 2002):

$$\begin{aligned} T(r, \varphi, \lambda) &= \frac{GM}{R} \sum_{l=2}^L \left(\frac{R}{r}\right)^{l+1} \sum_{m=0}^l (\overline{C}_{lm} \cos m\lambda + \overline{S}_{lm} \sin m\lambda) \overline{P}_{lm}(\sin \varphi) \\ &= \frac{GM}{R} \sum_{l=2}^L \left(\frac{R}{r}\right)^{l+1} \sum_{m=-l}^l K_{lm} Y_{lm}(\varphi, \lambda), \end{aligned} \quad (3.1)$$

where:

$\overline{P}_{lm}, Y_{lm}$	real and complex valued Legendre functions of degree l and order m , resp.
$\overline{C}_{lm}, \overline{S}_{lm}, K_{lm}$	spherical harmonic coefficients, where K_{lm} is the complex form of \overline{C}_{lm} , and \overline{S}_{lm}
G, M	gravitational constant and mass of the Earth
R	Earth's mean radius
$\left(\frac{R}{r}\right)^{l+1}$	field attenuation with altitude
r, φ, λ	spherical coordinates at the point of interest
l, m	spherical harmonic degree and order

The series coefficients \overline{C}_{lm} and \overline{S}_{lm} are the gravity field unknowns which are to be determined from gravity field observations. The spherical harmonics are usually truncated at the maximum resolvable degree to receive finest spatial information (Rummel et al, 2002). Figure 3.2 shows how degree and order of truncation impact the spatial resolution and the amplitude of TWS anomalies.

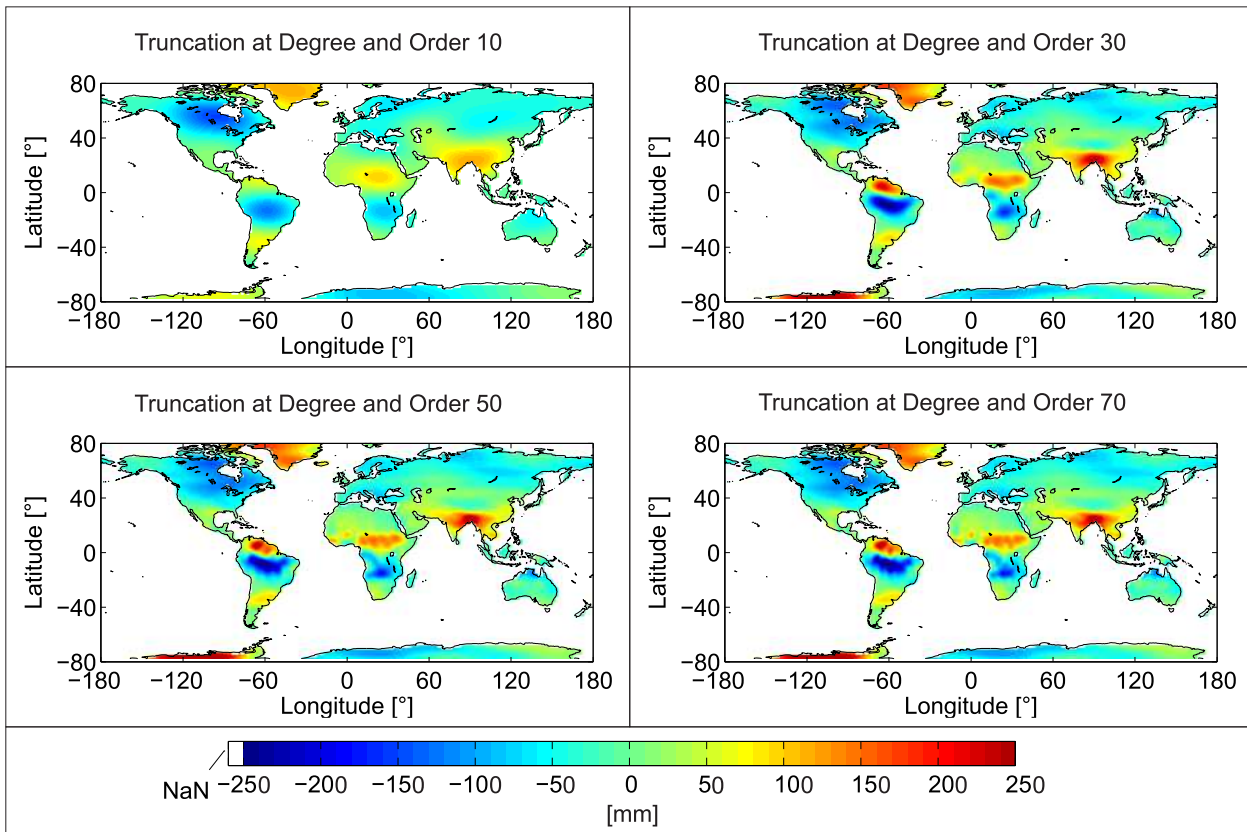


Figure 3.2: Impact of degree and order of truncation on amplitude and detail of TWS anomalies for August 2007 from GRACE data (five year mean from 2007-2012 has been subtracted), which have been filtered with a least-squares polynomial filter and smoothed with a Gauss filter of 300 km half-wavelength radius (the filtering is described in detail in Section 5.2).

The measurement of the change in TWS through satellite gravimetry is based on the assumption that mass changes over the continents mainly arise from the redistribution of water masses, when considering monthly to decadal time scales (Ramillien et al, 2008). However, this assumption is only valid if the signal is corrected for well-known and well-modeled signals from solid Earth and ocean tides, and atmospheric and ocean dynamics (Sakumura et al, 2014). Furthermore short-term non-hydrological mass changes need to be insignificant. Non-hydrological mass changes include for example those arising from post-glacial rebound (PGR) (Purcell et al, 2011; A et al, 2012), earthquakes (Fuchs et al, 2013), and erosion (Schnitzer et al, 2013). An overview on the magnitude and spatial resolution of different mass changes is provided by (Rummel, 2005).

As the absolute gravity signal is not only impacted by water masses but by all kinds of masses on the Earth's surface and its interior, it is not possible to obtain information on the absolute amount of water storage from satellite gravimetry. Only relative water mass changes with respect to some references value (e.g. long-term mean of the gravity signal) can be derived. Another limitation is that the measured relative mass change does not provide any information on the origin of mass change, meaning the contribution of individual hydrological storage components to the measured vertically-integrated water storage change (Cazenave and Chen, 2010). It requires ancillary information to define whether the mass change was caused for example by a change in surface water or groundwater or a non-hydrological process such as PGR (Wahr et al, 2006).

Satellite-to-satellite tracking (SST) and satellite gravity gradiometry (SGG) are two state of the art techniques to measure the Earth's gravity field with high precision (Rummel et al, 2002). SST relies on the fact that the satellite orbital motion is largely affected by gravitational force in addition to non-conservative forces (such as air drag). When passing over mass anomalies in Low Earth Orbit (LEO), the satellite orbit is disturbed, which provides indirect information on the gravity field. There are two techniques of SST. On the one hand there is high-low satellite-to-satellite tracking (SST-hl), where the position and the velocity of a satellite in LEO are tracked by global navigation satellites. An accelerometer onboard the LEO satellite accounts for non-gravitational forces. On the other hand there is low-low satellite-to-satellite tracking (SST-II), which employs two identical satellites in the same LEO. When the first satellite approaches a positive mass anomaly, the satellite is accelerated and the distance between the satellites increases. When the second satellite also approximates the mass anomaly it is also accelerated and the distance between the satellites decreases again. Based on this concept, the Earth's gravity field is then derived from the relative motion of the two satellites and the rate of change of the inter-satellite distance (Tapley et al, 2004).

SGG makes use of ideally three pairs of highly sensitive accelerometers, which are placed close to the satellite center. They measure acceleration differences in all three spatial direction over the short baselines of the gradiometer instrument (Rummel et al, 2011). From those measurements information on the Earth's gravity field can be derived as non-gravitational accelerations ideally drop of when taking the differences in gravitational acceleration at the test mass locations (Rummel et al, 2002). A more detailed description and graphical representation of SST-hl, SST-II, and SGG is given by Xu et al (2007) and Rummel et al (2002).

Due to the special mission design, such as the configuration of twin satellites (Wahr et al, 1998), the processing of satellite gravimetry data, does not only involve the correction of unwanted mass changes but also the filtering of the output data. Filters are used for example to suppress noisy high-resolution coefficients and to remove correlations between certain spherical harmonic coefficients (Swenson and Wahr, 2006, see Section 4.3). However, filtering does not only decrease the level of noise but also results in damping of signal (Landerer and Swenson, 2012). Furthermore, it may lead to leakage from outside of the region of interest, decrease in spatial resolution, and phase shifts in time series. Therefore, one main challenge in filter design is the balance between signal to noise ratio and spatial resolution (Werth et al, 2009).

Table 3.1: *Dedicated gravity field satellite missions, including CHAMP (CHALLENGING Minisatellite Payload), GRACE (Gravity Recovery And Climate Experiment), and GOCE (Gravity and Ocean Circular Exploration).*

Mission	Operation Time	Mapping Principle	Spatial Resolution	Reference
CHAMP	2000-2010	SST-hl	350 km (static)	Reigber et al, 1999
GRACE	2002-present	SST-II, SST-hl	275 km (static)	Tapley et al, 2004
			300 km (time-variable)	
GOCE	2009-2013	SSG	100 km (static)	Rummel et al, 2011

Recent dedicated gravity field satellite missions are listed in Table 3.1. The satellite mission CHAMP was the first dedicated satellite mission for the global mapping of the Earth's gravity field and improved previous gravity field models by about one order of magnitude (Reigber et al, 2003). GOCE is the most recent mission and has been designed to significantly increase the accuracy and the spatial resolution of the static gravity field (Rummel et al, 2002). In contrast to CHAMP and GOCE, the satellite mission GRACE focuses specifically on changes in the Earth's gravity field and not its static features. Therefore, it is the most relevant mission for this study, which focuses on inner-annual changes in TWS. The GRACE mission is described in more detail in Section 4.3.

3.3 Terrestrial Water Storage from Hydrological Models

A description on the basic principles and the main components of hydrological models as well as on their large diversity and different classification schemes has already been given in Section 2.3. Also global water balance models have been introduced, as possible source for estimates of soil moisture and TWS. In contrast to land surface models, which mainly have been developed to calculate fluxes from land to atmosphere for the purpose of climate modeling (Cazenave and Chen, 2010) those models focus specifically on closing the water balance for the area of interest and take account of all significant storage components (Güntner, 2008).

Regarding the global mapping of TWS there is in general a low comparability among hydrological models. Significant differences exist in the selection of storage components which are aggregated to represent TWS. For example GLDAS (Global Land Data Assimilating System; Rodell et al, 2004b) does not simulate groundwater and surface water stocks, as it only accounts for canopy storage, snow water and soil moisture. This may explain why GRACE observations and GLDAS estimates do not agree well in some large river basins, like the Amazon basin, where surface water and groundwater play a major role (Chen et al, 2009). Furthermore, a lack of delayed dynamics in a model (for example the lack of groundwater) may lead to an artificial earlier phase of seasonal storage dynamics (Yamamoto et al, 2007). In contrast to GLDAS, LaD (Land Dynamics World model; Milly and Shmakin, 2002) accounts (besides for snow and soil moisture) for groundwater. WGHM is different again as it simulates groundwater and surface water and various other storage components.

But not only the combination of storage components differs among models. There are also discrepancies for the simulation of individual storage components. For example while WGHM simulates soil moisture for only one layer of varying depth (depending on the rooting depth of vegetation), GLDAS provides information on 3 to 10 vertical layers, depending on the specific model (CLM: 10 layers, Mosaic: 3 layers, NOAH: 4 layers, VIC: 3 layers) as described by the Goddard Earth Science Data and Information Service Center (disc.gsfc.nasa.gov/hydrology/data-holdings/parameters/).

Despite those differences it has been found that in general hydrological models perform well in mapping seasonal dynamics and their continental-scale spatial patterns, accounting in most basins for 70-80% of the total signal (Cazenave and Chen, 2010; Güntner, 2008; Jiang et al, 2014). Larger differences were found for inter-annual variations and regional solutions for example due to erroneous precipitation data, systematic model biases, missing storage components in the simulation, and inadequate snow modeling. When being compared with GRACE poor correspondence may be based on signal leakage, aliasing effects, and stripe like features from GRACE. Furthermore, comparability is only given if GRACE and modeled data are filtered in a similar manner (Güntner, 2008).

Considering the scope of this study (combination of global data of TWS and soil moisture), the following aspects of hydrological models, addressing specifically the modeling of TWS, are essential:

- The scale of the model; e.g. does the model provide results for all major river basins of the world or just for a selection of basins?
- The number of sub-components modeled; e.g. does the model provide individual estimates of the main storage components (here specifically soil moisture is of interest) and then derives TWS from the sum of all components or is TWS calculated as an aggregate value?
- The purpose of the model; are all main components considered or is the focus on only one or two main components or on the calculation of fluxes from land to atmosphere?
- Comparability with GRACE; has the model been validated with other reference data and specifically with GRACE data?

One global water balance model, which meets the listed criteria, is WGHM (Döll et al, 2003; Müller Schmied et al, 2014). It provides global estimates of TWS for the world's major river basins for all continents except for Antarctica and simulates all storage components individually (other than e.g. the Basin-Scale Water Balance dataset from ETH Zurich; Mueller et al, 2011; Seneviratne et al, 2010). By simulating soil moisture, groundwater, snow, ice, canopy storage, and surface waters (including lakes, rivers, and reservoirs), it distinguishes between more components and sub-components than other models as for example the ISBA-TRIP (Interactions between Soil, Biosphere, and Atmosphere-Total Runoff Integrating Pathways) Continental Hydrological System, calculating TWS as the sum of soil moisture, snow water equivalent, vegetation interception and stream water content (Alkama et al, 2010). The purpose of WGHM is to assess water availability and water use at global scale for all main freshwater sources. Therefore, the focus is not only on one specific parameter.

Results of TWS from WGHM have been validated with various other data sources as for example independent rainfall measurements (Crossley et al, 2012), outputs of other hydrological models (Crossley et al, 2012; Jin and Feng, 2013) and GRACE (Schmidt et al, 2006a; Papa et al, 2008; Crossley et al, 2012; Forootan et al, 2012). Although soil moisture data from satellites could contribute to the validation and calibration of WGHM outputs (Werth, 2010), not much research has focused on this topic, yet. A detailed description on WGHM is provided in Section 4.4.

3.4 Validation

The quality of TWS estimates from hydrological models varies in space and time as it is strongly influenced by the quality and availability of adequate data for driving, tuning, calibrating, and validating the model (Güntner, 2008). One main factor causing erroneous modeling results is unrealistic precipitation data (Döll et al, 2003). Due to the lack of in-situ measurements for various storage components over large regions of the world (e.g. for soil moisture and groundwater, see Section 2.1 and Section 3.1, respectively), in the past hydrological models have been mainly validated with respect to river discharge, which is available for the world's largest river basins (Werth and Güntner, 2010). However, this validation only does not ensure that the partitioning between different components in the water cycle has been done correctly. Although GRACE data does not provide information on the change of individual storage components, it provides information on the integral change of all storage components, which is not reflected in river discharge. This is why GRACE data are valuable for the validation of modeled TWS data (Güntner, 2008; Jiang et al, 2014). Apart from the problem of data availability, models may also be deficient as they rely on assumptions and simplification of reality (Reager et al, 2015) and are limited by computational capability (Rodell and Famiglietti, 2001).

Also TWS estimates from satellite gravimetry are error-prone as the underlying processing is complex and requires various corrections (e.g. orbital corrections, removal of atmospheric masses and influences of tides and PGR) and filtering of the signal (e.g. to remove longitudinal stripes; Kerr et al, 2010, see Section 3.2).

Information on data quality is essential for researchers for the reliable interpretation of hydrological variations and trends (see Section 2.4). It helps users to choose the data product with the highest quality in their region of interest. This is specifically useful for GRACE data, as various GRACE solutions and filtering techniques exist. This complicates for non-experts the selection of the optimal product (the recommended average product of the three standard solutions from JPL, CSR, and GFZ is not yet available as stand-alone product but is promised to go online soon; JPL, 2015), and the selection of the optimal filtering technique for a specific application.

The comparison of TWS products is furthermore helpful to developers of hydrological models and developers of processing algorithms for GRACE, as they need to validate different TWS products to improve their modeling algorithms or filtering techniques. As this study focuses on the link between soil moisture and TWS, here validation studies, which address hydrological and application oriented aspects, are of major interest, rather than studies which investigate different processing techniques.

Due to the integrative nature of TWS, it is specifically challenging to validate large-scale TWS measurements with in-situ measurements. Gravimetric in-situ measurements provide aggregate information on TWS, but are not suitable to validate changes of TWS on global scale (see Section 3.1). Alternatively in-situ measurements from different storage components need to be linked to present in sum TWS. Also in this case data availability and quality are insufficient on global scale. Nevertheless, information from individual in-situ sites or large in-situ networks is highly beneficial for local studies. The use of remote sensing products of individual storage components is mostly limited by the lack of information on groundwater dynamics. Therefore, the global validation of TWS products is mainly done by the comparison of various global data sets from hydrological models and satellite gravimetry (Swenson and Wahr, 2006).

There are manifold methods which are applied to validate TWS products. Many studies perform a simple visual comparison of global maps and basin-averaged time series. Quantitative measures include the computation of bias (Klees et al, 2006), root-means square differences (Landerer and Swenson, 2012), and the computation of correlation values (Ngo-Duc et al, 2007; Long et al, 2013) for monthly time-series or spatial patterns of GRACE and modeled data. Furthermore, Taylor diagrams, combining standard deviations and correlation have been used (Ngo-Duc et al, 2007; Xiao et al, 2015) as well as principal (Frappart et al, 2013a; Rangelova et al, 2007) and independent component analysis (Frootan et al, 2012; Frappart et al, 2011).

There are two different approaches which are used for the validation of TWS products. In the first approach TWS information from one data source is compared with TWS information from another data source (e.g. TWS from one model is compared with TWS from another model). Although in general it is assumed that the comparability among TWS data sets is high, it has to be considered that storage components, which are aggregated to TWS, may differ among models. Additionally there might be difference in the modeling of individual storage components (see Section 3.3). A detailed list of numerous studies focusing on the comparison of different TWS products from hydrological models and GRACE is provided by Güntner (2008).

In the second approach TWS is analyzed with respect to a selection of storage components, which are assumed to dominate the signal or influence it in a significant way. For example, in a region which is covered by a glacier it is assumed that the dominating trend in TWS is primarily caused by changes

in the mass of the glacier and therefore TWS is compared to information on changes in the ice mass. In the following all major water storage components are listed and studies are described, which relate TWS to the respective water storage component:

Surface Waters:

- Comparison of changes in surface water extent in six large river basins with respect to precipitation, water level changes, variations in TWS and surface water from WGHM, and variations in TWS from GRACE (Papa et al, 2008).

Rivers:

- Comparison of variations in TWS from various models and GRACE with respect to precipitation data and records of river gauging stations in the Amazon River basin (Chen et al, 2009).
- Comparison of various GRACE products with respect to in-situ river level and discharge data sets in South America (Frappart et al, 2013a).

Lake:

- Comparison of water volume changes and river discharges for Aral Sea with respect to changes in TWS from GRACE (Singh et al, 2013).

Reservoirs:

- Comparison of changes in reservoir storage with respect to TWS from GRACE, and TWS from WGHM and with respect to soil moisture and snow water equivalent from GLDAS in the lower Nile basin and the Tigris Euphrates basin (Longuevergne et al, 2013).

Soil Moisture:

- Comparison of global changes in TWS from GRACE and WGHM with global changes of soil moisture from WGHM and ASCAT via correlation analysis (Abelen and Seitz, 2013).
- Comparison of changes in TWS from GRACE and WGHM with changes of soil moisture from WGHM and AMSR-E in Central Asia via principal component analysis (Abelen et al, 2011).

Groundwater:

- Comparison of seasonal variations of TWS from GRACE with in-situ groundwater observations and modeled soil moisture from a land surface model in the High Plains Aquifer, USA (Strassberg et al, 2007).

Snow:

- Comparison of GRACE mass trends with measurements of snow from remote sensing (ICE-Sat) and snow-stakes (Yamamoto et al, 2008).

Ice / Glaciers:

- Comparison of glacier mass changes from GRACE with glacier mass changes derived from satellite altimetry in the St. Elias Mountains (Arendt et al, 2008).

The list shows that almost all storage components have been directly compared with TWS. One exception is vegetation water content, as the seasonal amplitude of biomass changes just lies within

the sensitivity limits of GRACE (Rodell et al, 2005). Another special case is soil moisture. Although it is used in many studies as complementary source of information (primarily in the form of in-situ data), studies which focus primarily on soil moisture and TWS are lacking. Specifically remote sensing products of soil moisture are hardly exploited when analyzing TWS signatures, although they provide the opportunity to analyze spatial and temporal patterns of both parameters on global scale.

Studies from the past reflect that since the early phase of the GRACE mission, soil moisture has not been in the focus of research when investigating GRACE data. For example Güntner (2008) provided a table on TWS related studies. The table lists 42 studies which deal with the analysis and validation of TWS estimates from GRACE and hydrological models. None of these studies focus specifically on TWS and soil moisture but they are devoted to the comparison of various TWS products, the relation between TWS and evapotranspiration, snow, groundwater, or glacial isostatic adjustment, and the processing, filtering, and modeling of TWS data.

One reason for the little interest in the direct comparison of TWS and soil moisture is that its seasonal amplitude seems to be relatively low with respect to other storage components. This would imply that soil moisture is rarely the dominating component of TWS (this issue is discussed in detail in Section 7.1). However, soil moisture may still be closely linked to other dominating storage components and therefore show high agreement with changes in TWS (Abelen and Seitz, 2013).

3.5 Application

“GRACE provides an unprecedented opportunity to improve quantification, understanding, and simulation of TWS variability. Yet the fact that GRACE measures water at all depths simultaneously is also a challenge, and its spatial and temporal resolutions are coarse by any standard of earth science data.” (Zaitchik et al, 2008)

The quote of Zaitchik et al (2008) reflects that the application of TWS data has two facets. On the one hand specifically GRACE data have manifold limitations. Those include in particular the coarse spatial (300 km to 500 km) and temporal (monthly) resolution, the integrative nature of the signal (Seneviratne et al, 2010), and the latency of 2- to 6-month before GRACE data are released (Famiglietti and Rodell, 2013). Also no absolute but only relative values of TWS can be derived and the sensitivity of GRACE is limited (best estimates are around 25 mm at a spatial resolution of 340 km; see Section 4.3). Further problems arise from the complex data processing and filtering (see Section 3.2) which complicates the analysis and use of GRACE products, specifically for non-experts that are not familiar with the manifold GRACE solutions.

On the other hand GRACE data has been proven to deliver valuable information for many fields of application, which profit from a better understanding of the terrestrial water balance and its role in the global hydrologic cycle (Syed et al, 2008; Cazenave and Chen, 2010). In the following examples of fields of application for TWS data are listed:

Drought / Flood:

- Mapping of intense drought and subsequent flooding in large parts of western and southern Amazonia between mid-2005 and mid-2006 using regional four-dimensional gravity field solutions from GRACE (Schmidt et al, 2008a).
- Mapping of extreme weather fluctuations including droughts, excessive rain, snowfall, and flooding in Central Europe by using GRACE data (Seitz et al, 2008).

- Mapping and quantification of changes in TWS during droughts and floods in the Amazon basin and demonstration of interrelations with periods of La Niña and El Niño (Chen et al, 2010a).
- Using TWS changes of GRACE as drought indicator for the one-year drought in Texas in 2011 (Long et al, 2013).

Groundwater Extraction / Groundwater Change:

- Estimation of groundwater depletion in India using TWS change observations from GRACE (Rodell et al, 2009).
- Analysis of the impact of water withdrawals from groundwater and surface water on TWS as reflected in data from WGHM and GRACE (Döll et al, 2012).
- Detection of groundwater storage change within the Great Lakes Water Basin using GRACE (Huang et al, 2012).

Ice-Sheet Melting / Sea Level Rise:

- Investigation of the contribution of ice sheet melting in Antarctica and Greenland to sea level rise using GRACE data (Ramillien et al, 2006b).
- Detection of increasing rates of ice-mass loss and glacier dynamics of Greenland and Antarctic ice sheets based on GRACE (Velicogna, 2009; Shepherd et al, 2012).
- Measurement of land ice changes in the Antarctic outlet glaciers by combining GOCE gravity gradiometry observations with GRACE gravity data (Bouman et al, 2014).

Disaggregation:

- Use of GRACE measurements to derive high latitude snow mass anomalies using an inverse approach to separate soil waters from the snow signal (Frappart et al, 2006).
- Comparing in-situ measurements of groundwater with the disaggregated groundwater storage estimates from GRACE (for the disaggregation information on snow water equivalent, surface water reservoir storage and soil moisture storage from GLDAS are used; Scanlon et al, 2012).
- Assessment of changes in groundwater storage by disaggregating TWS from GRACE into individual storage components using estimates of surface water, soil moisture, snow, ice, and canopy storage from WGHM and GLDAS (Jin and Feng, 2013).

Assimilation:

- GRACE data are integrated into the Catchment Land Surface Model to improve model performance at sub-observation scale for groundwater and runoff simulation (Zaitchik et al, 2008).
- GRACE data are integrated into a numerical model of land surface and energy processes to derive information on groundwater and soil moisture, which serve as drought indicators (Houborg et al, 2012).
- Assimilation of TWS from GRACE in the snow-dominated Mackenzie River basin in northwest Canada (Forman et al, 2012).

Estimation of Vertical and Horizontal Fluxes:

- Estimation of evaporation rates over major river basin, using the water balance equation (Rodell et al, 2004a; Ramillien et al, 2006a).
- Estimation of river discharge by combining GRACE data with ancillary data sets and models (Syed et al, 2005).

The examples show that specifically the modeling, mapping, and quantification of TWS changes under extreme weather and climate conditions is under investigation. As in the case of soil moisture the main focus is on the comparison and analysis of hydrometeorological variables and events. Links to social and economic impacts are hardly provided.

Another study area is the investigation of individual storage components by disaggregation and assimilation of TWS data. This addresses the often mentioned limitation of receiving only aggregate information from GRACE. Various studies have shown that the assimilation of GRACE data, can improve the skill of hydrological models and that there is still a large potential for progress in the future (Güntner, 2008).

Another open challenge is the integration of GRACE data into operational decision support systems for water management (Famiglietti and Rodell, 2013). First attempts have been made to integrate GRACE data into the operational U.S. and North American Drought Monitor by developing drought indicators which are based on the assimilation of GRACE data into land surface models (Zaitchik et al, 2008). Furthermore, the European Union's Horizon 2020 research and innovation programme is funding the project European Gravity Service for Improved Emergency Management (EGSIEM; www.egsiem.eu/) which started in January 2015 and aims to demonstrate that TWS products from the current and the follow-on GRACE missions can be used for flood and drought monitoring and forecasting. Those efforts are only at the beginning. New processing algorithms, which improve the temporal and spatial resolution of GRACE data, and future satellite missions, delivering higher resolution and near-real time data may drive progress forward.

3.6 Contribution of the Study

Figure 3.3 shows main challenges which are associated with the large-scale mapping of TWS as summary of the previous sections. The figure shall highlight the diversity of challenges for different fields of research (characteristics of TWS, satellite gravimetry, hydrological modeling, validation and application). As for Figure 2.3 the objective is not to provide a complete picture of all existing problems. Challenges which are associated with the development of hydrological models or retrieval algorithms for satellite gravimetry are not mentioned. Out of the listed challenges the following ones are primarily addressed in this thesis:

TWS is highly complex by being the sum of all water storage components / Significance and characteristics of individual storage components vary in space and time / The source of mass change as sensed by GRACE is unknown:

This study focuses specifically on soil moisture and its direct and indirect connection to TWS (see Chapter 7). In contrast to other studies soil moisture is not used as ancillary source of information but is the main subject of comparison. Furthermore, new global data sets on soil moisture from satellite remote sensing are exploited (see Section 4.1 and Section 4.2). The aim is to better understand changes of TWS which are related to changes of soil moisture.

Interrelations between some smaller storage components such as soil moisture were not well understood and hardly investigated:

It might be argued that changes in soil moisture are not reflected in the signature of GRACE due to the limited sensitivity of the sensor and the dominance of other storage components. Here this issue is addressed in two ways. On the one hand it is examined if variations of soil moisture can lie above the sensitivity range of GRACE (see Section 7.1). On the other hand direct and indirect links between soil moisture and TWS are examined (see Section 7.2 and Section 7.3). For example it is analyzed if strong links between soil moisture and a dominant storage component exist, which then result in strong interrelations between soil moisture and TWS.

The quality of remote sensing products on different storage components varies in space and time / The quality of model outputs for TWS is heterogeneous:

To get a better understanding on the quality of global soil moisture products three different soil moisture data sets from active remote sensing (see Section 4.1), passive remote sensing (see Section 4.2) and one hydrological model (see Section 4.4) are used here. Prior to their comparison with GRACE their agreement is analyzed to improve the understanding of data quality for each data set (see Section 6.2). Furthermore changes in TWS from GRACE are compared with TWS outputs of one hydrological model (see Section 6.3).

Data from satellite gravimetry require special processing and filtering which may cause leakage, damping of the signal, and time shifts / Comparability with GRACE is only given if all data sets are filtered in a similar manner / From GRACE only relative changes of TWS can be derived:

In this study all data sets are treated in a harmonized way, as the filtering and special processing of GRACE data are also implemented for soil moisture and ancillary data (see Section 5.2). The impact of the harmonized processing is analyzed in detail (see Section 6.1). Being aware of artifacts that arise from filtering (e.g. damping of the signal), the data sets are not compared in absolute but in relative terms. For example the focus is not on the absolute amount of water storage or the bias and root-means square differences between various products but on correlation (see Section 5.4) and time shifts (see Section 5.5) between data pairs. As GRACE only provides information on relative mass changes, interrelations of soil moisture and TWS are only analyzed with respect to their variability, e.g. seasonal change.

For many applications the integrative nature of the GRACE signal represents a challenge:

As the disaggregation of GRACE data has not been developed to the stage of being operational and the availability of data for all storage components is not always given (especially for groundwater), this thesis examines the information content of the entire GRACE signal for disaster monitoring in combination with soil moisture data for one specific case study (see Chapter 8). The entire GRACE signal is expected to be valuable as it provides a holistic view on the state of water storage during extreme weather events. Soil moisture is expected to be an indicator for upcoming lack or surplus in TWS by being closely linked to precipitation.

Link to socioeconomic data is often missing:

As in the case of soil moisture (Section 2.5) TWS dynamics are most often analyzed with respect to hydrometeorological parameters. In order to increase the understanding on the applicability of TWS data for disaster monitoring, socioeconomic data from the International Disaster Database EM-DAT are also integrated in this study (see Section 5.7 and Section 8.4).

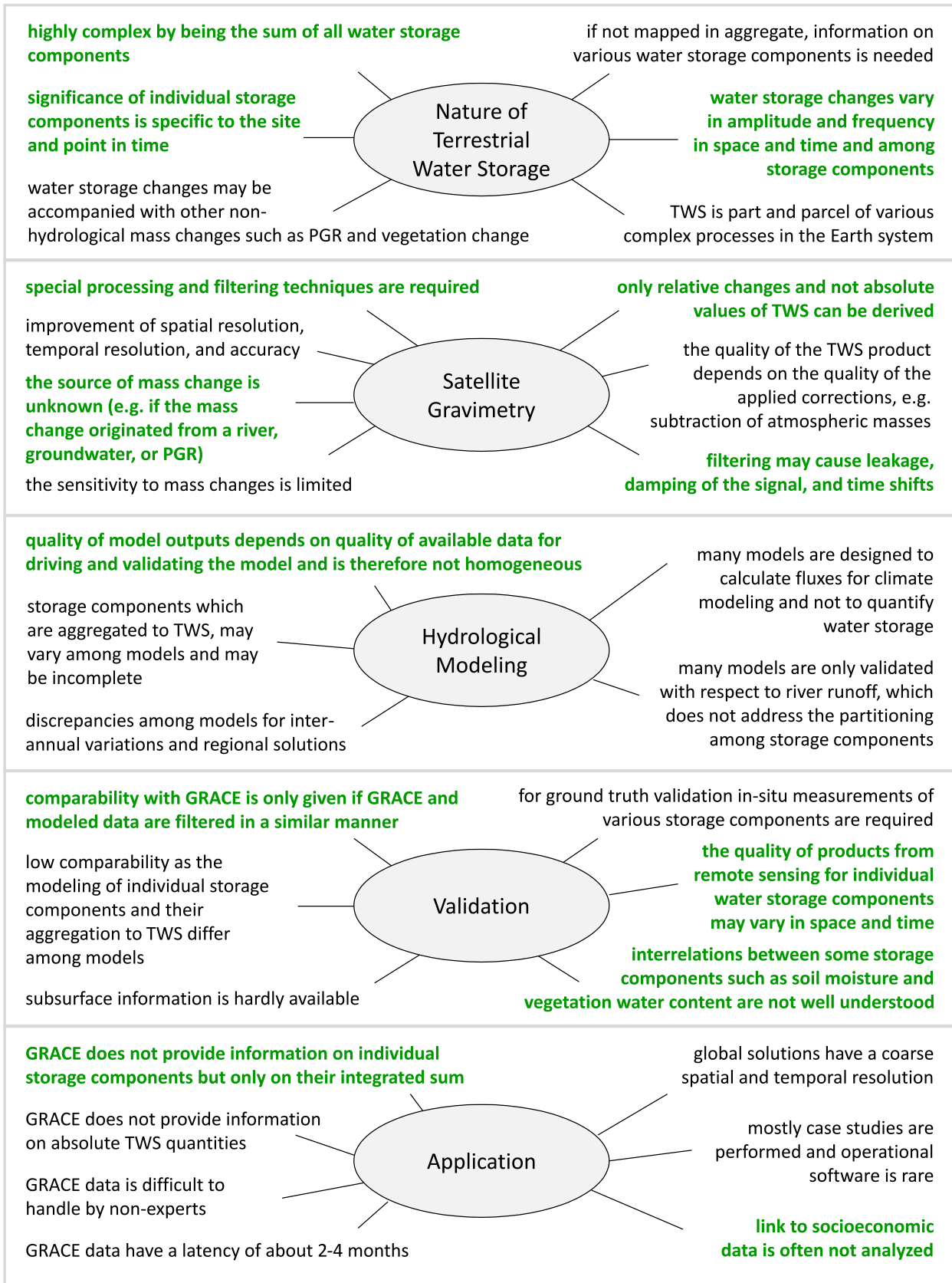


Figure 3.3: Examples of open challenges for the large-scale mapping of terrestrial water storage with respect to the nature of TWS, the used retrieval technique (satellite gravimetry vs. hydrological modeling), and its validation and application; challenges which are mainly addressed in this thesis are highlighted in green.

4 Data and Preprocessing

4.1 Surface Soil Moisture from ASCAT

One of the satellite-based surface soil moisture products used in this study is delivered by the active C-Band (5.3 GHz) microwave sensor ASCAT (Advanced SCATterometer) onboard the MetOp satellite (see Table 2.2 in Section 2.2). The mission, which is operated by EUMETSAT, started on October 2006 and is still operational. Orbiting the Earth at an altitude of 758 km, ASCAT achieves global coverage within about 2 days with a spatial resolution of 25 km. The product used herein contains Level 2 surface soil moisture (the captured surface layer is about 1-2 cm thin; Wagner et al, 2013) at 25 km swath grid and is provided by EUMETSAT and Vienna University of Technology (Bartalis et al, 2007).

◁ The mentioned ASCAT product contains additional information on quality control. Table 4.1 points out the criteria, which are used to exclude erroneous soil moisture data. Aiming at a better understanding of data quality and a large spatial coverage, these criteria are generally less stringent as those used in a data assimilation study such as Dharssi et al (2011). The soil moisture error is derived from error propagation of the backscatter noise, and soil moisture data are excluded if this error exceeds 10%. For the non-scatterometer based output variables containing information on topographic complexity, snow cover fraction, frozen land surface fraction, and inundation and wetland fraction a common threshold of 50% is applied. Furthermore, all data are excluded where processing flags are set. Those flags account for limitations of the instrument (such as noise levels and sensitivity) and the amount of land in the scene. Correction flags indicate data that allow for the calculation of soil moisture but might be of reduced quality based on the choice of references for minimum and maximum saturation levels of the soil, and backscattering. Those flags are not considered herein as they limit data availability significantly; in contrast a better understanding of the quality of those data is aimed at through the comparison with GRACE observations and soil moisture observations from other data

Table 4.1: *Quality control information for ASCAT data as provided by EUMETSAT and respective exclusion criteria applied for this study (as used by Abelen and Seitz, 2013).*

Flags ASCAT	Exclusion Criteria
Soil moisture error	>10%
Topographic complexity	>50%
Snow cover fraction	>50%
Frozen land surface fraction	>50%
Inundation and wetland fraction	>50%
Processing flags	On
Correction flags	Off

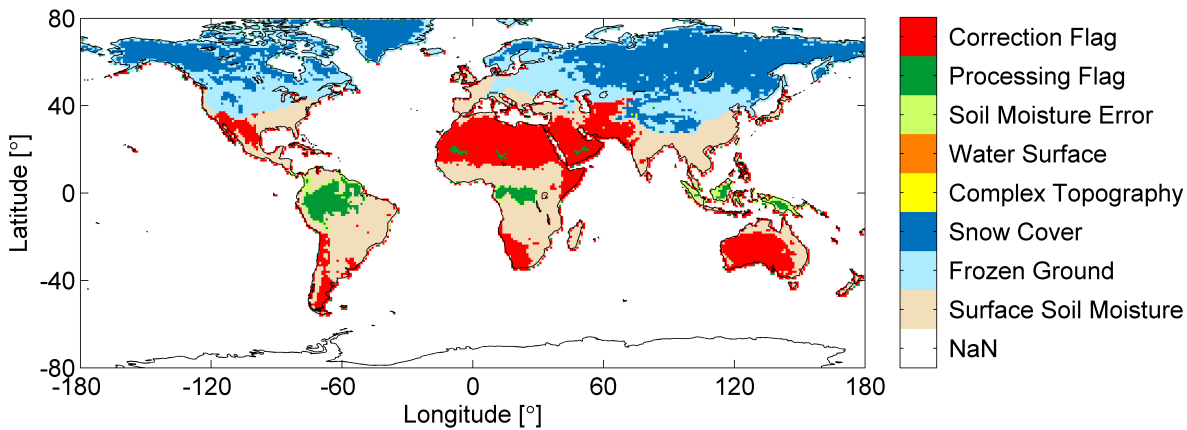


Figure 4.1: Global map showing exemplarily for December 2010 the flagging of ASCAT data, where the colors indicate that either surface soil moisture was captured (beige) or that all observation points falling within a $1^\circ \times 1^\circ$ grid cell were masked as the average fraction of frozen ground (light blue), snow cover (dark blue), complex topography (yellow), or surface water (orange) exceeded 50%. Furthermore grid points are shown where the average soil moisture error exceeded 10% (light green) and where processing (dark green) and correction (red, not applied in this study due to large coverage) were set.

sets. \triangleright (Abelen and Seitz, 2013) Figure 4.1 shows the coverage of different flags exemplarily for December, 2010.

\triangleleft ASCAT data are provided as percentages of dryness, where 0% corresponds to the driest soil surface conditions (lowest backscatter coefficients) and 100% corresponds to wettest soil surface conditions (highest backscatter coefficients). \triangleright (Abelen et al, 2015)

4.2 Surface Soil Moisture from AMSR-E

The second satellite-based surface soil moisture data set is the daily LPRM / AMSR-E / Aqua Level 3 Surface Soil Moisture product. It is based on the Land Parameter Retrieval Model (LPRM), which was developed by Vrije Universiteit Amsterdam and NASA's Goddard Space Flight Center (Owe et al, 2008). AMSR-E (Advanced Microwave Scanning Radiometer for Earth Observing System) is a passive microwave sensor on the satellite platform AQUA, which operates (in addition to other Bands) in the C-Band at 6.9 GHz and in the X-Band at 10.7 GHz. Only solutions for C-Band were used herein as they are less influenced by vegetation cover and represent a deeper surface layer (see Section 2.2). The C-Band gridded product provides information on the volumetric soil moisture content [$\text{m}^3_{\text{water}}/\text{m}^3_{\text{soil}}$] for the uppermost portion of the soil (around 1 cm deep; Njoku et al, 2003) with a grid size of $0.25^\circ \times 0.25^\circ$.

The product is provided for the time span July 2002 to September 2011. Solutions for subsequent months are not available because AMSR-E stopped delivering data due to a problem with the rotation of its antenna. AQUA has a polar orbit, where ascending paths move over the equator at night (at around 1:30 a.m. local time) and descending paths move over the equator during the day (at around 1:30 p.m. local time; de Jeu et al, 2008). As in many other studies (Draper et al, 2009; Liu et al, 2011, 2012; de Jeu et al, 2008), only descending tracks are used herein. This is due to the greater stability of nighttime soil, canopy, and air temperatures (Owe et al, 2001).

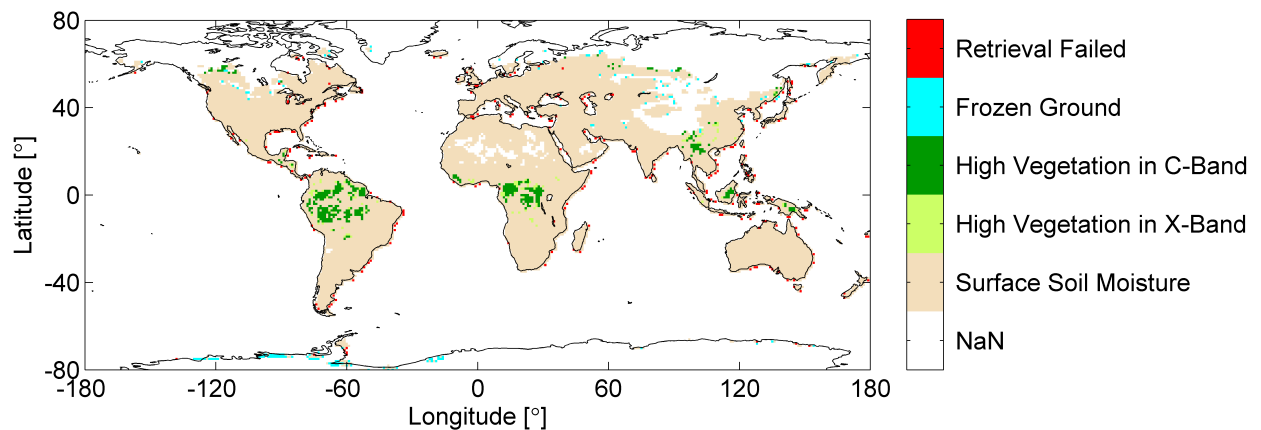


Figure 4.2: Global map showing exemplarily for December 2010 the flagging of AMSR-E data, where the colors indicate that either surface soil moisture was captured (beige) or that all observation points falling within a $1^\circ \times 1^\circ$ grid cell were masked due to high vegetation in X-Band (light green), high vegetation in C-Band (dark green), frozen ground (light blue), or that no retrieval was possible, for example due to large fractions of ocean in the pixel (red).

The described AMSR-E surface soil moisture product also contains flagging information for quality control. In this study data points are excluded if any of the flags indicating high vegetation in the X-Band, high vegetation in the C-Band, or frozen ground are set. Furthermore, pixels are masked out if the retrieval was not possible for example due to high fraction of oceans in the field of view. The coverage of those flags is shown exemplarily for December, 2010 in Figure 4.2. In addition to the flagged pixels there are also large areas where no information on soil moisture is provided. Those include areas in hyper-arid zones such as the Sahara desert and areas of continuous snow cover or frozen ground like large parts of Siberia, Alaska and the Tibetan Plateau (see Figure 4.2).

4.3 Terrestrial Water Storage from GRACE

The GRACE mission is a joint scientific satellite mission between the US National Aeronautics and Space Administration (NASA) and the German Aerospace Center (DLR), which has been launched in March 2002 and is still operational. It is a twin satellite configuration (using SST-II and SST-I, both concepts are described in Section 3.2) with two identical satellites orbiting about 220 km apart in the same LEO at an altitude of 500 km (Xu et al, 2007).

Official processing centers providing GRACE data include the German Research Centre for Geosciences (GFZ), the Center for Space Research at University of Texas, Austin, USA (CSR) and the Jet Propulsion Laboratory (JPL), Pasadena, USA. Results on the Earth's gravity field or the respective water mass variation differ among those groups due to varying processing strategies and tuning parameters (Sakumura et al, 2014). The three official data sets have been compared in the spectral and spatial domain by Sakumura et al (2014). They conclude that all solutions lie within a certain analysis scatter (regardless of the local relative water height variation) and that the noise in the gravity field solutions is reduced in the ensemble model.

In this study the GRACE RL05 Level-2 data provided by the GFZ (Dahle et al, 2012) is used. This product is calculated using the EPOS (Earth Parameter and Orbit System) software suite providing

monthly gravity field solutions in spherical harmonics up to degree and order 90 and weekly solutions up to degree and order 30. The data is available from January 2003 onwards but due to problems with the accelerometer or K-Band data or due to orbit maneuvers, solutions are not provided for June 2003, January and June 2011, May and October 2012, March and August 2013, January, February, July, and December 2014, and May 2015 (Flechtner et al, 2015). The level of mm-geoid accuracy is ~ 350 km (Dahle et al, 2012).

During preprocessing the gravity signal is corrected for non-gravitational forces acting on the satellite and gravitational forces originating from solid Earth tides, ocean and atmospheric tides, ocean pole tides, non-tidal variability in the atmosphere and ocean, rotation deformation forces, perturbations due to sun, moon and 5 planets (Mercury, Venus, Mars, Jupiter, and Saturn), and general relativistic contributions (Dahle et al, 2012). Remaining gravitational variations, contained in the RL05 GFZ product, are predominantly caused by hydrology, cryosphere, episodic events such as large earthquakes, PGR, and errors or non-modeled effects of the applied background models (Dahle et al, 2012).

As the GRACE signal contains some level of noise, the data need to be filtered. Noise is in particular manifested in the presence of stripes in unfiltered solutions and implies correlation in certain spherical harmonic coefficients (Swenson and Wahr, 2006). Further errors result from the orbit configuration of the twin satellites such as system-noise error in the satellite-to-satellite microwave ranging measurements, or accelerometer and orbit error (Wahr et al, 1998). Also noisy high-resolution coefficients need to be suppressed (Swenson and Wahr, 2006; Zhang et al, 2009). A significant fraction of sub-monthly mass changes is not captured by the background models and leads to the corruption of the GRACE estimate through aliasing (Bettadpur, 2007). Errors in sub-monthly atmospheric or oceanic variability provided by background models (used to reduce the GRACE signal for non-hydrological masses and non-continental water masses) may lead to aliasing as well. Furthermore, the derived signal for water storage may contain unwanted mass changes such as mass variations in the Earth's interior, which were not modeled and consequently also not reduced from the signal during pre-processing (Wahr et al, 2006). In order to reduce the level of noise, GRACE data need to be filtered, having also the consequence that the signal is damped (Landerer and Swenson, 2012), and that it might be effected by leakage, and phase shifts in time (Werth et al, 2009, see Section 3.2).

Several studies have focused on the design and improvement of filtering techniques for GRACE data (Kusche, 2007; Klees et al, 2008; Seo et al, 2006; Swenson and Wahr, 2006) or the introduction of scaling factors to reduce damping effects (Chen et al, 2007; Velicogna and Wahr, 2006). Further studies focus specifically on the increase of spatial and temporal resolution (Kurtenbach et al, 2009; Lemoine et al, 2007; Schmidt et al, 2006b). An overview on several filters is given by Kusche (2007) and Werth et al (2009).

Due to the different filter designs there is no fixed spatial resolution and accuracy for monthly estimates of changes in TWS from GRACE. Wahr et al (2006) estimated that the accuracy of GRACE amounts to about 38 mm for 500 km and 15 mm for 1000 km Gaussian-averaged mass estimates. A similar result was obtained by Schmidt et al (2006c), who estimated the error to amount to 35 mm water height, when using a Gauss filter of 750 km averaging radius. For more recent GRACE releases (GFZ RL04) the accuracy was improved to around 25 mm and 40 mm for a Gauss filter of 500 km and 400 km half-wavelength radius, respectively (Schmidt et al, 2008b). For the latest version, GFZ RL05, the accuracy was again improved. It is estimated that GFZ RL05 at a spatial scale of about 340 km is as accurate as GFZ RL04 at a spatial scale of about 530 km (Dahle et al, 2014).

4.4 Water Storage Components from WGHM

The WaterGAP Global Hydrology Model (WGHM; Müller Schmied et al, 2014; Döll et al, 2003) is (in addition to water use models for five different sectors) part of the global hydrology and water use model WaterGAP (WaterGlobal Assessment and Prognosis). WaterGAP has been developed for the simulation of water balances of large river basins to assess water availability and water use at global scale for all main freshwater sources (Döll et al, 2003). WGHM calculates daily water storage and water flow for all large river basins over the continents (except Antarctica) with a spatial resolution of 0.5° . In the scope of this thesis, the latest version of WGHM in WaterGAP2.2 is used (Müller Schmied et al, 2014).

The model is calibrated against mean annual river discharge using data from 1319 gauging stations worldwide. The precipitation data which is used as input to the model is the Monitoring Product Version 4.0 from the Global Precipitation Climatology Center (GPCC; Schneider et al, 2011, see Section 4.5). Other climate forcing data such as temperature, cloudiness, and number of rainy days per month are taken from operational forecast or analysis data of the European Centre for Medium-Range Weather Forecasts (ECMWF).

WGHM simulates all main storage components including soil moisture, groundwater, snow, ice, canopy storage, and surface water from lakes, rivers, and reservoirs. The water mass of all these storage components is added together to derive TWS. A schematic view of the structure of the water fluxes and storages as computed by WGHM within each $0.5^\circ \times 0.5^\circ$ grid cell is provided by (Müller Schmied et al, 2014).

Soil moisture is calculated for one soil layer of varying thickness, depending on the rooting depth of vegetation. The effective rooting depth is derived from a land cover map, using MODIS observations for the year 2004 (see Figure 4.3; Müller Schmied et al, 2014). The soil water balance takes into account the soil moisture within the effective root zone, effective precipitation (throughfall and snowmelt), evapotranspiration, and runoff. The maximum available water capacity, which is crucial for the estimation of runoff, is calculated by multiplying the total available water capacity in the uppermost meter of the soil (Batjes, 1996) with the rooting depth of vegetation (Döll et al, 2003).

In Section 3.3 WGHM has been introduced as suitable complementary data set to satellite based observations on TWS and soil moisture.

4.5 Precipitation from GPCC

In the previous section it has been mentioned that WGHM receives as model input precipitation data from the Monitoring Product Version 4.0 of the Global Precipitation Climatology Center (GPCC; Schneider et al, 2011). The precipitation data used in this thesis originates from this precipitation product. The monthly global land-surface precipitation is based on 7,000 to 9,000 globally distributed in-situ stations. Monthly products at a resolution of 1° are available two month after the end of an analysis month.

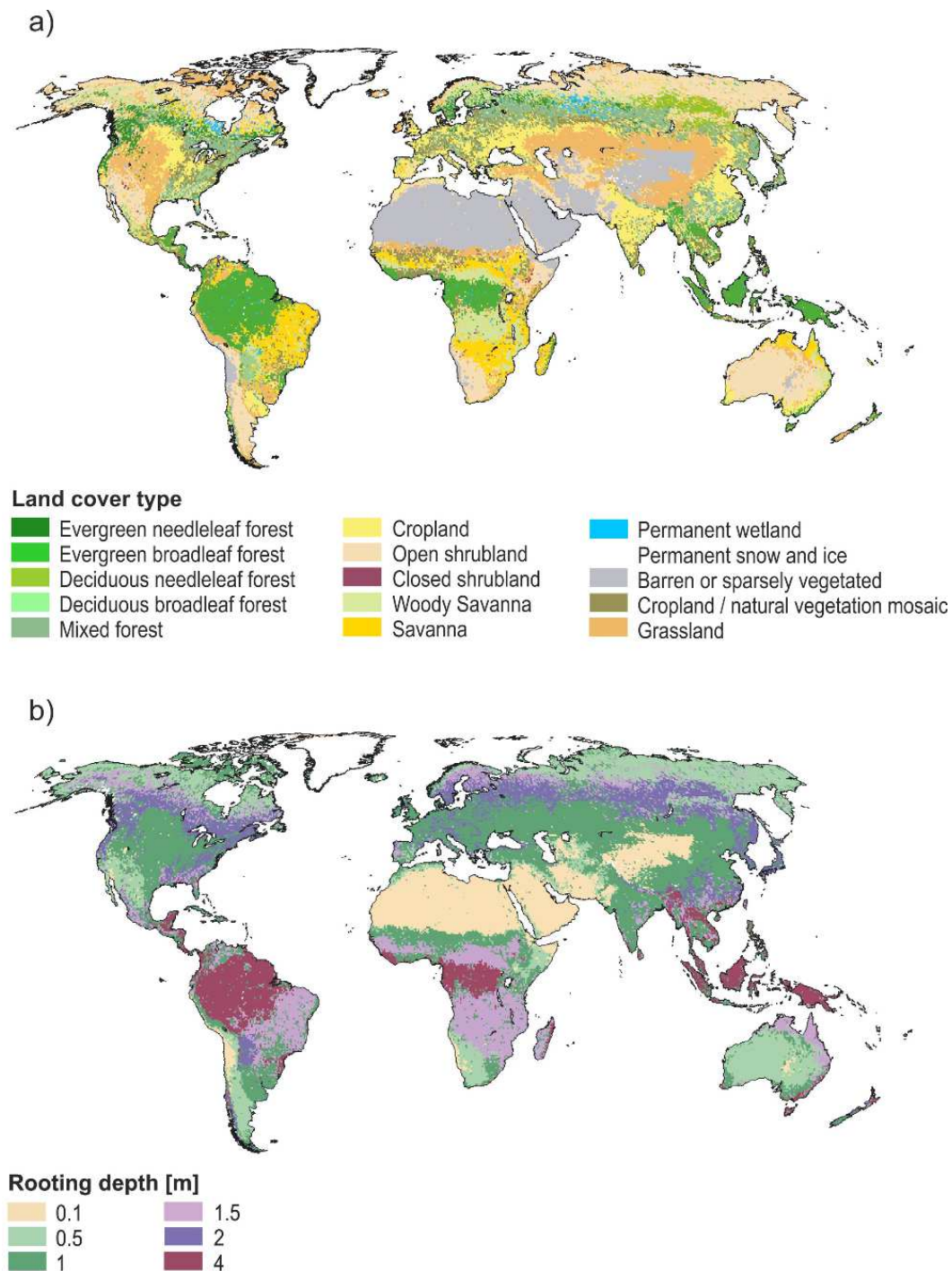


Figure 4.3: Global map with a spatial resolution of $0.5^\circ \times 0.5^\circ$ showing a) the land cover, which is used as input for WaterGAP being based on MODIS observations for the year 2004 (the map has been taken from Müller Schmied et al, 2014), and b) the respective rooting depth of vegetation as used in WaterGAP (the map has been modified from Müller Schmied et al, 2014, by replacing the land cover information with the respective rooting depth of vegetation).

4.6 Oceanic Niño Index

◁ The Climate Prediction Center of the United States National Oceanic and Atmospheric Administration (NOAA) provides the Oceanic Niño Index (ONI) to identify El Niño and La Niña events in the tropical Pacific (Climate Prediction Center of NOAA, 2014). The ONI is calculated from the three-month mean sea surface temperature anomaly for the Niño 3.4 region (5°N-5°S, 120°-170°W). If five consecutive overlapping three-month periods exceed a certain threshold, they are classified as El Niño (warm, positive anomaly) or La Niña (cool, negative anomaly) events (Larkin, 2005). The threshold is set to 1.5 for strong events, 1.0-1.4 for moderate events, and 0.5-0.9 for weak events (Golden Gate Weather Service, 2014). ▷ (Abelen et al, 2015)

4.7 The International Disaster Database EM-DAT

◁ EM-DAT (the OFDA/CRED International Disaster Database - www.emdat.be - Université Catholique de Louvain, Brussels, Belgium) is a global database on natural and technological disasters, and it is maintained by the Centre for Research on the Epidemiology of Disasters. From 1900 onward, more than 17,000 disasters that meet at least one of the following criteria have been registered (Guha-Sapir et al, 2009):

- ten or more people killed;
- one hundred or more people affected;
- declaration of a state of emergency; and
- call for international assistance. ▷ (Abelen et al, 2015)

Within EM-DAT natural disasters are classified into five subgroups to which certain disaster types are assigned. For example the subgroup “Hydrological Disasters” contains the disaster types flood, landslide and wave action, and the subgroup “Climatological Disasters” contains the disaster types drought, glacial lake outburst and wildfire. The database collects for each registered disaster information on the location, date, duration, the estimated total damage (amount of damage to property, crops, and livestock given in US-Dollar true to the year of the event) and the number of total affected (being injured, homeless, or requiring immediate assistance during a period of emergency), missing or dead people. However, due to lack of knowledge or lack of knowledge transfer this information might be incomplete (or deficient) for individual disasters and certain disasters might not be registered at all.

5 Linking Soil Moisture to Terrestrial Water Storage

5.1 Theoretical Background

◁ Putting the signal from GRACE in relation to soil moisture is not directly possible. This is mainly based on the fact that GRACE is not only sensitive to signals of soil moisture but to all sources of mass changes on the Earth's surface and its interior. ▷ (Abelen and Seitz, 2013)

For the GRACE product used herein, the gravity signal has been reduced for several gravitational and non-gravitational forces (see Section 4.3). Over non-polar continental regions the remaining GRACE signal contains mass changes originating from hydrology, episodic events such as large earthquakes (magnitude 8 or higher; De Viron et al, 2008) and glacial isostatic adjustment (A et al, 2012; Purcell et al, 2011), but also errors or non-modeled effects of the applied background models (Dahle et al, 2012). Figure 5.1 illustrates these contributions, neglecting erroneous contributions of applied background models. It shows that terrestrial mass changes as sensed by GRACE, originate on the one hand from changes in TWS and on the other hand from non-hydrological mass changes (as for example from PGR and large earthquakes).

While on first sight soil moisture and TWS appear to be totally different parameters, Figure 5.1 shows that they are related, because soil moisture is (together with surface water, ground water, canopy storage and snow and ice) an integral part of TWS. Therefore, it is also one component of the terrestrial mass, which is sensed by GRACE. If soil moisture changes, the terrestrial mass changes as well. In order to put changes in soil moisture in direct relation to changes in TWS, several assumptions are made (see Abelen and Seitz, 2013):

1. Errors or non-modeled effects of the applied background models are - after filtering - assumed to lie within the uncertainty of GRACE data, which is here estimated to range approximately from 20 mm to 40 mm (when using a Gauss filter of 500 km and 300 km half-wavelength respectively; see Section 4.3).
2. It is assumed that after masking regions affected by PGR and after considering effects of very strong earthquakes (magnitude 8 or higher), the main non-hydrological contributions are removed

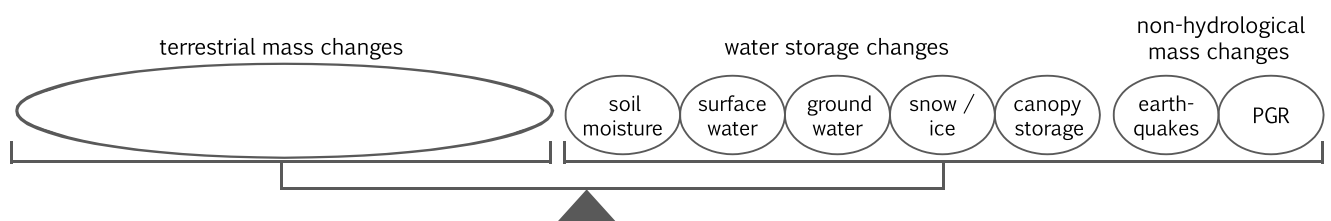


Figure 5.1: Balance illustrating main continental mass components on Earth, adding up to the terrestrial masses as sensed by GRACE.

from the GRACE signal. It is assumed that variations in the remaining GRACE signal are only related to changes in TWS.

3. The focus is on areas, where signals from snow and ice can be neglected. In this way contributions to TWS from these storage components do not need to be considered.
4. As soil moisture cannot be captured by satellites over regions with dense vegetation cover (see Section 2.4) those regions are masked out (see Figure 4.1 and Figure 4.2). Therefore, contributions of canopy storage to TWS are neglected herein.
5. Considering the prior assumptions we are only left with three components that make up the change in continental water storage, namely surface water, groundwater and the target parameter soil moisture. It is assumed that correlations between changes in soil moisture and changes in TWS are high if:
 - a) soil moisture is dominant, meaning that the change in soil moisture is much larger than the change of groundwater and surface water combined,
 - b) soil moisture changes proportionally with another dominant storage component, being ground water and/or surface water.

Assumption 5a) is considered to be possible, as surface water is rather a point-like (lake) or line-like (river) phenomenon, while soil moisture changes over large areas. Furthermore groundwater does not show strong short-term variation (recharge ≤ 5 mm/year) over wide areas, unless excessively impacted by humans for example through irrigation (Taylor et al, 2013). Assumption 5b) is based on the idea that soil moisture serves as transition zone between surface and groundwater and therefore may show similar variations (for example in wetlands). Accounting for assumptions 1 to 5 in the following it is assumed that under certain circumstances changes in soil moisture can be put in relation to changes in TWS as sensed by GRACE.

5.2 Data Harmonization

“For a fair comparison of water storage variations, hydrological model data have to be treated in the same way as the GRACE data.” (Güntner, 2008)

GRACE data have very specific characteristics as they are provided in spherical harmonics and require special filtering (see Section 3.2 and Section 4.3). Therefore, they differ significantly from the other soil moisture data sets, which are provided in grid format and do not require filtering. Furthermore, the spatial and temporal resolution differs among the various data sets (see Table 5.1). If those distinct data sets were compared directly, it would not be clear whether observed differences are of hydrological origin or if they result from different processing or representation. To avoid differences in data structures that strongly impact the analysis, all data sets are harmonized (Abelen and Seitz, 2013). The harmonization process is described in Figure 5.2. The impact of the described processing steps is shown and discussed in the next chapter in Section 6.1.

Table 5.1: Individual specifications of the main data sets of soil moisture and water storage and harmonized specifications for all data sets.

	Satellite Gravimetry	Remote Sensing		Hydrological Model	Harmonized Specifications
Source	GRACE	ASCAT	AMSR-E	WGHM	
Product	Level 2, RL05, German Research Centre for Geosciences (GFZ)	Level 2 Soil Moisture at 25 km Swath Grid EUMETSAT, Vienna University of Technology (TU Wien)	LPRM/AMSR-E/Aqua Daily L3 Surface Soil Moisture, Vrije Universiteit Amsterdam, and NASA GSFC	Version 2.2, German Research Centre for Geosciences (GFZ), University of Frankfurt	
Reference	Dahle et al, 2012	Bartalis et al, 2007	Owe et al, 2008	Müller Schmied et al, 2014	Abelen and Seitz, 2013
Parameter	change in terrestrial water storage	surface soil moisture	surface soil moisture	terrestrial water storage, root zone soil moisture, groundwater, surface water, snow and ice	only changes can be compared
Unit	mm	% (0% dry, 100% wet)	m ³ /m ³	mm	mm
Availability	2002 - present	2007 - present	2002 - 2011	1901 - present	Sept. 2007 - Aug. 2011
Temporal Resolution	monthly	daily	daily	monthly	monthly
Spatial Resolution	300 km	25 km	25 km	0.5°	300 km
Representation	spherical harmonics	ascending and descending tracks	0.25° world map with descending tracks	0.5° world map	1° world map
Post-processing	least-squares filtering, Gauss filtering				least-squares filtering for GRACE only, Gauss filtering for all data sets

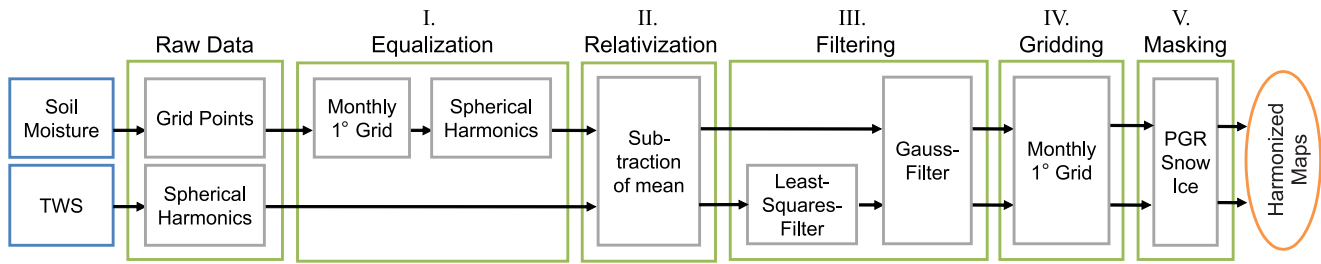


Figure 5.2: Flowchart describing the data harmonization process for equalizing soil moisture products and satellite gravimetry data on terrestrial water storage (taken from Abelen and Seitz, 2013).

The raw data, which are harmoniously processed, include GRACE data on TWS (see Section 4.3), surface soil moisture from remote sensing (see Section 4.1 and Section 4.2) and root zone soil moisture from WGHM (see Section 4.4). The data sets are mainly processed for the overlapping time period September 2007 to August 2011 as during these four complete annual cycles all data sets are available (see Table 5.1). As mentioned before the data sets of soil moisture and TWS differ in their representation because GRACE data are commonly provided in spherical harmonics (Wahr et al, 1998) and soil moisture products are provided in grid formats for example with a grid size of $25 \text{ km} \times 25 \text{ km}$ or $0.5^\circ \times 0.5^\circ$. Furthermore, GRACE provides monthly solutions while remote sensing products are available in daily time intervals (see Table 5.1). The following description of the harmonious processing follows the flowchart shown in Figure 5.2:

- I. First, the spatial resolution of all soil moisture data products is brought to a $1^\circ \times 1^\circ$ grid (by computing the simple average of all data points falling within a $1^\circ \times 1^\circ$ grid cell) and the temporal resolution is aggregated monthly (by computing the simple average of all daily $1^\circ \times 1^\circ$ grid solutions of one month to ensure global coverage for the subsequent conversion into spherical harmonics).

Second, the grid points are converted into spherical harmonics. For all data sets the spherical harmonics series are truncated at degree and order 70. Higher terms up to degree and order 90 (which are available for the RL05 GFZ product) are not considered as their impact is masked by the subsequent Gauss filtering (see Figure 3.2 in Section 3.2).

- II. As described in Section 3.2, satellite gravimetry only delivers information on the change in TWS with respect to some reference value (and not its absolute value). Therefore, the spherical harmonic coefficients are reduced either by their long-term mean over the observed time period (the observed time period is here the overlapping time period of all compared products) or by their monthly mean values (for each month the mean of the same month for the overlapping time period is subtracted). The subtraction of mean values implies that the subsequent analysis focuses on hydrologic anomalies from different data sets.

- III. As next step the GRACE data are filtered, following a widely used procedure. First a least-squares polynomial filter is applied which has been introduced by (Swenson and Wahr, 2006) to reduce spatially correlated errors in GRACE data. Those errors are manifested on maps of surface mass anomaly as long, linear features, commonly referred to as “stripes” (see Figure 5.3). The destriping effect of the least-squares polynomial filter results from negative lobes north and south of the filter’s center and positive lobes to the east and west (a spatial representation of the filter is shown by Swenson and Wahr, 2006), differentiating between correlated north-to-south noise (visible as stripes) and geophysical signals (Swenson and Wahr, 2006). Herein the least-squares

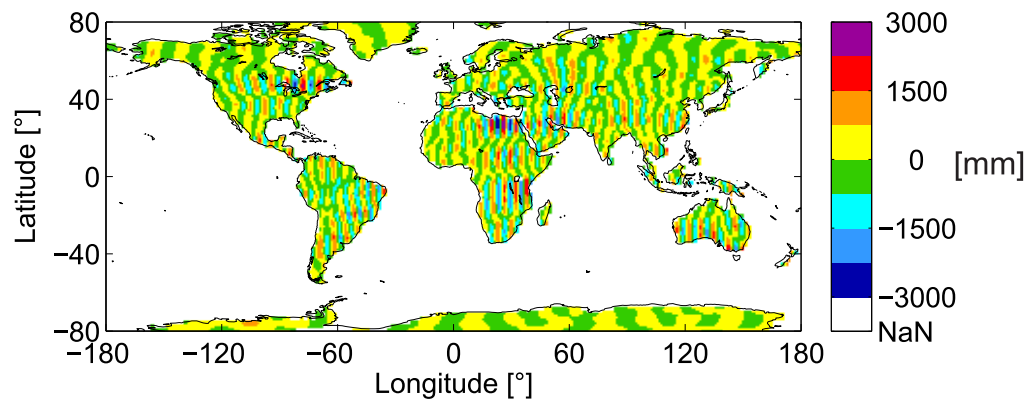


Figure 5.3: Global map showing the stripes of unfiltered GRACE data for October 2008 (long-term mean of the time period January 2007 to December 2012 has been subtracted).

polynomial filter is only applied to the GRACE data as it has been demonstrated by Swenson and Wahr (2006) that it only marginally influences data sets, which are not affected by correlated errors (like the converted fields of the soil moisture data used herein).

The second filter, which is applied to the GRACE data in the course of the conversion of spherical harmonic coefficients into monthly fields of Equivalent Water Heights (EWHs), is the widely used isotropic Gaussian smoothing filter (Wahr et al, 1998). The weighting of this symmetric bell-shaped filter is derived from the Gaussian probability density function. The highest weight is in the center and with increasing distance from the center the weighing converges to zero. The width of the filter (e.g. 300 km half-wavelength) defines at which distance the weighting function reaches 50% of its maximum value (Werth et al, 2009). It is well-known that Gauss filtering decreases the level of noise (by reducing noisy short wavelength components in the GRACE signal). At the same time also the amplitude of the desired signal is reduced, whereby the impact of filtering increases with increasing filter width (see Figure 5.4). Without applying the Gauss filter to all data sets, soil moisture patterns would be much finer than those of GRACE. Furthermore, Gauss filtering may lead to phase shifts in the seasonal signal and cause leakage from surrounding regions into the study area (Werth et al, 2009). Due to these artifacts the Gauss filter is applied also to the soil moisture data sets to obtain comparable data. A radius of 300 km half-wavelength is chosen as this is the limit in spatial resolution for GRACE data (Schmidt et al, 2008b).

- IV. After the filtering the spherical harmonic coefficients of all data sets are converted back into geographical grids of $1^\circ \times 1^\circ$.
- V. Following the assumptions of the previous section, as last step regions are excluded if they are affected by PGR, contain ice cover or receive significant snowfall. \triangleleft The snow mask is derived from snowfall data from WGHM, excluding areas where the sum of all variation in snowfall over the observed time span is bigger than 20 mm and therefore lies above the accuracy of the filtered GRACE fields (see first assumption in Section 5.1). Respectively areas are also masked in which (according to A et al, 2012) PGR-rates exceed ± 5 mm per year (using a Gauss filter with 200 km radius and truncating at degree and order 60). \triangleright (Abelen and Seitz, 2013) The PGR mask and the snow mask are shown in Figure 5.5 and Figure 5.6 respectively.

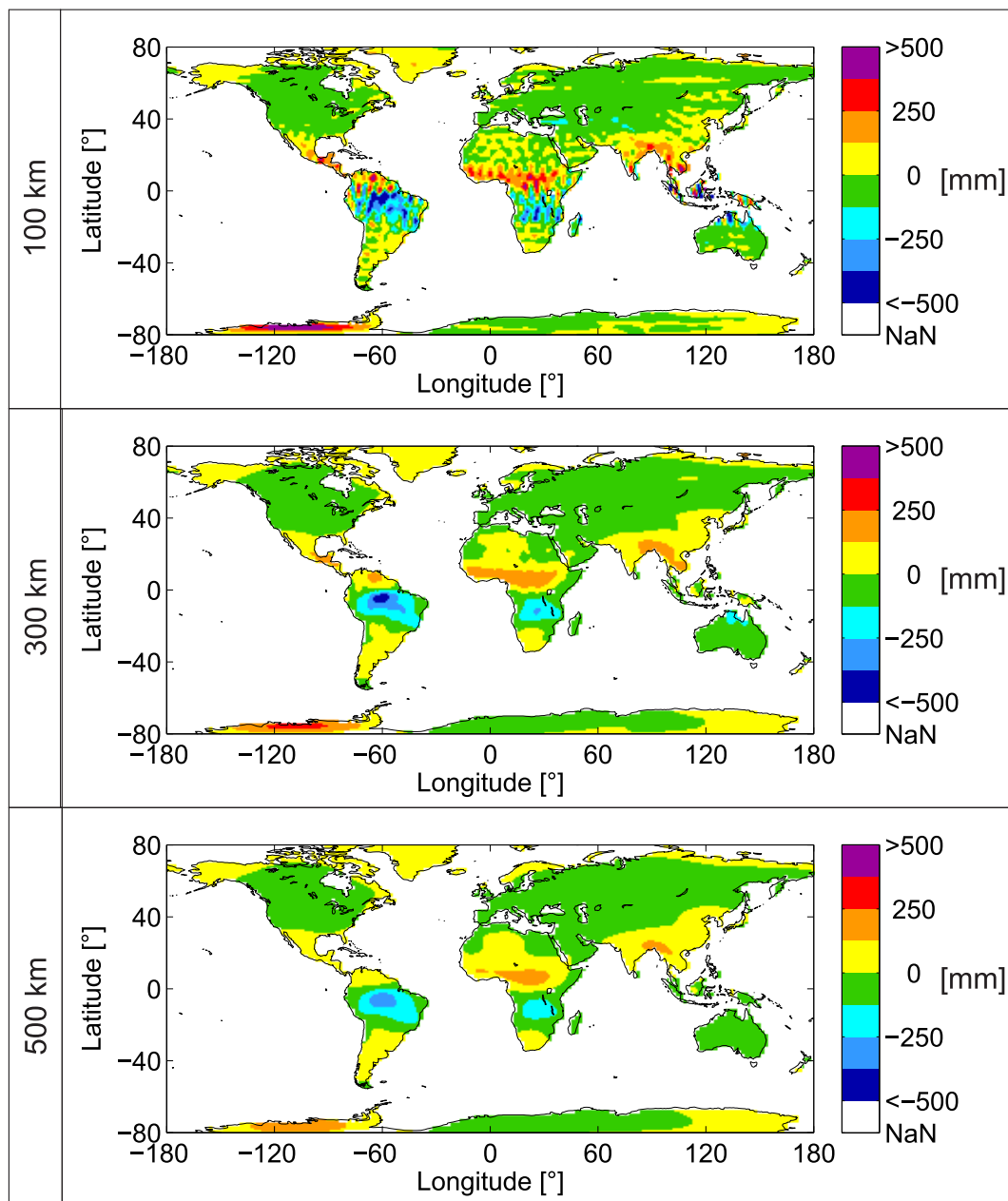


Figure 5.4: Global maps of terrestrial water storage from GRACE for October 2008 showing the impact of smoothing when using a Gauss filter of 100 km (row 1), 300 km (row 2), or 500 km (row 3) half-wavelength radius (long-term mean of the time period January 2007 to December 2012 has been subtracted).

Information on strong earthquakes, which happened globally between September 2007 and August 2011 is provided in Table 5.2. Regions affected by earthquakes are not masked here, as the spatial and temporal significance of these events is not well defined. Therefore, Table 5.2 is meant to give complementary information to assist the interpretation of results in affected regions. Apart from the earthquake in southern Sumatra, the remaining three earthquakes in Table 5.2 either affected small islands, which are not visible on large-scale maps (Samoa Islands) or lie in regions which are to a large extent already masked out due to intense snowfall (Honshun, Japan and Bio-Bio, Chile).

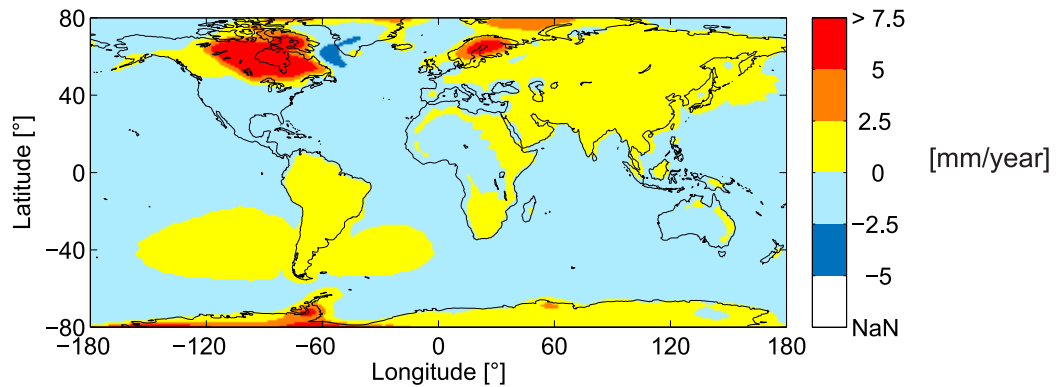


Figure 5.5: Global map showing yearly rates of post glacial rebound according to A et al (2012); red areas mark regions which are masked out in the course of the harmonization process.

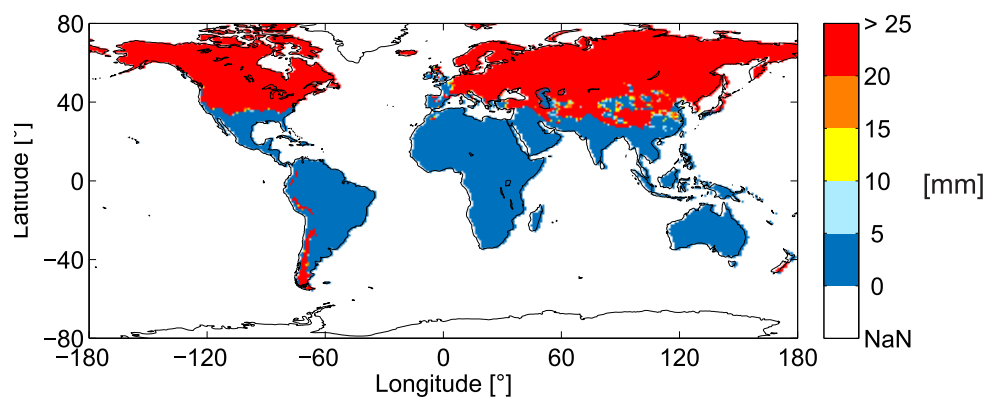


Figure 5.6: Global map showing the accumulation (total sum of all variation) of snow fall over the time period September 2007 to August 2011 based on WGHM data; red areas mark regions which are masked out in the course of the harmonization process.

Table 5.2: List of severe earthquakes with magnitude 8 or higher, which happened around the world from September 2007 to August 2011 as provided by the United States Geological Survey (USGS, 2015).

Date	Location	Magnitude
2007 09 12	Southern Sumatra, Indonesia	8.5
2009 09 29	Samoa Islands region	8.1
2010 02 27	Offshore Bio-Bio, Chile	8.8
2011 03 11	Near the East Coast of Honshu, Japan	9.0

Table 5.1 summarizes the diverse characteristics of the compared data sets (column 1-4) and the final unified characteristics of the harmonized maps (column 5). As mentioned before, the main impact of the harmonious processing is the spatial smoothing of the data, which leads to loss of detail, damping of the signal, spatial leakage and possibly temporal time shifts (these artifacts are analyzed in detail in Section 6.1). As all data sets are processed in a unified way, it is assumed that they are similarly affected by these artifacts. This is specifically important when a comparison with GRACE data is sought (e.g. comparing GRACE with satellite soil moisture products). Therefore, the harmonization procedure is not only done for soil moisture data but also for complementary data products (as precipitation data or information on surface water variation from WGHM), when being linked to GRACE data.

In contrast the harmonization procedure is not applied if for example different remote sensing soil moisture products are compared (meaning GRACE data is not subject of the comparison). By this means artifacts are avoided, when filtering is not necessary for the sake of comparability. In this case only the spatial resolution is harmonized by computing the simple average of all data points falling into a $1^\circ \times 1^\circ$ grid cell and the temporal resolution is unified to one month.

5.3 Scaling

◁ ASCAT and AMSR-E only map the near-surface soil moisture, whereas WGHM provides the soil moisture content for the entire root zone. Therefore, all three data sets cannot be compared directly in terms of magnitude. Additionally, the units of the different soil moisture data sets are not unified as for example ASCAT data are provided as percentages of dryness and AMSR-E as volumetric soil moisture content [m^3/m^3]. To harmonize the units and approximate the root zone soil moisture for all data sets, the ASCAT and AMSR-E data were scaled with respect to the soil moisture content provided by WGHM. A pixel-wise scaling algorithm was applied because the depth of the soil column may vary among the pixels. The time series of each pixel was scaled with respect to the minimum and maximum soil moisture values of the same pixel, as provided in the reference soil moisture data (WGHM herein).

The simple scaling has the advantage that it does not influence the correlation between data sets, as shown by (Liu et al, 2011). For example, the correlation between scaled ASCAT soil moisture and GRACE TWS yields the same correlation coefficients as the correlation between unscaled ASCAT soil moisture and GRACE TWS. However, the simple scaling has the disadvantage that it does not account for the heterogeneous vertical distribution of soil moisture. Also the maximum and minimum values of root zone soil moisture, taken from the WGHM for the scaling, may contain errors. Due to this limitation, soil moisture values from ASCAT and AMSR-E are not discussed in absolute terms in this study.

Alternative algorithms exist, which derive root zone soil moisture from satellite surface soil moisture. For example, several studies suggest the use of an exponential filter to calculate the so called soil water index (SWI; Albergel et al, 2008b; Wagner et al, 1999). The algorithm comprises a parameter (called time characteristic length), which depends on the depth of the root zone and the soil properties. Such an algorithm is not used here, as it requires reference data (which is optimally in situ data) for calibration. Furthermore, in the case of filtered data, correlation results are not any more independent from the reference data. For example, the correlation between the SWI from ASCAT and GRACE TWS does not yield the same correlation coefficients as the correlation between unscaled ASCAT soil moisture and GRACE TWS. ▷ (Abelen et al, 2015)

5.4 Correlation Analysis and Fisher's z Transformation

◁ One well-known method used for the comparison of data sets is the Pearson product-moment correlation coefficient (Rodgers and Nicewander, 2008), which is defined as the covariance of two variables divided by the product of their standard deviations. As in other studies, which focus on the correlation of various soil moisture data sets (Draper et al, 2012; Albergel et al, 2013a,b; Su et al, 2013), Fisher's z-transformation is used to calculate confidence limits for the Pearson product-moment coefficients. ▷ (Abelen et al, 2015)

For a correlation coefficient r which has been calculated from n observations (e.g. two time lines with n time points) the upper (Lim_{up}) and lower (Lim_{low}) limits for e.g. a confidence interval of 90% is calculated as follows (Fan and Thompson, 2001):

$$z = \frac{1}{2} \ln \left(\frac{1+r}{1-r} \right) = \operatorname{arctanh}(r)$$

$$Lim_{up} = \tanh \left(z + 1.65 \frac{1}{\sqrt{n-3}} \right)$$

$$Lim_{low} = \tanh \left(z - 1.65 \frac{1}{\sqrt{n-3}} \right)$$
(5.1)

5.5 Time Shift Analysis

◁ To identify possible time shifts in the signals of different data pairs, the time lag maximizing the correlation between two signals was calculated. Therefore, the sample cross-covariance function described by Box et al (1994) was used. It provides an estimate of the covariance (c) between two time series x_t ($[x_1, x_2, \dots, x_t]$) and y_t ($[y_1, y_2, \dots, y_t]$) for a defined time lag k :

$$c_{xy}(k) = \begin{cases} \frac{1}{T} \sum_{t=1}^{T-k} (x_t - \bar{x})(y_{t+k} - \bar{y}) & \text{for } k = 0, 1, 2, \dots, n \\ \frac{1}{T} \sum_{t=1}^{T+k} (y_t - \bar{y})(x_{t+k} - \bar{x}) & \text{for } k = 0, -1, -2, \dots, -n \end{cases}$$
(5.2)

where \bar{x} is the mean of the first time series and \bar{y} is the mean of the second time series. The formula for estimating the cross correlation (r) is:

$$r_{xy}(k) = \frac{c_{xy}(k)}{s_x s_y} \quad \text{for } k = 0, \pm 1, \pm 2, \dots, \pm n$$
(5.3)

where s_x is the variance of the time series $x_t(\sqrt{c_{xx}(0)})$ and s_y is the variance of the time series $y_t(\sqrt{c_{yy}(0)})$. In this study, x_t is the signal of one data set, y_t is the signal of another data set, $T=48$ months, and $n=6$ months. ▷ (Abelen et al, 2015)

5.6 Principal Component Analysis

The Principal Component Analysis (PCA; Preisendorfer and Mobley, 1988) is used to split a spatio-temporal signal (e.g. a time series of maps) into a series of Empirical Orthogonal Functions (EOFs) that describe the spatial pattern of the signal, and a series of corresponding coefficients, called Principal Components (PCs), which describe the temporal behavior of the signal:

$$S(\lambda, \varphi, t) = PC(t)_{mode1} EOF(\lambda, \varphi)_{mode1} + PC(t)_{mode2} EOF(\lambda, \varphi)_{mode2} \dots + PC(t)_{modeN} EOF(\lambda, \varphi)_{modeN} \quad (5.4)$$

where:

PC Principal Component (temporal information)
 EOF Empirical Orthogonal Function (spatial information)
 $S(\lambda, \varphi, t)$ Signal at location λ (Latitude), φ (Longitude) and time t

The first mode (first pair of EOF and PC in the series, here: $mode1$) describes the most dominant part of the signal. Higher modes have decreasing importance (here $modeN$ has least importance). A detailed description of PCA is given by Forootan and Kusche (2012).

5.7 Analysis of Hydrological Extremes

This study analyses the interdependency between the two hydrological parameters soil moisture and TWS. Therefore, also a potential field of application is brought into focus, which is the monitoring of natural disasters. As extremes in soil moisture can propagate into extremes in TWS, one target of this study is to better understand interactions between soil moisture and TWS under extreme hydrological conditions.

◁ As soil moisture is closely linked to precipitation and evaporation, it is expected to provide information on the initial phase of hydrologic extremes. Variations of TWS are analyzed to identify possible complementary information on water cycle dynamics during hydrological extremes by considering the sum of all water storage components. Consequently, GRACE TWS is not disaggregated into individual TWS components such as soil moisture, groundwater, and surface water (as for example investigated by Houborg et al, 2012; Zaitchik et al, 2008). Instead the integral information contained in TWS is used. ▷ (Abelen et al, 2015)

The analysis of hydrologic extreme events focuses on the La Plata Basin in South America, which is described in detail in Section 8.1. In this study area some hydrological extreme events could be linked to patterns of El Niño and La Niña. For example Chen et al (2010b) assigned the La Plata drought in 2009 to the weak La Niña period during boreal winter 2008/2009. To better understand interrelations between hydrological extremes and La Niña and El Niño events in this basin, variations of the Oceanic Niño Index (ONI; see Section 4.6) are compared with hydrological anomalies, which are reflected in soil moisture, TWS and other complementary data sets (precipitation from GPCC and surface and groundwater variation from WGHM).

Another data set which is integrated into the analysis of hydrologic extreme events is the International Disaster Database EM-DAT (see Section 4.7). ◁ It provides information on natural disasters that occurred in the La Plata Basin. The definition of a natural disaster is based on the number of

people affected or killed by an event; moreover, it applies if a state declares an emergency or calls for international assistance (see Section 4.7). Therefore, the definition is completely independent of any hydrological and meteorological parameter. The EM-DAT list of natural disasters is integrated in this study to focus on hydrologic extreme events that had a significant impact on society.

The main EM-DAT disaster types, which are considered in this study, were hydrometeorological in nature and classified as storms, floods, extreme temperature, and droughts. Wet mass movements, landslides, avalanches, and land subsidence are neglected as their impacts are limited to local scales and are not visible in satellite data of coarse spatial resolution. For the same reason small-scale events, which for example only affected one town, are not considered. ▷ (Abelen et al, 2015)

6 Comparability of Data Sets

6.1 Impacts of Data Harmonization

The harmonious processing of the various soil moisture data sets and the GRACE data to achieve comparability among those data sets in terms of spatial detail, temporal resolution, and other artifacts from filtering, has been described in detail in Section 5.2. Here the impact of this harmonization process is analyzed. Figure 6.1 shows the impact of each processing step exemplarily for surface soil moisture from AMSR-E and for TWS from GRACE for October 2008. Starting with the first row, which shows the raw data for both data sets, it appears as if the information content of both data sets differs tremendously. This is due to the fact, that the initial absolute GRACE signal is mainly based on the static mass distribution of the Earth, which is visible as horizontal stripes on the map reflecting the oblateness or ellipsoidal shape of the Earth. This stresses the need to subtract the static component of the gravity field by subtracting some long-term mean in order to derive variations of the gravity field, which can be related to changes in water masses. Those anomalies are several magnitudes smaller than the static component as shown in the color scales of the different maps.

The raw AMSR-E product has a daily resolution (in the first row soil moisture measurements for the 2nd of October 2008 are shown) and as in several other studies only descending satellite tracks are used herein (see Section 4.2), which explains the vertical stripe like data gaps for example over Africa. As second step the AMSR-E data are brought to a monthly $1^\circ \times 1^\circ$ grid and subsequently they are converted into spherical harmonics to achieve the same spatial and temporal representation as the raw GRACE data (shown in row 1). Data gaps which appear for AMSR-E data in row 2 and row 3 result from the flagging of the data (see Section 4.2).

The map in row 3 for AMSR-E reveals that the conversion into spherical harmonics impacts the data in at least two ways. On the one hand the magnitude of the signal is damped. For example in India soil moisture decreases in some regions by more than $0.1 \text{ m}^3/\text{m}^3$ (some regions are shown in yellow in row 2 and in light blue in row 3). On the other hand in regions with very low soil moisture (such as the Sahara Desert, the Arabian Desert, the Turkestan Desert and the Kalahari Desert) negative soil moisture values appear (which can be as low as $-0.2 \text{ m}^3/\text{m}^3$).

The next step shown in row 4 is the subtraction of the long-term mean of the time period September 2007 to August 2011. For GRACE the subtraction of a mean is essential as it removes the static component of the gravity field. However, patterns which can be related to water mass changes are still not visible (see row 4 for GRACE data). This is due to the fact that the signal is now dominated by vertical stripes, which result from certain correlated errors in the spherical harmonic coefficients and high-frequency aliasing (see Section 4.3). In order to remove those stripes a least-squares filter is applied to the GRACE data (see Section 5.2).

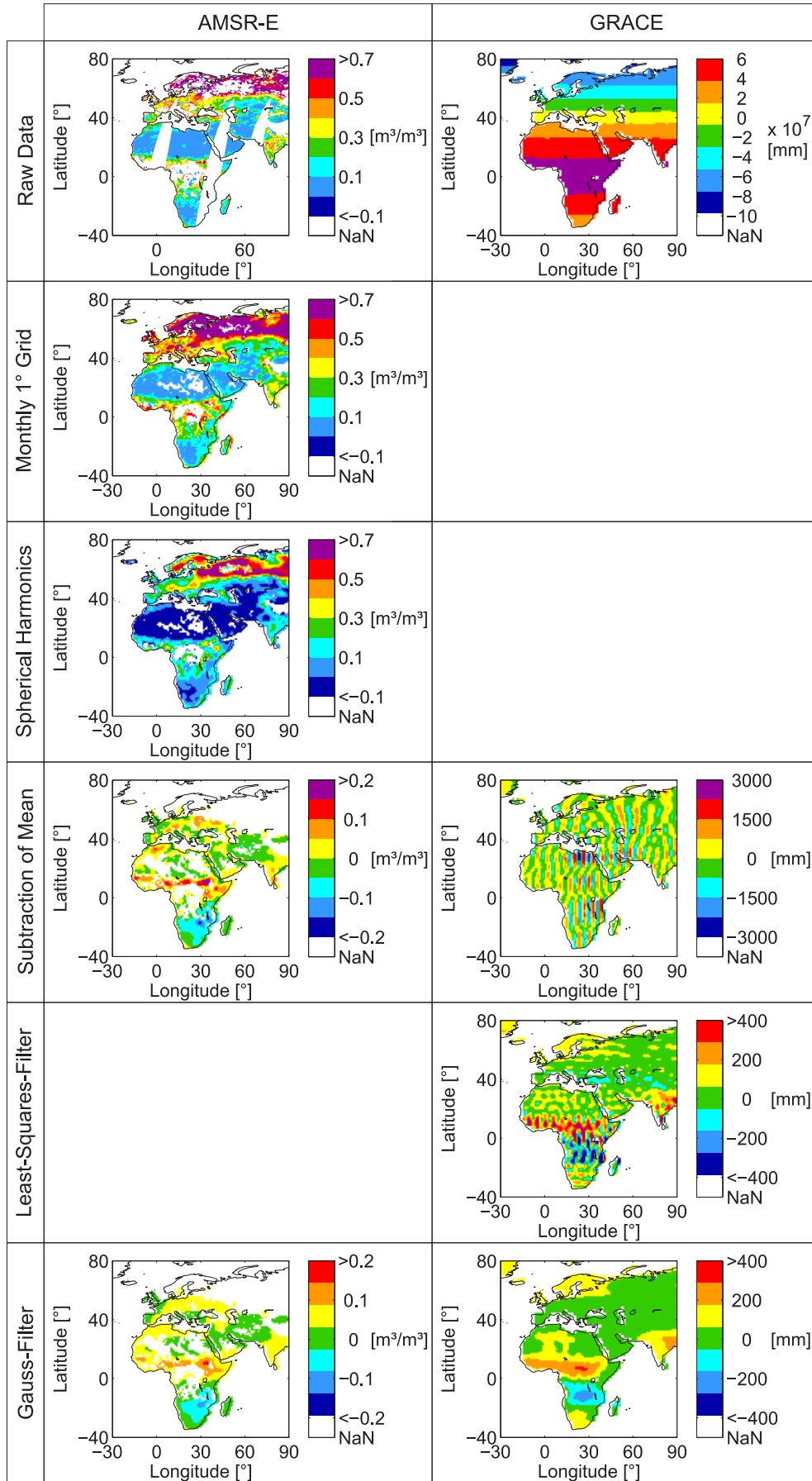


Figure 6.1: *Impacts of the data harmonization process (shown with respect to the flowchart of Figure 5.2) for soil moisture from AMSR-E (column 1; row 1 shows the raw data for the 2nd of October 2008 and the other rows show monthly maps for October 2008) and terrestrial water storage from GRACE (column 2; all rows show monthly maps for October 2008) for different processing steps starting with the raw data (row 1; raw GRACE data are provided in spherical harmonics and presented in a monthly $1^\circ \times 1^\circ$ grid, which is why the next two steps are not shown for GRACE), which are first converted into monthly $1^\circ \times 1^\circ$ grid maps (row 2), then converted into spherical harmonics (row 3), afterwards the long-term mean for the time period September 2007 to August 2011 is subtracted (row 4), then a least-squares filter is applied to the GRACE data (row 5), and finally both data sets are smoothed with a Gauss filter of 300 km half-wavelength radius (row 6), whereby all steps are shown in grid format as spherical harmonics can hardly be visualized.*

The impact of the least-squares filtering is shown in row 5 for GRACE data. Although some hydrological patterns become visible (e.g. surplus of soil moisture to the north of the equator and deficit of soil moisture to the south of the equator) the patterns are still noisy. This noise disappears after applying a Gauss filter of 300 km half-wavelength radius (see row 6 for GRACE data). The strong smoothing of this filter, which again implies a damping of the signal is clearly reflected in the AMSR-E data (compare row 4 with row 6 for AMSR-E data).

One main method, which is used in this study to determine the interrelation between soil moisture and TWS, is the calculation of correlation coefficients (see Section 5.4). Figure 6.1 has shown that the harmonious processing of all data sets and in specific the conversion into spherical harmonics and the Gauss filtering, results in certain artifacts (damping of the signal, appearance of negative values). Therefore, as next step it is analyzed how correlation values are impacted by both processes.

Figure 6.2 highlights in row 1 to row 3 how the conversion of gridded data into spherical harmonics impacts the correlation values for the soil moisture data pairs ASCAT and WGHM (column 1, as shown by Abelen and Seitz, 2013, slight differences results from the different WGHM versions) and AMSR-E and WGHM (column 2). The first row shows the correlation coefficients for the mean-reduced ASCAT and WGHM data, when being brought to a $1^\circ \times 1^\circ$ grid and the second row shows the correlation of the same data sets with the sole difference that this time the data have been converted into spherical harmonics up to degree and order 70 and then brought back onto a $1^\circ \times 1^\circ$ grid. Differences between the correlations in row 1 and row 2 are presented in row 3, emphasizing two main impacts, which result from the conversion into spherical harmonics.

First, correlation coefficients increase over large areas from row 1 to row 2, resulting in a difference between 0 and -0.2 in the correlation coefficients as shown in row 3. Second, regions which have very low variation in soil moisture like the world's large deserts are exceptions. On the one hand there are some data points gained for example over the Sahara Desert (compare row 1 and row 2 in column 1). \triangleleft The gain in data points is caused by the spherical harmonic conversion of the WGHM data. Prior to the conversion for extended regions over the Sahara the standard deviation of soil moisture change provided by the model is equal to zero. Therefore, no correlation value can be calculated (denominator becomes zero). Due to the conversion in spherical harmonics the standard deviation becomes unequal zero (and with it also the denominator of the correlation coefficient), leading to additional correlation coefficients on the map. \triangleright (Abelen and Seitz, 2013) The phenomena of increase in standard deviation from zero to above zero is shown in the time series of WGHM data in Figure 6.3 for a pixel in Africa.

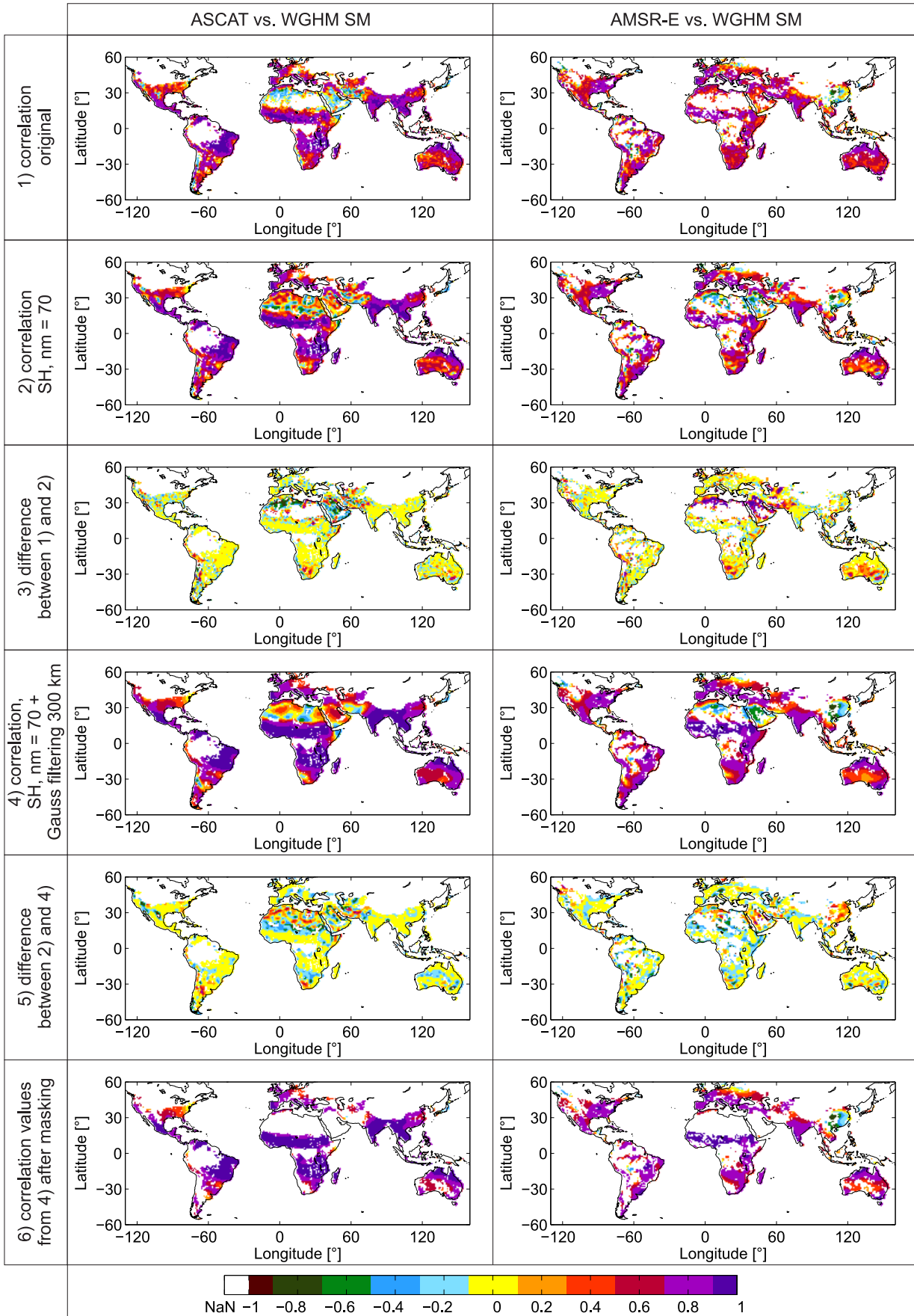


Figure 6.2: *Correlation coefficients for change (long-term mean for the time span September 2007 to August 2011 has been subtracted) in soil moisture from ASCAT and WGHM (column 1) and AMSR-E and WGHM (column 2), showing a) (row 1) results for the monthly original data when being brought to a $1^\circ \times 1^\circ$ grid, b) (row 2) the results from a) after spherical harmonic conversion of maximal degree and order 70, and c) (row 3) the difference between the map from a) and the map from b). In d) (row 4) the results from b) are shown after Gauss filtering with a 300 km half-wavelength radius, e) (row 5) shows the difference between the map from b) and the map from d), and in f) (row 6) results from d) are shown after masking all pixels, where the correlation coefficient between the original time series of a data set and the harmonized time series (after conversion in spherical harmonics and Gauss filtering) of the same data set takes values lower than 0.7 (masked pixels are mainly located in the world's large deserts).*

Additionally some correlation coefficients change substantially in those areas. For example in parts of Algeria correlation coefficients increase significantly for the data pair AMSR-E and WGHM and decrease significantly for the data pair ASCAT and WGHM. This is due to the fact that in arid environments the standard deviation of soil moisture is very close to zero. Those extreme low values are also artificially modified in the course of the conversion into spherical harmonics, which is also visible in Figure 6.1. Therefore, correlation coefficients become biased at locations where the standard deviation is very close to zero. At locations with large soil moisture dynamics as in India the impact of the harmonious processing is low (as also visible in Figure 6.3).

How correlation coefficients change due to Gauss filtering is shown in Figure 6.2 in row 4 and row 5. Again correlation coefficients increase over large areas due to smoothing (resulting in a difference between 0 and -0.2 in the correlation coefficients as shown in row 5 in Figure 6.2) whereby very dry regions show again exceptionally high changes in correlation coefficients. For example in the Sahara Desert some correlation coefficients increase or decrease significantly (reflected by red and blue pixels in row 5 in Figure 6.2). This is due to the fact that dispersed correlation patterns which result from the conversion in spherical harmonics are smoothed (compare the spatial patterns of the correlation coefficients over the Sahara Desert in row 2 with those of row 4) and with it also become subject to leakage from surrounding areas. This leakage is specifically significant in regions where the magnitude of the actual signal is much lower than the signal from surrounding regions, which is why again arid environments are specifically affected (see also Güntner, 2008). The artificial modification of a soil moisture signal by Gauss filtering in arid environments is also visible in the time series of AMSR-E data for one pixel in Africa in Figure 6.3.

The results from row 1 to row 5 of Figure 6.2 show that the conversion into spherical harmonics and the Gauss filtering can modify the variation of soil moisture significantly, specifically in the world's large deserts. Therefore, those areas have to be masked when comparing harmonized soil moisture data sets with GRACE. Prior it has been suggested to mask areas of low variation by excluding pixels, which have a very low standard deviation with respect to the value range of the observed parameter (pixels with a standard deviation, which take values smaller than a certain percentage of the data range are excluded; see Abelen and Seitz, 2013). This approach has the disadvantage that it is sensitive to outliers, which can significantly increase or decrease the value range. Furthermore, the threshold for excluding pixels with a low standard deviation varies among data sets, as the relation between standard deviation and value range is not fixed.

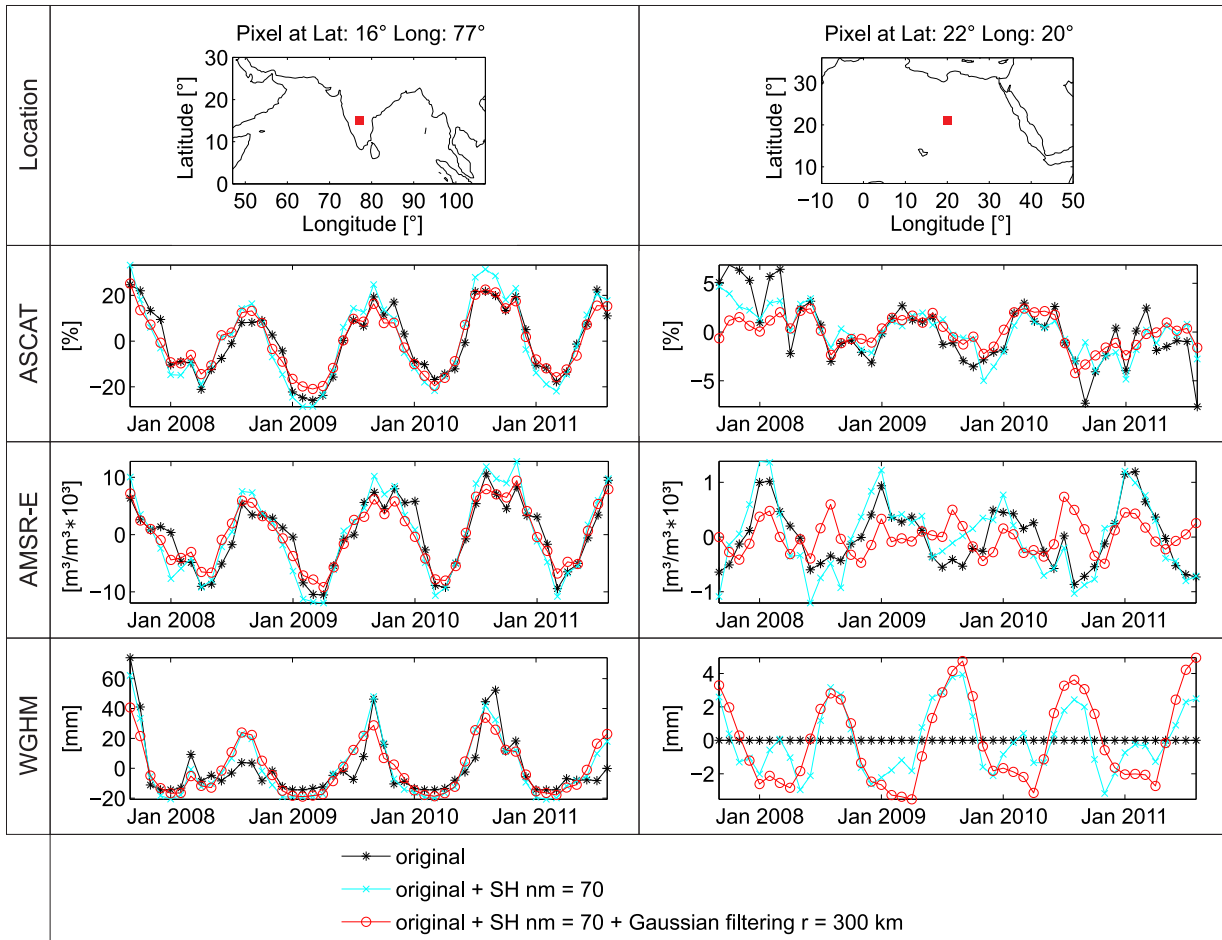


Figure 6.3: Time series showing impacts of data harmonization (conversion into spherical harmonics of degree and order 70, and Gauss filtering with a 300 km half-wavelength radius) for soil moisture variation (long-term mean for the time span September 2007 to August 2011 has been subtracted) from ASCAT (row 2), AMSR-E (row 3), and WGHM (row 4) at one location in India (column 1) and one location in the Sahara Desert (column 2).

Therefore, here another kind of masking is proposed, which excludes pixels where the correlation coefficients between the original time-series of a data sets and the harmoniously processed time series of the same data set take values lower than 0.7 (by lowering the threshold e.g. to 0.6 less values are excluded and by increasing the threshold e.g. to 0.8 more values are excluded). This threshold can be equally applied to all data sets. The resulting masks for the soil moisture data sets and TWS from WGHM are shown in Figure 6.4.

In row 6 of Figure 6.2 the correlation coefficients of row 4 are shown after those masks have been applied (the mask for soil moisture from ASCAT and WGHM in column 1, and the mask for soil moisture from AMSR-E and WGHM in column 2). As consequence mainly pixels over the world's large deserts with very low variation in soil moisture were excluded.

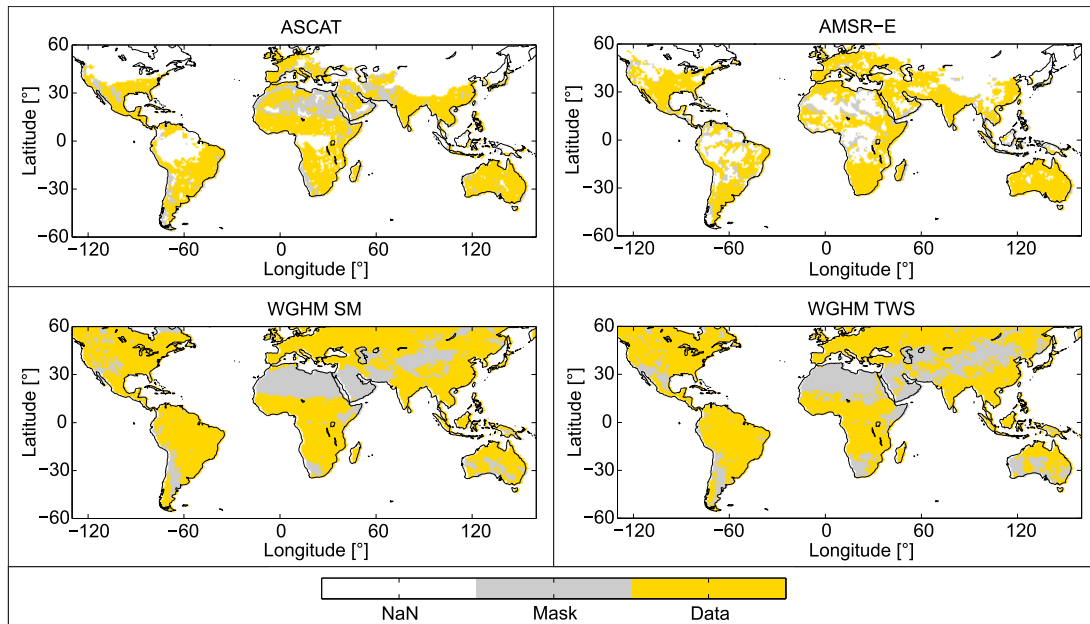


Figure 6.4: Masks for surface soil moisture from ASCAT (upper left), surface soil moisture from AMSR-E (upper right), root zone soil moisture from WGHM (lower left) and terrestrial water storage from WGHM (lower right), showing pixels, where the correlation coefficient between the original data and the harmonized data (after conversion in spherical harmonics and Gauss filtering) is lower than 0.7; NaN values are either over the oceans or result from the flagging of the input data (as described in the respective data description in Chapter 4).

6.2 Comparison of Soil Moisture Products

Next, the various soil moisture products are compared to gain information on the consistency of the data sets. Figure 6.5 shows the correlation coefficients for different pairs of soil moisture products (here the original monthly one degree gridded data is correlated). For the data pairs ASCAT and AMSR-E (row 1), and ASCAT and WGHM (row 2) correlation coefficients take in most regions of the world values of 0.7 or higher. For the data pair AMSR-E and WGHM (row 3) correlations are slightly lower, ranging mainly between 0.6 and 0.9.

For ASCAT data, deserts are an exception, where correlation values are lower than zero. The low quality of ASCAT data over arid regions, resulting from volume scattering of very dry sand, has been observed in various studies (see Section 2.4). For AMSR-E an exception is East and Southeast Asia. This region is partly covered by dense forests (e.g. in northeastern China; see Xiao et al, 2002), which is problematic especially for passive soil moisture retrieval (see Section 2.4). For the desert areas of western and southern Australia correlations are low for all data sets.

The identification of the described error patterns on the maps is possible due to the moderate flagging of soil moisture data from remote sensing (see Section 4.1 and Section 4.2), leaving the data coverage almost at global scale. When correlating those data sets with GRACE, the described quality issues of each data set need to be taken into account. However, in general a high agreement exist among the soil moisture data sets, specifically when considering that desert areas are to a large extent masked out after data harmonization to avoid artificial biases (see Section 6.1).

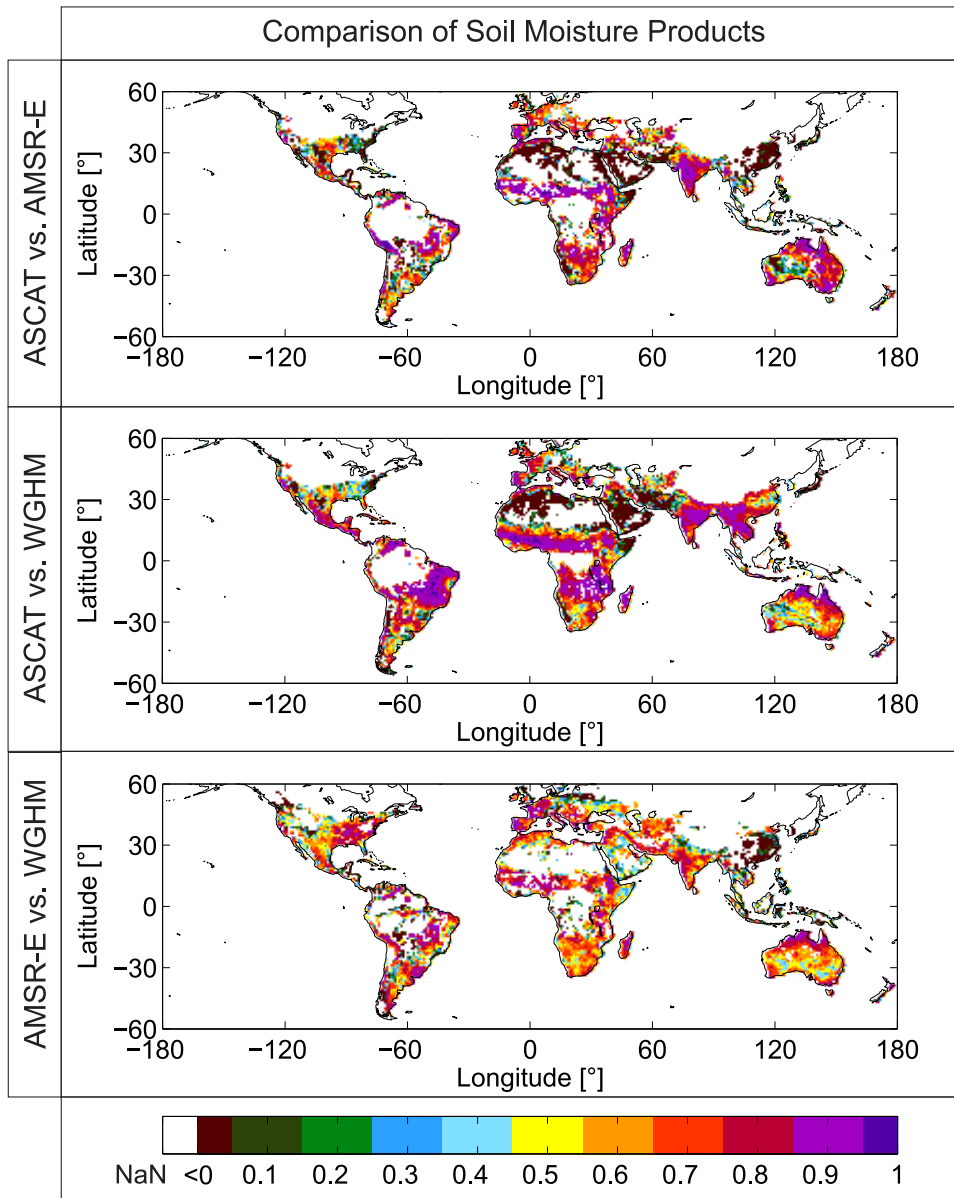


Figure 6.5: Correlation for the original soil moisture data of ASCAT and AMSR-E (row 1), ASCAT and WGHM (row 2), and AMSR-E and WGHM (row 3) over the time span September 2007 to August 2011 (in contrast to Figure 6.2 only positive correlation values are distinguished and the color scale is finer for positive values).

6.3 Comparison of Terrestrial Water Storage Products

In the following the two products for TWS from GRACE and WGHM are compared to assess the agreement between both data sets. Figure 6.6 shows that the correlation coefficients (row 1) take values of 0.7 or higher over wide areas around the world. Exceptions are for example the western part of the La Plata Basin in South America, several states of the US to the north of Mexico, large parts of China, and South Africa. In those regions also Schmidt et al (2008c) found large differences in the annual periods of TWS from GRACE and WGHM.

Other studies have shown that TWS from WGHM may be shifted with respect to GRACE data by a few months, because in the model water often drains too quickly from river basins (e.g. if groundwater recharge and volume are underestimated; Werth and Güntner, 2010; Schmidt et al, 2008c). This is also supported by Figure 6.6, which shows in the second row the time shift of TWS from WGHM with respect to GRACE and in the third row correlation coefficient for the time series of both data sets after implementing the time shift for WGHM. The map of time shifts is in agreement with the differences in annual phases between GRACE and WGHM provided by Schmidt et al (2008c), indicating that TWS from WGHM is preceding GRACE in several river basins.

The time shift between both data sets is shown exemplarily for the time series of one location in the USA and one location to the east of Aral Sea in Figure 6.7. It shows (in combination with Figure 6.6, row 3) that the implementation of the time shift does not necessarily improve the correlation significantly. For example for the location in the USA the correlation coefficient is after the time shift still as low as 0.2. In contrast for the location to the east of Aral Sea, there is a much higher agreement between the seasonal signals of both data sets after shifting the WGHM data back in time. An improvement is also visible for the Lower Amazon Basin (Figure 6.6, row 3), where the inundation storage is often underestimated by models (Swenson and Milly, 2006; Güntner, 2008).

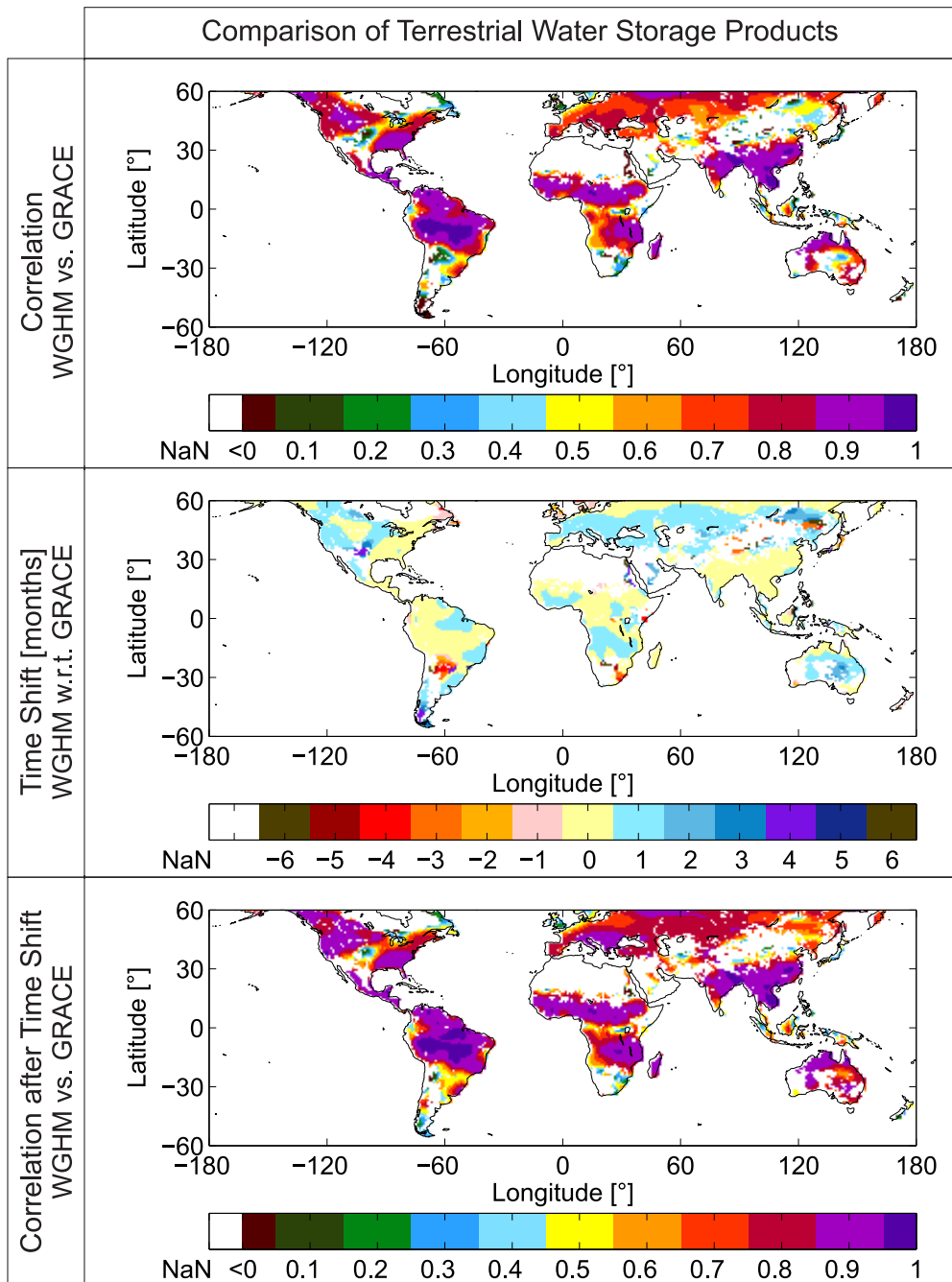


Figure 6.6: Correlation (row 1), time shift in months (row 2; negative values indicate that the seasonality of TWS from WGHM lags behind GRACE), and correlation after the implementation of time shift (row 3) for TWS from WGHM and GRACE, whereby both data sets have been harmoniously processed (subtraction of long-term mean, conversion into spherical harmonics of degree and order 70, and Gauss filtering with a 300 km half-wavelength radius) over the time span September 2007 to August 2011. Regions, which have artificial correlation coefficients (where the standard deviation of the original TWS signal from WGHM is equal zero) or are affected by PGR or other artifacts from the harmonious processing (see mask in the lower right of Figure 6.4 for TWS data from WGHM) have been masked out.

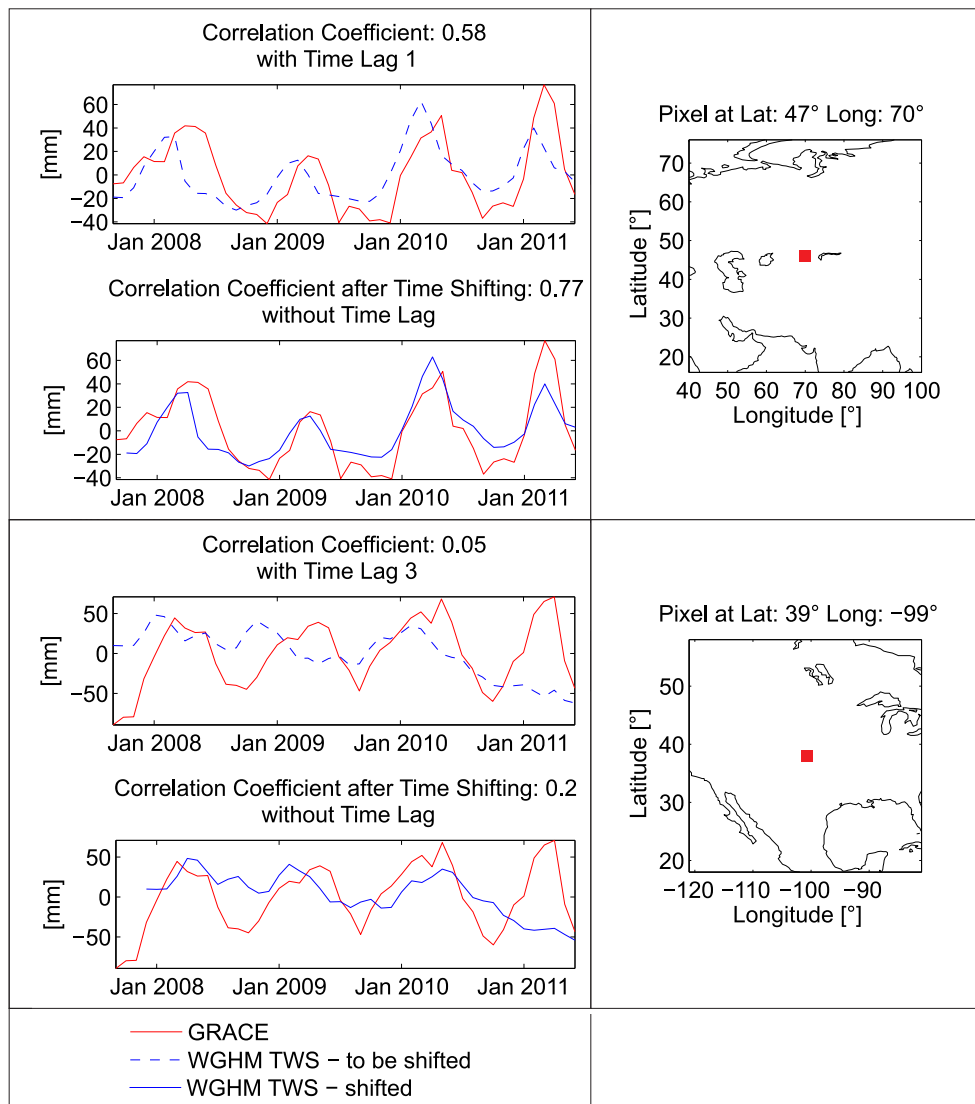


Figure 6.7: Time series, showing the impact of shifting TWS data from WGHM in time with respect to GRACE (both data sets have been harmoniously processed) for one location East to the Aral Sea (row 1) and one location in the USA (row 2).

6.4 Summary

This chapter addressed the first research question which focuses on the feasibility to compare the various data sets from soil moisture and TWS in terms of their different data structures (RQ 1a) and their consistency in information content (RQ 1b). In terms of the data structure specifically, the impact of the harmonious processing of all data sets was analyzed (see Section 6.1). Results show that the conversion into spherical harmonics and the transformation back in geographical grids of $1^\circ \times 1^\circ$ change the variation of soil moisture in at least two ways. Generally the spatial patterns become smoother, which in turn increases the correlation coefficients among the data sets (correlation coefficients may increase by 0.2). Secondly, observations which show very low or no variability (standard deviation is close to or equal zero) become biased and produce artificial or altered correlation coefficients.

For Gauss filtering similar impacts were observed. On the one hand the Gauss filtering again smoothes the data which leads to higher correlation coefficients (again in the order of up to 0.2). On the other hand the smoothing also causes leakage of surrounding areas into the signal. The leakage is specifically significant in regions where the magnitude of the actual signal is low and the signal of surrounding regions is relatively high. Therefore, biased observations resulting from the conversion into spherical harmonics in arid environments become additionally biased by Gauss filtering.

As consequence of artifacts which result from the conversion into spherical harmonics and the Gauss filtering pixels need to be masked where the original signal differs significantly from the harmoniously processed signal. Those regions are mainly located in the world's large deserts. In this study pixels are masked out where the correlation coefficient between the original signal and the harmoniously processed signal of the same data set is lower than 0.7.

In terms of data quality it was found that the soil moisture products are in high agreement over large parts of the world with correlation coefficients mostly above 0.7. Exceptions are again desert areas which are for the most part masked out after the harmonious processing (as described in the paragraphs above). However, the specific characteristics of each data set still have to be kept in mind when doing the comparison with GRACE, as for example AMSR-E data have lower quality in regions with dense vegetation cover (e.g., eastern China) and ASCAT data are prone to volume scattering in arid regions.

The analysis also showed that the two TWS products are consistent with correlation coefficients of 0.7 or higher in most parts of the world. However, in several river basins the seasonal signals are shifted, which may significantly lower the agreement of both data sets.

7 Hydrological Interdependencies

7.1 Analysis of Seasonal Amplitudes

As mentioned in Section 3.4 there are few studies which directly link “small” water storage components such as soil moisture or vegetation water content to GRACE measurements. This is due to the fact that the accuracy of GRACE is relatively low on smaller scales, taking values of approximately 40 mm when using a Gauss filter of 300 km half-wavelength (see Section 4.3). This means that changes in soil moisture will only be reflected in the GRACE signal if the variability, which is mostly dominated by the seasonal signal (Cazenave and Chen, 2010, suggest that in most basins 70-80% of the signal results from seasonal variation), lies above 40 mm over wide-ranging areas, which are several hundred square kilometers large. Furthermore, the variation in soil moisture might not be dominant, meaning that even if reaching above 40 mm it would be masked by much stronger variations from other storage components such as surface water or groundwater.

In this section the seasonal part of the signal and its anomaly are analyzed. Herein, the seasonal signal is defined as the average monthly variation of the signal (when looking at a time period of four years for each month four values are averaged, yielding 12 values, which describe the average annual signal). The anomaly is calculated by subtracting the seasonal signal from the entire signal (for each individual month the respective four year average of that month is subtracted, yielding 48 values, which describe the anomaly of each month with respect to the seasonal signal).

Figure 7.1a shows the seasonal amplitude of soil moisture based on the root zone soil moisture of WGHM. It emphasizes that the seasonal amplitude (herein defined as maximum value of the seasonal signal minus minimum value of the seasonal signal) is in several parts of the world above 40 mm. Some of the regions with variation in soil moisture above 100 mm are located in the world’s largest river basins such as the Amazon and Niger Basin. In these regions it is expected that despite of the large seasonal amplitude, the soil moisture signal is dominated by surface water.

Figure 7.1b indicates in which region of the world the variation (not the absolute amount) of a certain storage component is dominant, meaning that its seasonal amplitude is larger than the sum of the seasonal amplitudes of all other storage components. The map shows that in most parts of the world the variation of a certain storage component is dominant. In the northern hemisphere surface waters or snow and ice have the largest share of TWS with respect to the seasonal signals. In the southern hemisphere soil moisture plays a prominent role.

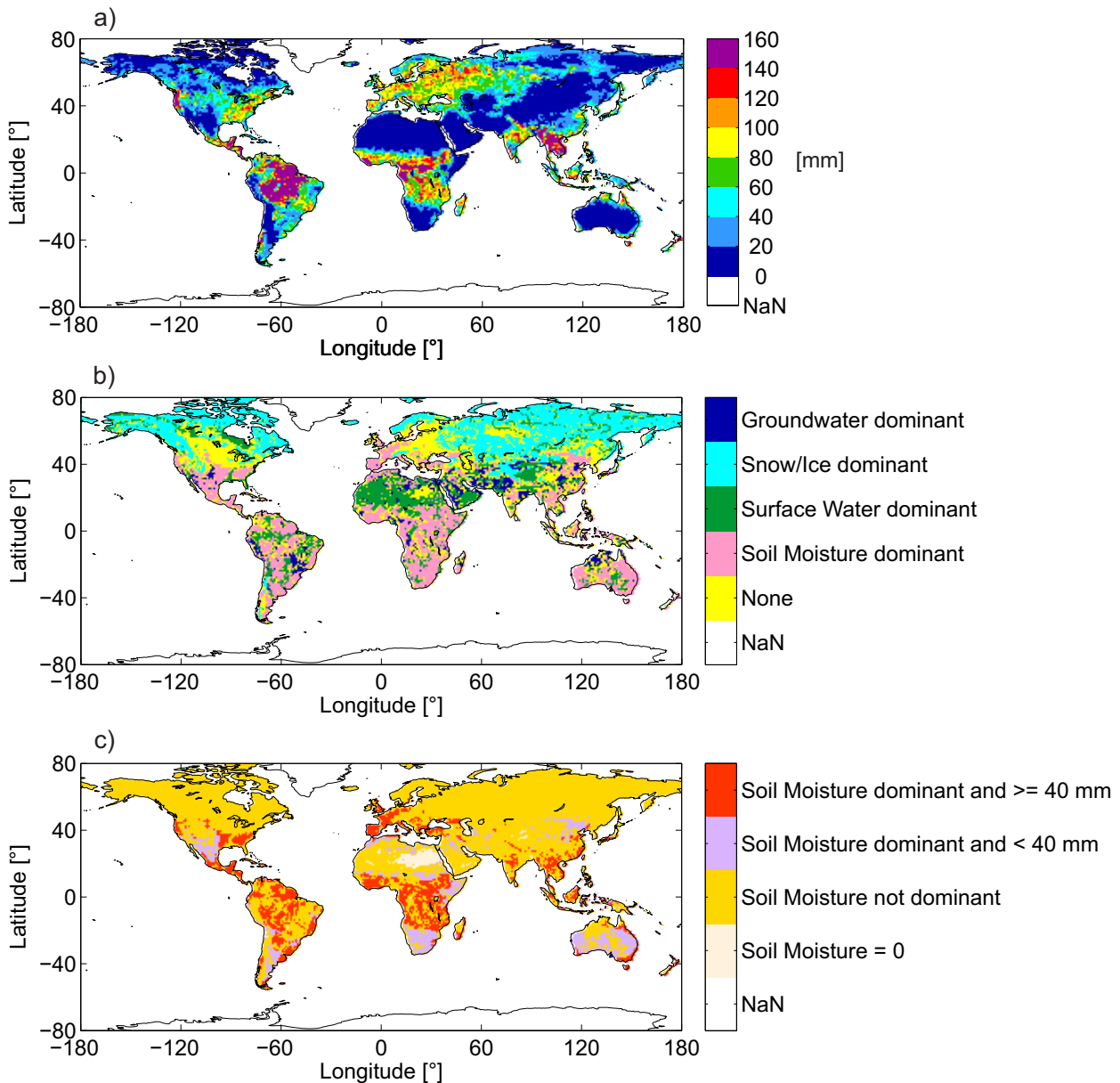


Figure 7.1: Global map showing a) the seasonal amplitude (maximum value of seasonal signal minus minimum value of seasonal signal) of root zone soil moisture from WGHM over the time period September 2007 to August 2011, b) the storage component which dominates all other seasonal signals (the seasonal amplitude of a certain component is bigger than the sum of all other individual seasonal amplitudes, whereby “None”, indicates that no single storage component dominates all others), and c) regions where the seasonal amplitude of soil moisture is dominant and takes values of 40 mm or higher (herein shown in dark orange).

Figure 7.1c links the information of Figure 7.1a and b, highlighting regions where the variation in soil moisture is dominant and at the same time has a seasonal amplitude, which is large enough to be captured by GRACE. Especially between latitudes 5°N to 30°S these two criteria are over large areas fulfilled. This emphasizes that there are regions in the world where it can be expected that soil moisture contributes to the largest part to the seasonal signal of GRACE, and therefore should have a stronger

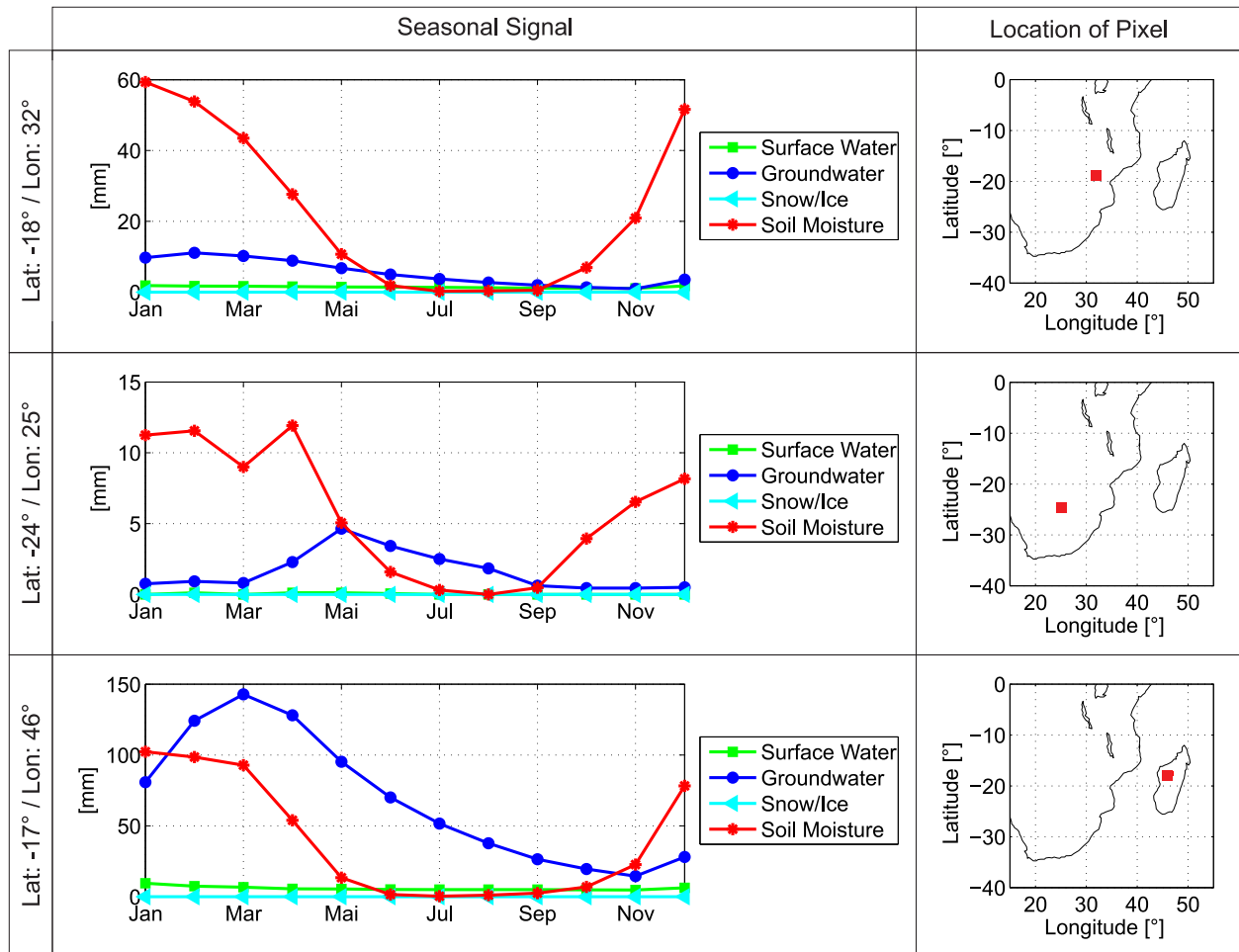


Figure 7.2: Seasonal signal for the time period September 2007 to August 2011 for surface water, groundwater, snow and ice, and root zone soil moisture from WGHM, for a) an example location (row 1, column 2) where the seasonal amplitude of soil moisture is higher than 40 mm and bigger than the sum of all other individual seasonal amplitudes (row 1, column 1), b) an example location (row 2, column 2) where the seasonal amplitude of soil moisture is lower than 40 mm but still bigger than the sum of all other individual seasonal amplitudes (row 2, column 1), and c) an example location (row 3, column 2) where the seasonal signal of soil moisture is not dominant (in this case it is the seasonal signal of groundwater; row 3, column 1).

link to TWS than other hydrological components. This result is also supported by Figure 7.2, showing in the first row for a location in the eastern part of South Africa (Latitude: -18° , Longitude: 32°) the strong seasonal variation of soil moisture with respect to other storage components. In the second and third row examples are given for the case that the seasonal signal of soil moisture is dominant but has a low amplitude (row 2) and for the case that the seasonal signal of soil moisture is high in amplitude but not dominant (row 3). Although the seasonal signal normally reflects the largest part of the signal (Cazenave and Chen, 2010), there are also regions where the amplitude of the anomaly is larger than the seasonal amplitude (as for example in the Pampas region in the La Plata Basin; see Section 8.3). In these areas variations in soil moisture might dominate the seasonal signal but not necessarily the entire signal, if the anomaly of other storage components is much larger than the one of soil moisture.

7.2 Interdependency of Soil Moisture and Terrestrial Water Storage

One main objective of this section is to analyze if soil moisture and TWS are interrelated. Figure 7.3 shows in the first column global maps with the correlation coefficients for the various soil moisture data sets in combination with GRACE. The maps indicate that soil moisture and TWS are over wide regions of the world closely linked with correlation coefficients above 0.6. Especially in humid climate zones like the Amazonian region and south and south-east Asia correlation coefficients are above or equal 0.7. But also in the semi-arid Sahel zone correlation coefficients are high. In the Kalahari Desert in southern Africa all soil moisture data set show no agreement with GRACE.

The second column of Figure 7.3 shows the time shifts between soil moisture and GRACE, which range between zero and two months. In areas where AMSR-E data has low quality as for example in eastern China (see Section 6.2), the time shift for AMSR-E with respect to GRACE is unrealistically high and reflects the low agreement among those data sets in this region (which is reflected by low correlation values in the first column). For ASCAT data the same phenomena occurs over the northern part of Morocco and Tunisia, as in arid environments the quality of soil moisture data from ASCAT is low (see Section 2.4). In the Kalahari Desert in southern Africa all soil moisture products are in relatively low agreement (see Figure 6.5). Therefore, the low correlation values and the extremely high time shifts rather indicate that the two hydrological quantities soil moisture and TWS are not strongly interrelated in this region (also see Section 7.3).

Figure 7.4 shows how soil moisture and TWS are correlated if the signal is split into a seasonal component (column 1) and its anomaly (column 2). For the seasonal signal correlations are very similar to the ones of the entire signal, shown in Figure 7.3. This is expected as the seasonal component is in most areas the dominant part of the entire signal (Cazenave and Chen, 2010). For the anomaly correlations are much lower taking values of around 0.4. Only in a few parts of the world like in the La Plata Basin (this region is analyzed in detail in Chapter 8) and in Australia (this region would be interesting to look at in a future study, see Chapter 10) correlation coefficients take values above 0.7. In eastern China for the satellite soil moisture products the correlation is higher for the anomaly than for the seasonal signal, indicating that the satellite signal might be disturbed by a strong seasonal component, which could be for example the seasonal change of vegetation. Another explanation could be that the surface soil moisture from satellites is not able to map the seasonal change in TWS in this region as the storage capacity of the root zone plays a large role there (see Figure 4.3). Also other storage components might dominate the signal (see Section 7.3).

In Figure 7.5 and Figure 7.6 the results of the first column of Figure 7.3 are combined and the correlation values of different data pairs are compared. Figure 7.5a shows in which regions ASCAT and Figure 7.5b shows in which region AMSR-E correlates better, worse or similar with TWS from GRACE than with soil moisture data from WGHM. It is expected that the soil moisture products show a higher agreement among each other than with respect to GRACE. Therefore, regions which show higher agreement with GRACE (marked in red herein) may indicate areas where the WGHM needs to be improved (as for example in eastern Australia, see Figure 6.5) or where the quality of the satellite soil moisture products is low (as for example in Mexico for AMSR-E, see Figure 6.5).

In general there are few regions in both maps where GRACE correlates better with one of the soil moisture products, as for example in the North China Plain and around Texas for ASCAT, and in Mexico, the North China Plain, parts of South East Asia, and eastern Australia for AMSR-E. Furthermore, both data sets show higher correlation values with GRACE for India. The regions highlighted here are slightly different to the ones shown by Abelen and Seitz (2013), because in this study a later version of WGHM and a later TWS product from GRACE is used. Based on the maps of Abelen and Seitz

(2013) and the maps shown in Figure 7.5 there is for the later data versions a better agreement among the soil moisture products in the southern USA. However, for other regions the agreement seems to be lower in comparison with GRACE as for example in India.

Figure 7.6 shows in which regions of the world TWS from GRACE correlates better, worse or similar with soil moisture from ASCAT (Figure 7.6a) or AMSR-E (Figure 7.6b) than with soil moisture from WGHM. In both maps clear patterns are visible, which can be to a large extent related to the soil moisture regime map, provided by the Soil Science Division of the Natural Resource Conservation Service of the United States Department of Agriculture (NRCS-USDA, 1997). ◁ The comparison of Figure 7.6 with the map of the world's soil moisture regimes shows in accordance with the results of Abelen and Seitz (2013) that:

1. ASCAT or AMSR-E correlate better than WGHM with GRACE in
 - ustic regimes (semi-arid climate): southern part of the Great Plains, USA; North-East Brazil; Africa's savanna, scrub and woodland; India
 - aridic regimes (arid climate): world deserts like the deserts of Australia (an exception is the Kalahari Desert in Africa)
2. ASCAT or AMSR-E correlate worse than WGHM with GRACE in
 - udic regimes (humid or subhumid climate): Eastern USA; Brazil; China
 - xeric regimes (Mediterranean climate): Mediterranean countries; Western Australia
3. ASCAT or AMSR-E correlate similar than WGHM with GRACE in
 - the transitions zones between different regimes.

In summary there is a higher agreement between satellite soil moisture and GRACE TWS in arid and semi-arid environments, and a higher agreement between WGHM and GRACE in humid and Mediterranean environments. This observation is in concordance with the characteristics of each soil moisture data set. ASCAT and AMSR-E deliver information on soil moisture for the soil surface, as the signal only penetrates a few centimeters into the ground. On a daily basis it is able to capture short-term variations. This functionality is favorable for arid environments. Soil moisture changes quickly and mainly at the surface, as precipitation evaporates rapidly due to high solar radiation. In addition, surface soil moisture is more likely to present the moisture in the whole soil column as the soil layer is shallow and its water holding capacity is low. Also soil moisture has a proportionally large impact on the whole water balance as there are fewer surface water bodies and there are only low variations in (fossil) ground water, unless excessively used by humans. It is therefore expectable that surface soil moisture from satellites shows similar variations in arid climate regimes as TWS from GRACE. In contrast, the hydrological model shows lower correspondence since it is more difficult to model fast changes in those highly sensible environments, where often less data from river gauges are available for the calibration of the model.

In humid climate regimes it is expected that deeper soil layers have a larger correspondence to TWS, since the water holding capacity is high and the soil profile reaches several meters into the ground. Consequently, changes in surface soil moisture are less representative for changes in total soil moisture, and along with this also for changes in TWS. This behavior is also reflected in the result of the correlation analysis: in humid climate regimes (like in large parts of Asia) surface soil moisture from ASCAT and AMSR-E showed lower correlations with GRACE than root zone soil moisture from WGHM (see Figure 7.3). ▷ (Abelen and Seitz, 2013)

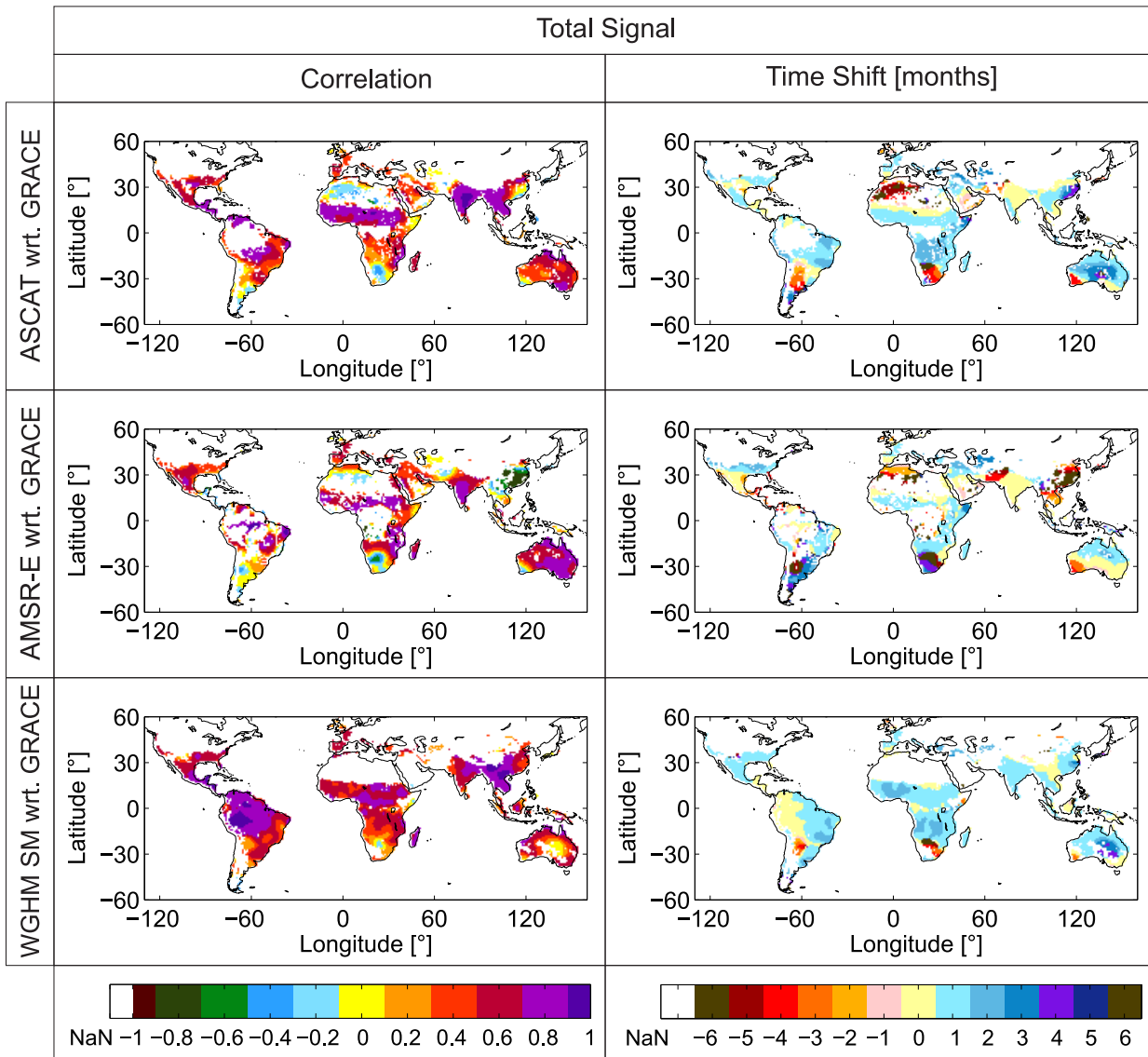


Figure 7.3: Correlation (without time shift; column 1) and time shift in months (column 2; positive values indicate that soil moisture changes prior to TWS from GRACE) for surface soil moisture from ASCAT and TWS from GRACE (row 1), surface soil moisture from AMSR-E and TWS from GRACE (row 2) and root zone soil moisture from WGHM and TWS from GRACE (row 3), whereby all data sets have been harmoniously processed (subtraction of long-term mean, conversion into spherical harmonics of degree and order 70, and Gauss filtering with a 300 km half-wavelength radius) over the time span September 2007 to August 2011, and regions have been masked which are subject to PGR, covered by snow or ice or are significantly affected by the harmonious processing.

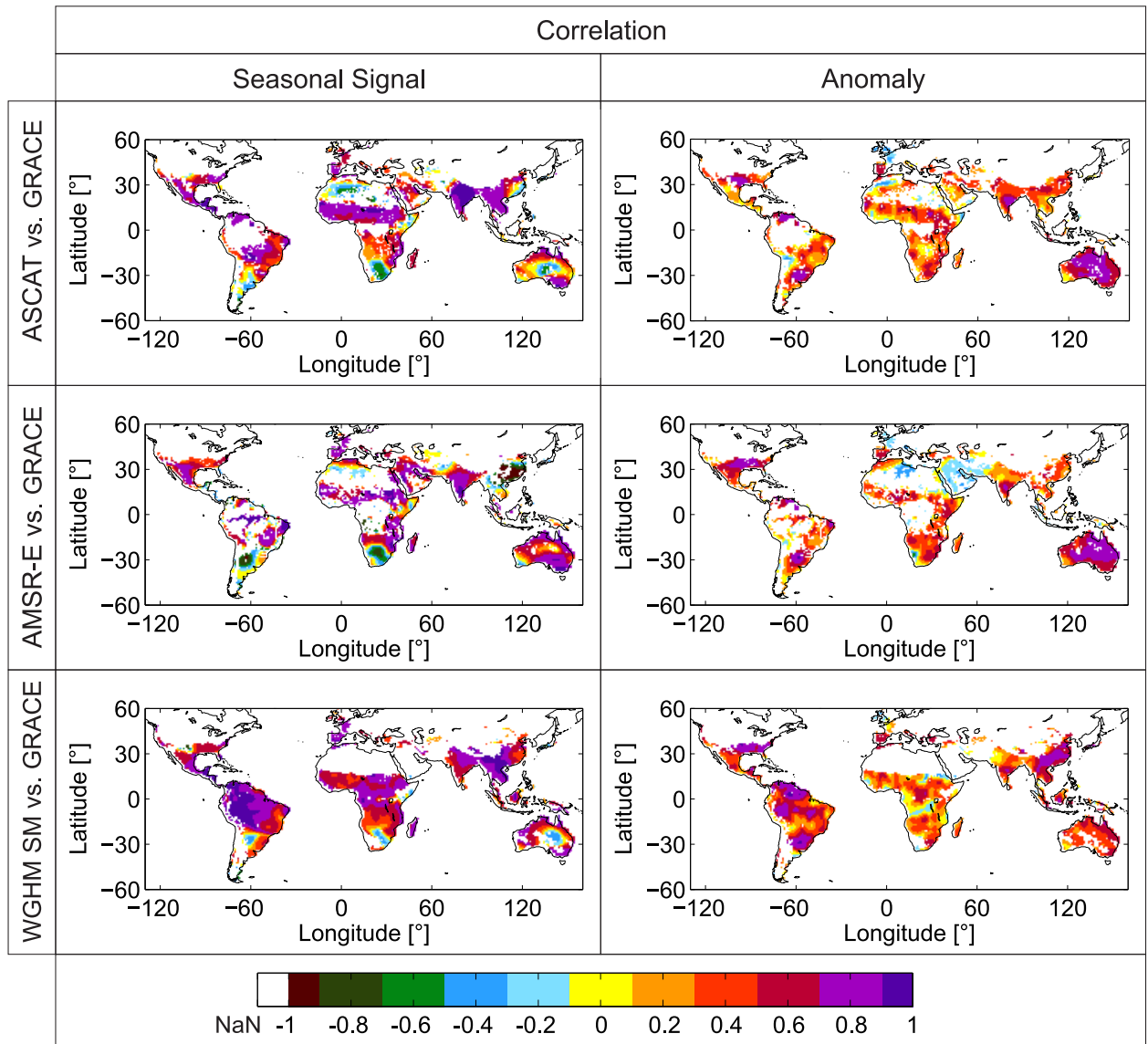


Figure 7.4: Correlation for the seasonal signal (column 1, all values of the same month over the observed time-span are averaged, resulting in twelve average values for each month) and the seasonal anomaly (column 2, variation with respect to the seasonal signal) for surface soil moisture from ASCAT and TWS from GRACE (row 1), surface soil moisture from AMSR-E and TWS from GRACE (row 2) and root zone soil moisture from WGHM and TWS from GRACE (row 3), whereby all data sets have been harmoniously processed (subtraction of long-term mean, conversion into spherical harmonics of degree and order 70, and Gauss filtering with a 300 km half-wavelength radius) over the time span September 2007 to August 2011, and regions have been masked which are subject to PGR, covered by snow or ice or are significantly affected by the harmonious processing.

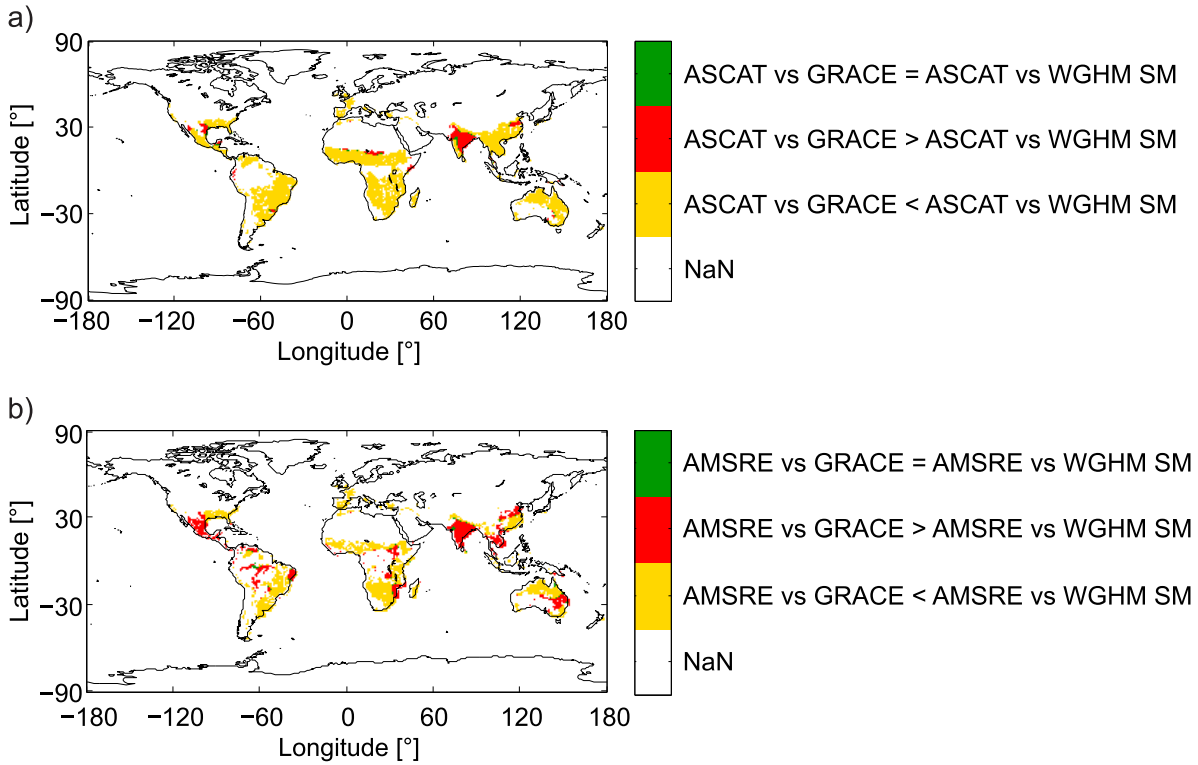


Figure 7.5: Map indicating in which regions of the world a) ASCAT or b) AMSR-E correlates better, worse or similar with TWS from GRACE than with soil moisture from WGHM.

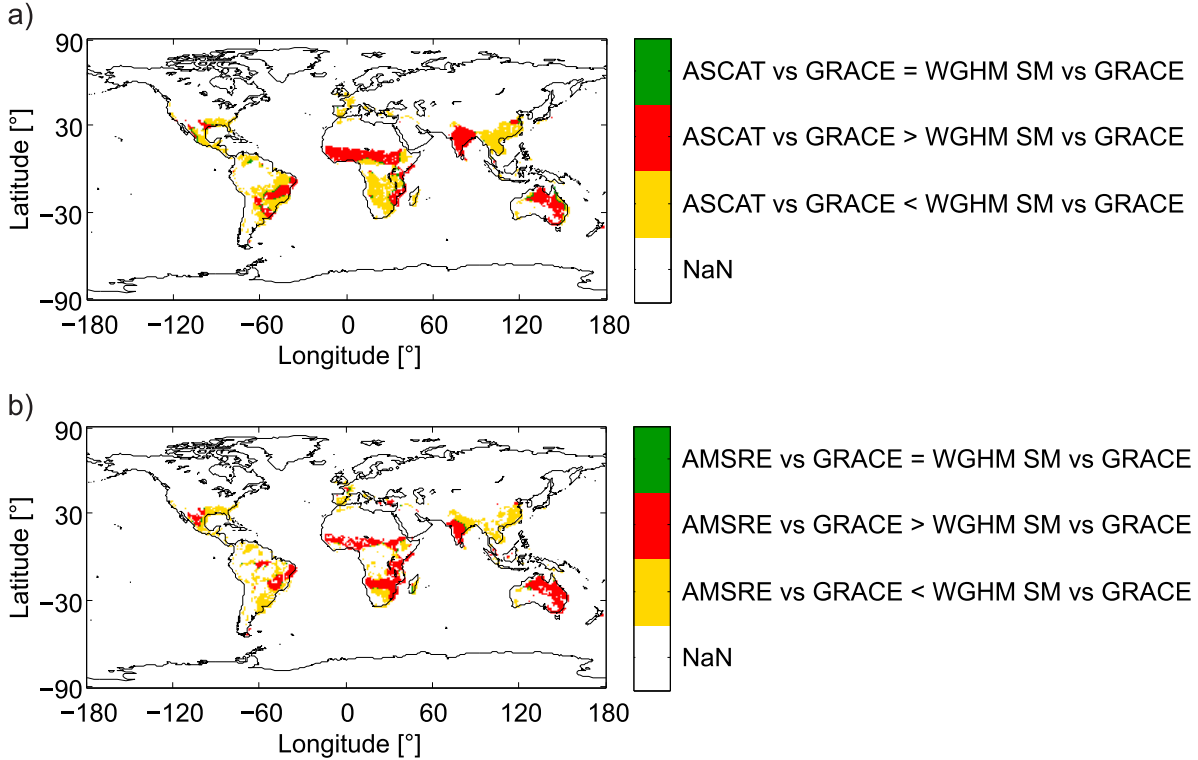


Figure 7.6: Map indicating in which regions of the world TWS from GRACE correlates better, worse or similar with soil moisture from a) ASCAT or b) AMSR-E than with soil moisture from WGHM.

7.3 Interdependencies with other Hydrological Parameters

To further analyze why in certain regions the soil moisture products are in high or low agreement with GRACE, this section focuses on the interrelation of here exemplarily the soil moisture product ASCAT with precipitation from GPCC, and with surface water (SUR) and groundwater (GW) from WGHM (see Figure 7.7).

As expected precipitation shows the highest correlation with soil moisture and positive phase shifts, indicating that it takes time until changes in precipitation translate into changes in soil moisture. In regions where soil moisture and TWS correlate well, there is generally also a high agreement between the variation of surface water and soil moisture, or groundwater and soil moisture. For example in India soil moisture and TWS are highly correlated (see Figure 7.3). In eastern India soil moisture correlates well with surface water and groundwater, which dominate the seasonal signal in this region (see Figure 7.1b). In western India soil moisture and surface water are strongly linked. Also in northern Australia, where the variation in groundwater is dominant (see Figure 7.1b), the correlation between soil moisture and GRACE is very similar to the correlation between soil moisture and groundwater. In south-east Asia and southern China all main storage components are closely linked with correlation coefficients of 0.6 or higher.

An exception is the Sahel zone. In this region soil moisture correlates very well with TWS from GRACE but the other storage components surface water and groundwater show lower agreement with soil moisture. This emphasizes that in this region variations in soil moisture play a significant role in the water balance (as indicated in Figure 7.1) and that the variation is large enough to be sensed by GRACE. This finding is also supported by Figure 7.8, which shows for two locations in the Sahel zone the strong seasonal signal of soil moisture and its time shift with respect to the other storage components. The time series also show that the seasonal signal of GRACE is shifted forward in time with respect to the seasonal signal of groundwater and surface water due to the early seasonal phase of soil moisture.

The time shifts in the second column of Figure 7.7 show similar patterns for groundwater, surface water and GRACE. The lack in time shift for example between surface water and groundwater might be one reason why the model usually is ahead in time (see Section 6.3) and indicates as already emphasized in other studies that inundation might not be properly modeled (Swenson and Milly, 2006; Güntner, 2008).

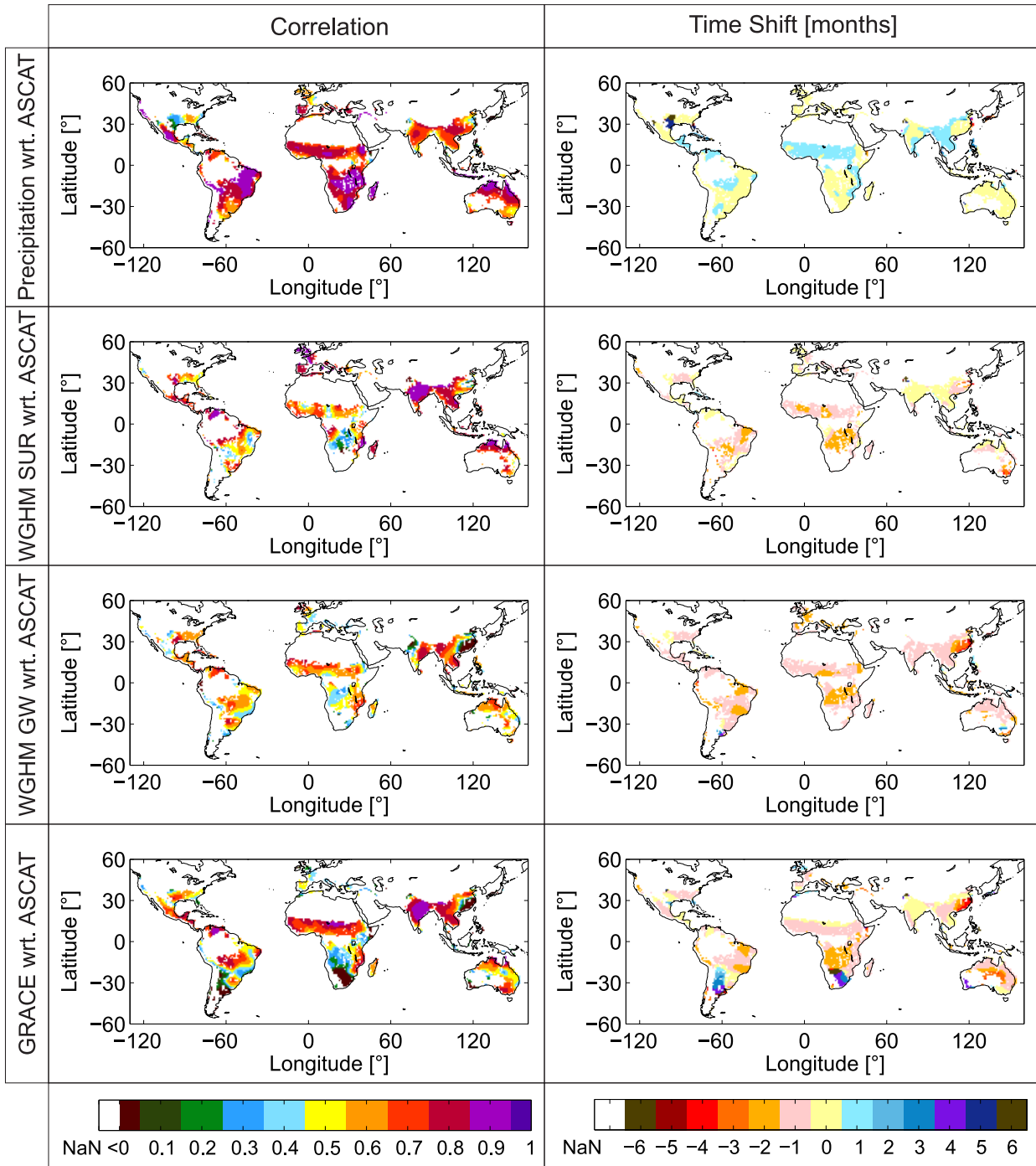


Figure 7.7: Correlation (without time shift; column 1) and time shift in months (column 2; positive values indicate e.g. that precipitation from GPCC changes prior to soil moisture from ASCAT) for precipitation from GPCC (row 1), surface waters from WGHM (row 2), groundwater from WGHM (row 3), or TWS from GRACE (row 4) with respect to soil moisture from ASCAT, whereby all data sets have been harmoniously processed (subtraction of long-term mean, conversion into spherical harmonics of degree and order 70, and Gauss filtering with a 300 km half-wavelength radius) over the time span September 2007 to August 2011, and regions have been masked which are subject to PGR, covered by snow or ice, are significantly affected by the harmonious processing, or are very dry with an annual average sum of monthly precipitation equal or lower than 300 mm (as ASCAT has low quality in those areas).

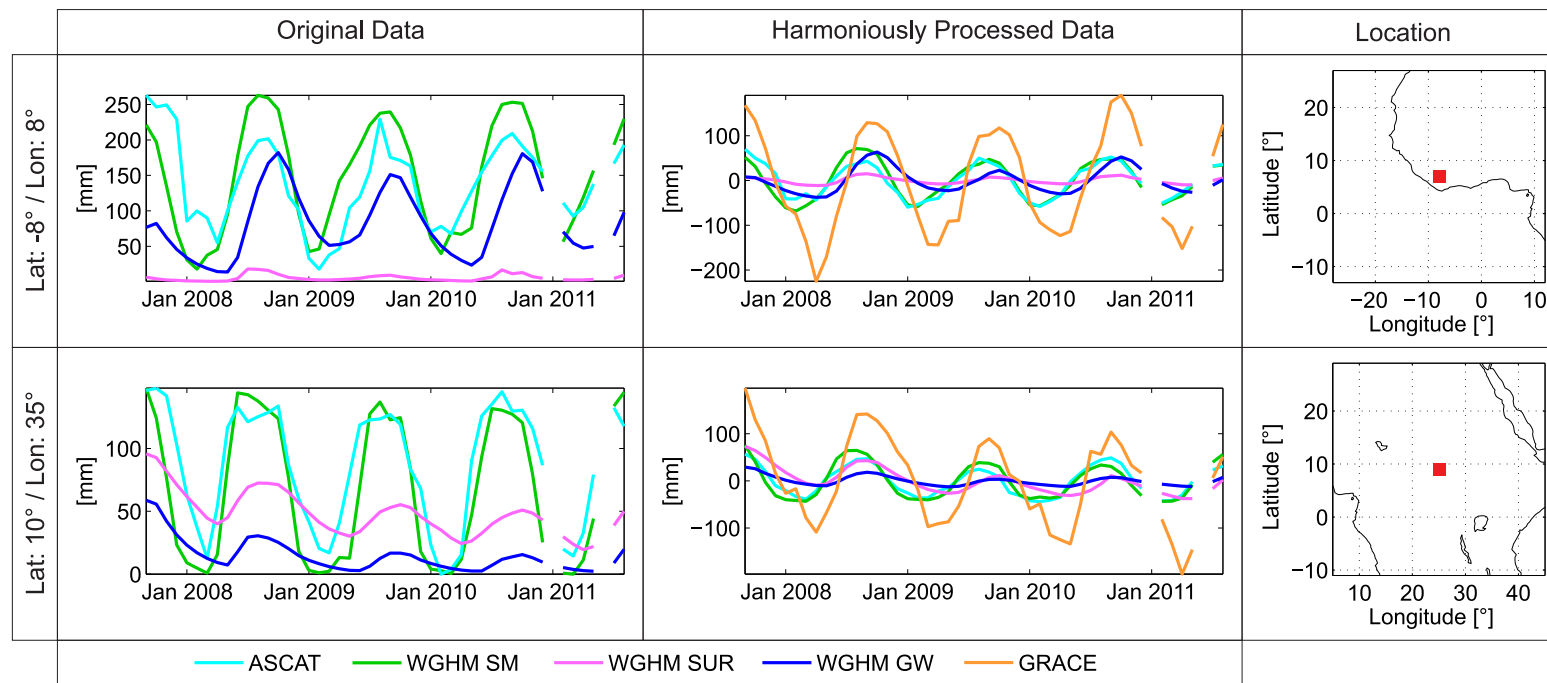


Figure 7.8: Time series showing the dynamics of soil moisture from ASCAT and WGHM (ASCAT data are scaled with respect to WGHM; see Section 5.3) in comparison to the dynamics of other water storage components from WGHM and TWS from GRACE for two locations in the western (row 1) and central (row 2) Sahel zone; the first column shows the original data and the second column shows the harmoniously processed data (subtraction of long-term mean, conversion into spherical harmonics of degree and order 70 and Gauss filtering with a 300 km half-wavelength radius).

7.4 Summary

In this chapter it has been analyzed where and why soil moisture and TWS dynamics are linked (RQ 2). In terms of the magnitudes of seasonal cycles (RQ 2a), it has been found that in most parts of the world a certain water storage component dominates the seasonal signal. Soil moisture dominates most regions south of the equator, snow and ice mainly polar regions e.g. in Russia and Canada, and surface water and groundwater mostly desert regions like the Sahara. Regions where soil moisture dominates the seasonal signal and where its seasonal amplitude is larger or equal to 40 mm (and with it should be reflected in the GRACE signal) are mainly located in central America, central Africa, south-east Asia and southern Europe. This result (which is only based on WGHM as the other soil moisture products do not provide root zone soil moisture) indicates that there are several regions in the world where soil moisture largely impacts TWS and represents not a “small” but a significant part of the seasonal TWS signal. In regions where the entire signal is dominated by anomalies (like e.g. in the Pampas region of the La Plata Basin; see Section 8.3) additional information on the amplitudes of anomalies is needed to conclude on the significance of soil moisture for the entire signal (and not only for the seasonal signal).

In terms of correlations and time shifts between the soil moisture data sets and GRACE (RQ 2b), it has been found that correlations between the entire signals mainly result from high correlations between seasonal signals (as correlation patterns for the entire signals and for seasonal signals are very similar). However, in some regions correlations are also high for seasonal anomalies like in the La Plata Basin, and in parts of Australia and India. Time shifts between soil moisture and TWS range between 0 and two months. In regions of low data quality (e.g. in south-east Asia and southern China for AMSR-E) time shifts are much higher, reflecting the low agreement among data sets.

The findings in terms of the magnitude of correlations between soil moisture and TWS (RQ 2b) and in terms of interdependencies of soil moisture and other storage components (RQ 2c) are exemplarily summarized in Table 7.1 for some regions of the world. Also information on the consistency among the soil moisture products and the TWS products from Section 6.2 and Section 6.3 is included in the table. The focus is on humid and arid regions of the world (polar regions are excluded as they receive snowfall and may be covered by ice; see Section 5.1), whereby humid areas refer to udic and xeric soil moisture regimes and arid areas refer to ustic and aridic regimes, herein (NRCS-USDA, 1997).

In general the results show that there is a higher correlation between soil moisture and TWS in humid areas around the equator than in arid environments. This information mainly results from the correlation of soil moisture data from WGHM with TWS data from GRACE, as the satellite soil moisture products do not provide information on soil moisture over regions with dense vegetation cover. For example ASCAT and AMSR-E data are not available over the Amazon, which is why the quality of the soil moisture data from WGHM cannot be assessed in this region with the data sets used in this study (as indicated in Table 7.1). Also humid regions that have not been masked during preprocessing may show low data quality for satellite soil moisture products. For example in eastern China no soil moisture data pair shows high correlation values. The low data quality also explains why the soil moisture data sets are neither in agreement with groundwater or surface water dynamics nor with variations of TWS from GRACE in this region.

For southern China and Myanmar the data quality of AMSR-E remains low, but soil moisture variation from ASCAT and WGHM are in agreement. The high correlation coefficients (meaning greater than or equal to 0.6 herein) of ASCAT and WGHM with respect to GRACE in this region can be related to the fact that soil moisture is also closely linked to the partly dominating storage components surface water and groundwater.

Table 7.1: Summary of findings about consistencies among soil moisture and TWS products and about interrelations between soil moisture and TWS, and soil moisture and other storage components for selected humid and arid regions of the world.

High: correlation ≥ 0.6 Low: correlation < 0.6	Humid Soil Moisture Regimes (udic and xeric)			Arid Soil Moisture Regimes (ustic and aridic)			
	Southern China / Myanmar	Eastern China	Amazonas	Eastern Australia	Kalahari Desert	India	Sahel Zone
Seasonal signal dominated by:	Mix of all	Mix of all	Soil moisture and surface water	Soil moisture (< 40 mm)	Soil moisture (< 40 mm)	Mix of all	Soil moisture (≥ 40 mm) / None
Agreement among soil moisture data sets:	ASCAT: high AMSRE: low WGHM: high	ASCAT: low AMSRE: low WGHM: low	ASCAT: - AMSRE: - WGHM: ?	ASCAT: high AMSRE: high WGHM: low	ASCAT: high AMSRE: high WGHM: low	ASCAT: high AMSRE: high WGHM: high	ASCAT: high AMSRE: high WGHM: high
Agreement among TWS products (GRACE and WGHM):	high	high	high	low	low	high	High
Correlation of soil moisture products with TWS:	ASCAT: high AMSRE: low WGHM: high	ASCAT: low AMSRE: low WGHM: low	ASCAT: - AMSRE: - WGHM: high	ASCAT: low AMSRE: high WGHM: low	ASCAT: low AMSRE: low WGHM: low	ASCAT: high AMSRE: high WGHM: high	ASCAT: high AMSRE: high WGHM: high
Correlation of ASCAT and surface water from WGHM:	high	low	-	low	low	high	low
Correlation of ASCAT and groundwater from WGHM:	high	low	-	low	low	high and low	low

The analysis of dry regions mainly focuses on semi-arid regions. This is due to the fact that hyper-arid deserts and most arid regions are masked out after the harmonious processing to avoid artifacts from the conversion into spherical harmonics and the spatial smoothing (see Section 6.1). Furthermore, ASCAT data have low data quality in dry sandy regions due to volume scattering effects (see Section 2.4).

The results of two arid to semi-arid regions, which include eastern Australia and the Kalahari Desert in southern Africa, show that soil moisture is not closely related to TWS, although the variation in soil moisture is dominant. This is mainly due to the fact that the amplitude of the seasonal soil moisture signal is lower than 40 mm (see Figure 7.1). Also soil moisture does not correlate well with surface water and groundwater in these two regions. A contrasting example is the Sahel Zone. In this semi-arid region the variation of soil moisture is over large areas in low agreement with the variation of surface water and groundwater. However, soil moisture and TWS are still interrelated. This can be explained by the fact that the variation in soil moisture is dominant and that the amplitude of the seasonal soil moisture signal is larger than 40 mm. This indicates that in the Sahel zone the GRACE signal can only be understood if soil moisture is considered as a significant contributing storage component to changes in TWS.

Another region where all soil moisture products are highly correlated with TWS from GRACE is India. As various storage components dominate different parts of India, the correlation is based on the high interdependence of soil moisture, surface water and groundwater in this region.

8 Hydrological Extremes in Soil Moisture and Terrestrial Water Storage

8.1 Study Area: La Plata Basin

The results of Section 7.2 indicate that soil moisture and TWS are closely linked in many parts of the world, not only with respect to seasonal signals but also in terms of seasonal anomalies. Specifically for the La Plata Basin the anomalies of the various soil moisture products are highly correlated with GRACE (see Figure 7.4). These findings suggest that the combination of soil moisture and GRACE data can contribute to a better understanding of hydrological extremes in this river basin. Therefore, this chapter explores exemplarily for the La Plata Basin the potential of combining soil moisture and TWS data for the monitoring of extreme weather events. The focus is on destructive events, which had significant impact on society.

◁ The La Plata Basin is the world's fifth largest river basin and covers parts of Argentina, Brazil, Bolivia, Paraguay, and Uruguay (Chen et al, 2010b). It has three main contributing rivers: the Paraguay, Paraná, and Uruguay Rivers. Despite of its large size of approximately 3,100,000 km² (Pereira et al, 2012), the region has low topographic complexity. This is favorable, especially for signals from active microwave systems that are degraded by mountainous terrain. The main land cover classes of the La Plata Basin are shown in Figure 8.1. The mean annual cycle of precipitation and river runoff varies significantly within the La Plata Basin (Su and Lettenmaier, 2009). The following description of the sub-regions outlined in Figure 8.1 is summarized from Caffera and Berbery (2006) (unless otherwise cited), who describe the climatology of the La Plata Basin in great detail.

- Southern cropland (Pampas; Figure 8.1, sub-region 1) and southern grassland (Campos; Figure 8.1, sub-region 6): The Pampas and the Campos are two major sub-regions of the major South American grassland, which stretches from the south of Brazil to Argentina, comprising more than 700,000 km². The climate changes from west to east from humid to dry-subhumid (Politis, 2008). The plain contains the most fertile soils of the La Plata Basin. The Campos has continental climate with frequent frost in winter and daily maximum temperature above 36 °C in summer. Rainfall is distributed throughout the year but changes strongly between years (Pallarés et al, 2005). The annual mean precipitation in the North (1600 mm) is larger than in the South (1200 mm). The Campos is mainly used for grassland-based livestock production (Viglizzo and Frank, 2006). This is different for the Pampas. This region is intensively used by agriculture. The climate is similar to the Chaco with the main precipitation falling from October to March.
- Western deciduous broadleaf forest (Chaco; Figure 8.1, sub-region 2): The Chaco is a subtropical area and located west of the Paraguay River and east of the Andes (Coronel et al, 2006). It is the warmest region in the La Plata Basin. In summer, the daily maximum temperature often exceeds 45 °C. The rainy season usually takes place between September and April. The semi-arid plains of the Chaco are dominated by dry woodland, which (approaching to the east) transform into more open savannas (Figure 8.1).

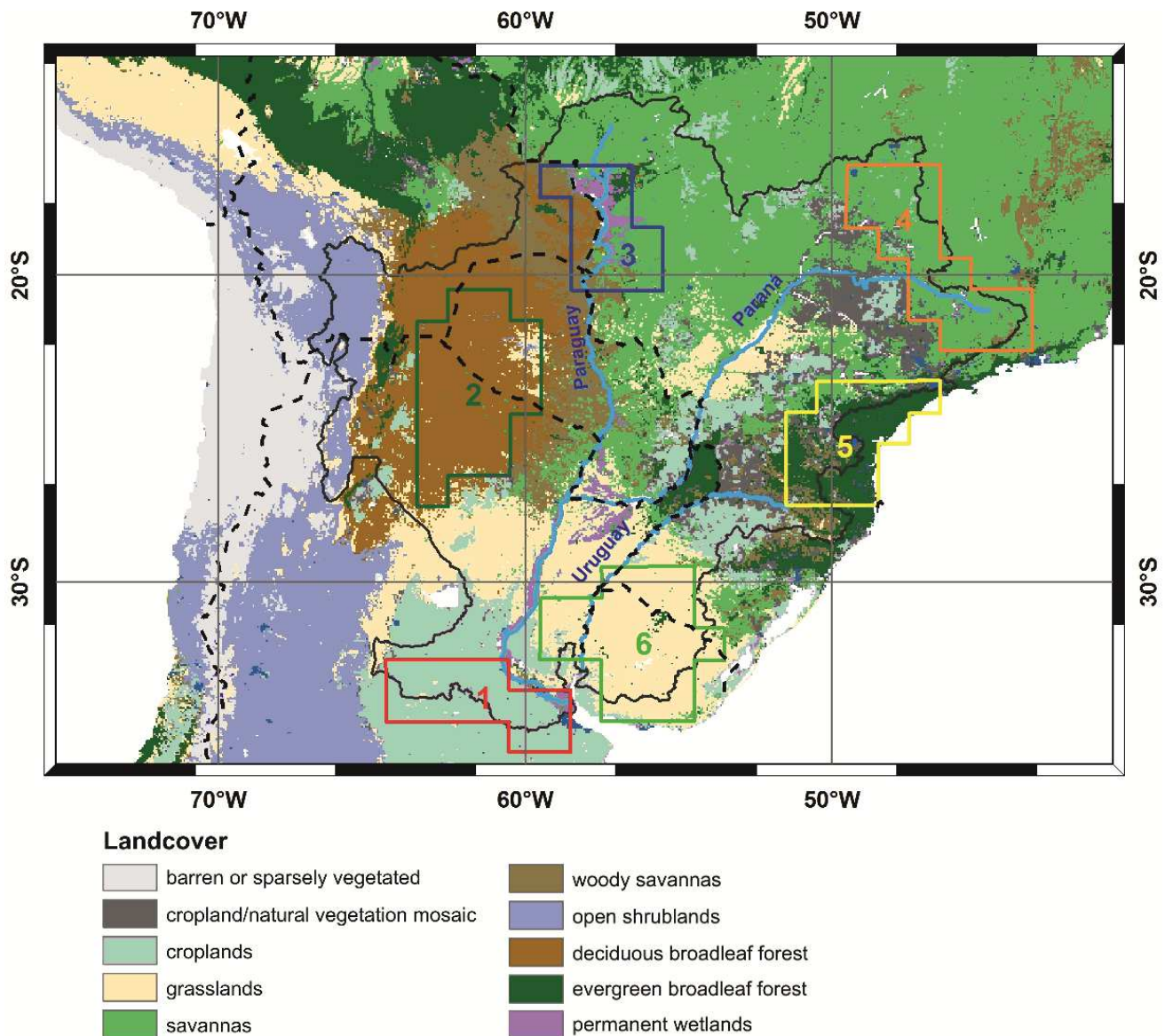


Figure 8.1: Land cover map of the La Plata Basin in South America (USGS, 2012) with its three main contributing rivers (Paraguay, Paraná, and Uruguay). The sub-regions selected for this study are shown with contours and include: 1, southern cropland (Pampas); 2, western deciduous broadleaf forest (Chaco); 3, wetland Pantanal; 4, northern savanna (Cerrado); 5, eastern evergreen broadleaf forest (Mata Atlantica); and 6, southern grassland (Campos). The black continuous line shows the outline of the La Plata Basin and the black dashed lines indicate the boundaries of the countries (as shown in Abelen et al, 2015).

- Wetland Pantanal (Figure 8.1, sub-region 3): The Pantanal is one of the world's largest wet lands with enormous biodiversity, covering about 100,000 km² of the Paraguay Basin (Berbery and Barros, 2002). It behaves as a regulator for the entire La Plata Basin, by slowing the streamflow of the Paraguay River before its junction with the Paraná River (Ferrazzoli et al, 2010). Annual totals of precipitation exceed 1300 mm. In December, the precipitation maximum takes place, reaching about 200 mm. In July and August, the precipitation is close to zero (Garcia, 1996).

- Northern savanna (Cerrado; Figure 8.1, sub-region 4): The Cerrado is a rather moist savanna region with an average annual precipitation of around 1500 mm. The climate is seasonal with a very strong dry period, spanning from April to September. The temperatures are mild, ranging from 22 to 27 °C. Large parts of the Cerrado have been transformed into pasture or are used for cash cropping (Klink and Machado, 2005).
- Eastern evergreen broadleaf forest (Mata Atlantica; Figure 8.1, sub-region 5): Originally the Atlantic forest was one of the world's largest rainforests, covering approximately 150 million ha. Nowadays, only smaller fragments exist due to intensive deforestation and agricultural use (Ribeiro et al, 2009). The region has the highest average annual precipitation (above 2000 mm) in the La Plata Basin (Su and Lettenmaier, 2009) and receives precipitation during the whole year. The climate is tropical to subtropical. The month of maximum precipitation varies from north (boreal summer) to south (boreal winter). Therefore, the annual cycle of precipitation for the whole region shows three peaks (Grimm et al, 2000): one at the beginning of spring, one in the middle of summer, and one in winter (with respect to boreal seasons). Due to the altitude of the region, frost occurs frequently during winter and precipitation may fall in some sub-region as snow (e.g. high places of Santa Catarina State). ▷ (Abelen et al, 2015)

◁ Previous studies showed that GRACE can monitor large-scale hydrologic events such as droughts and floods in the La Plata Basin (Chen et al, 2010b; Pereira et al, 2012; Pereira and Pacino, 2012; Frappart et al, 2013b) and AMSR-E data proved to be sensible for flooding events along the Paraná River (Ferrazzoli et al, 2010). Figure 8.2 shows a rough spatial distribution of natural disasters, which happened in the La Plata Basin between October 2007 and July 2011 based on the International Disaster Database EM-DAT (here hydrometeorological disasters are of interest; see Section 5.7). Most of the disasters were registered in densely populated regions such as the east coast of South Brazil and the surroundings of the metropolitan area Gran Asunción in Paraguay (Encyclopedia Britannica, 2011). In sparsely populated regions such as the Chaco, the Pantanal, and the Campos, only a few events were listed. This is due to the fact that extreme weather events are only classified as natural disasters within EM-DAT if they had a high impact on society. ▷ (Abelen et al, 2015)

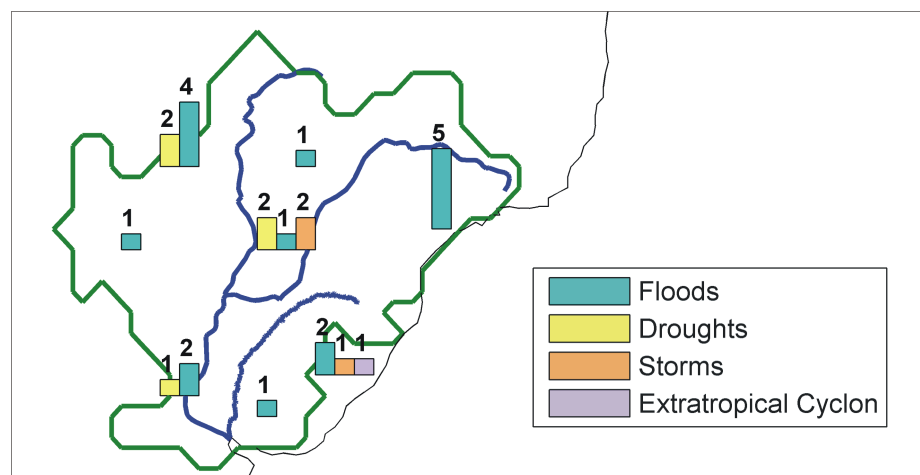


Figure 8.2: Location of natural disasters in the La Plata Basin from October 2007 to July 2011 based on the International Disaster Database EM-DAT (as shown in Abelen et al, 2015).

8.2 Regional Comparison of Soil Moisture Products

◁ Before linking the signatures of soil moisture to extreme weather conditions, the different global soil moisture data sets of the hydrological model WGHM and the two satellite products ASCAT and AMSR-E are compared more in detail for the La Plata Basin. Figure 8.3 and Figure 8.4 show that ASCAT and WGHM agree well in most parts of the basin with correlation coefficients above 0.7 for the monthly time series (90% confidence interval ranges from 0.6 to 1). Exclusively in the evergreen broadleaf forest in the eastern part of the study area, the soil moisture signal from WGHM lags several months behind the ASCAT signal (lag ranges from -3 to -6) and therefore has to be shifted forward in time (Figure 8.3, row 2, column 3). However, even if the time shift is implemented, the correlation does not improve much (Figure 8.3, row 3, column 3). For soil moisture from AMSR-E and WGHM, the correlation coefficients are lower than those for ASCAT and WGHM. Especially in the western part of the basin, they are negative or close to zero since the seasonal signals are out of phase (Figure 8.4, column 1, rows 3-4 and Figure 8.3, row 1, column 2). The poor correlation values agree with the results of Dorigo et al (2010), which reports large errors for the AMSR-E signal in the La Plata Basin.

In the eastern evergreen broadleaf forest, neither ASCAT nor AMSR-E data agree well with soil moisture from WGHM. Although WGHM model deficits cannot be excluded, this indicates that in this region, the microwave signal received by ASCAT and AMSR-E is severely degraded by the topographic complexity (Draper et al, 2012) and/or the very high foliage density, which shield the soil moisture signal (de Jeu et al, 2008). ▷ (Abelen et al, 2015)

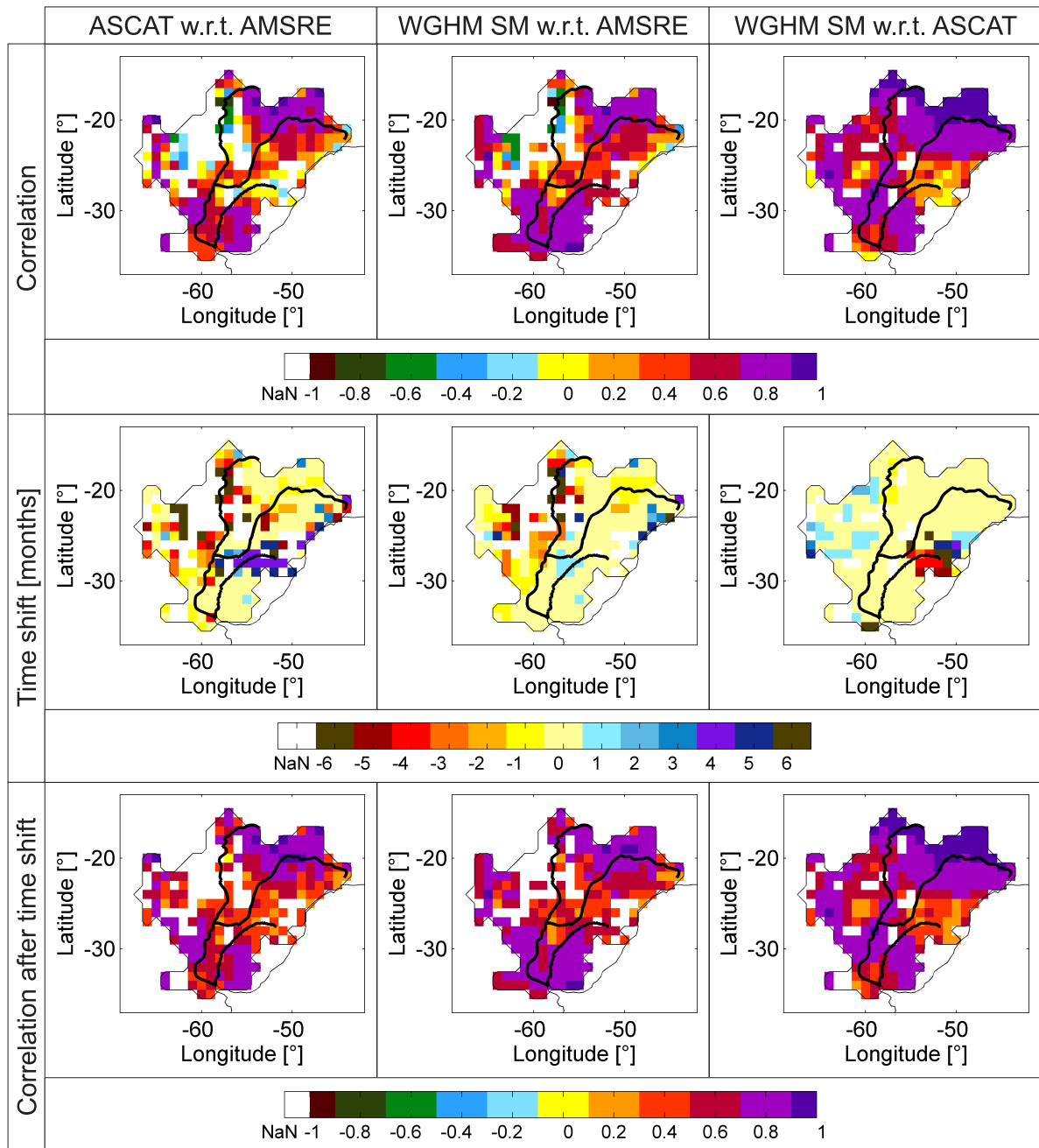


Figure 8.3: Correlation (row 1), time shift in months (row 2; negative values indicate that the seasonality of the first soil moisture product lags behind the second product), and correlation after the implementation of time shift (row 3) for soil moisture from AMSR-E and ASCAT (column 1), AMSR-E and WGHM (column 2), and ASCAT and WGHM (column 3) (as shown in Abelen et al, 2015).

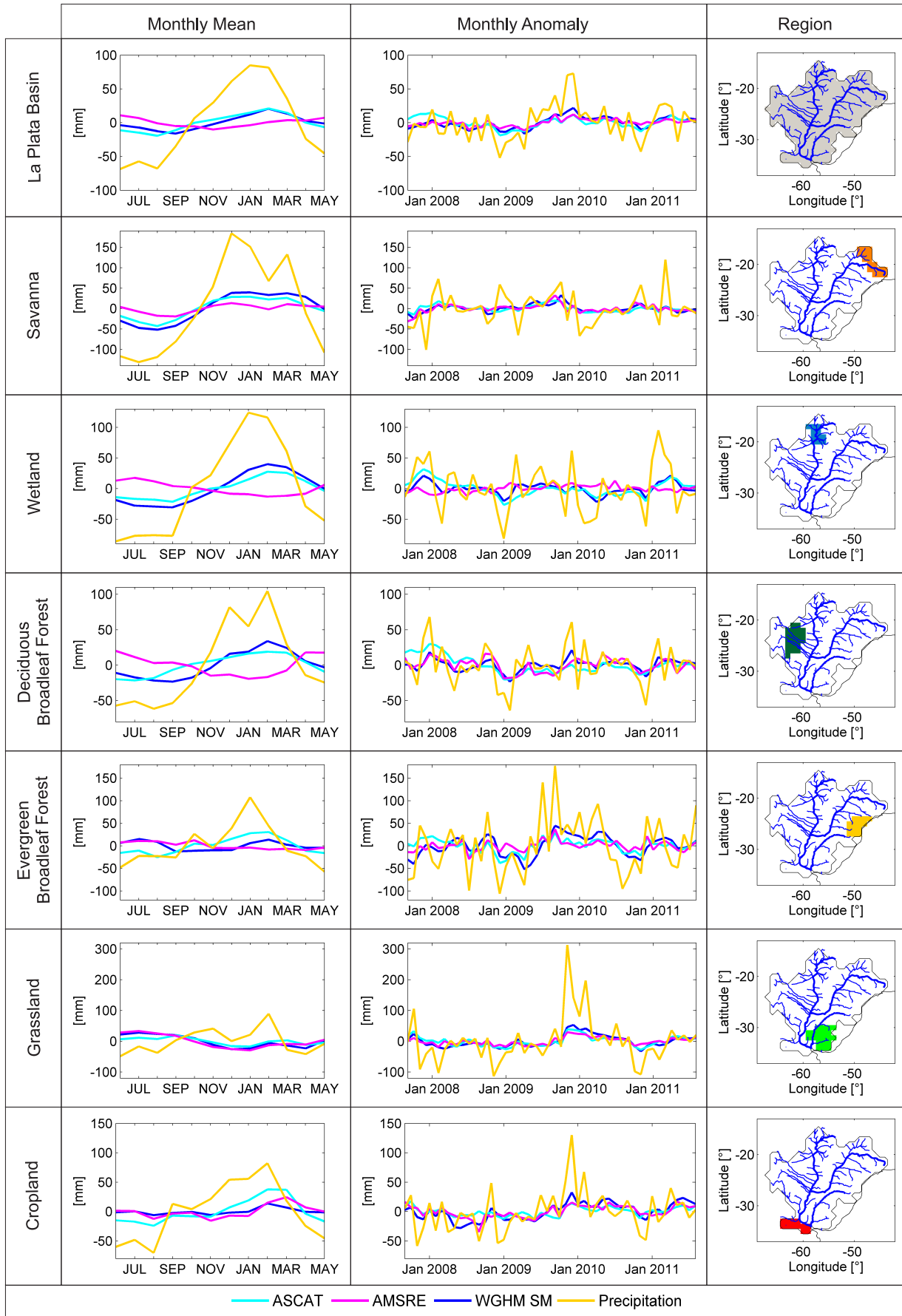


Figure 8.4: *Monthly mean (column 1) and monthly anomaly (column 2) for soil moisture from ASCAT, AMSR-E and WGHM (ASCAT and AMSR-E are scaled with respect to WGHM), and for precipitation from GPCC for the entire La Plata Basin (row 1) and the different sub-regions delineated in Figure 8.1 including the northern savanna (row 2), the wetland Pantanal (row 3), the western deciduous forest (row 4), the eastern evergreen broadleaf forest (row 5), the southern grassland (row 6), and the southern cropland (row 7) (as shown in Abelen et al, 2015).*

8.3 Regional Interdependency of Soil Moisture and TWS

◁ As shown in Figure 8.5 there are two regions in the La Plata Basin where soil moisture (here exemplarily from ASCAT) and TWS from GRACE are interrelated. The first region is the wetland Pantanal (correlation coefficients are around 0.8, 90% confidence interval ranges from 0.7 to 0.9). In the Pantanal, the shallow groundwater table may rise and saturate the surface soil or fall and leave the surface soil dry (Hamilton, 2002). Therefore, near-surface soil moisture dynamics monitored by ASCAT can be expected to be a good indicator of TWS variations.

The second region with a good correlation between ASCAT and GRACE (correlation coefficients range from 0.6 to 0.7; 90% confidence interval is 0.5 to 0.8) ranges from the junction of the Paraguay and Paraná Rivers, which is surrounded by wetlands (Figure 8.1), to the southeastern coast of the basin. Again, in the wetland region, the dynamics of groundwater and soil moisture tend to be closely linked. Approaching the coast, the connection to surface water is stronger. Although the seasonal signal of soil moisture is dominant in this part of the basin (see Figure 7.1), soil moisture does not dominate the entire TWS signal. This is due to the fact that in this region the amplitude of the anomaly is very high. This is visible in Figure 8.4 (rows 6 and 7), where the seasonal pattern of precipitation and soil moisture for the relatively short study period considered here is dominated by the anomaly of the El Niño event in the boreal winter of 2009/2010. The absence of a marked seasonality in this region in the absence of extreme events is also described by (Su and Lettenmaier, 2009) for stream flow data. ▷ (Abelen et al, 2015) The high agreement between variations of soil moisture and changes of TWS from GRACE is therefore not based on the stronger seasonal signal of soil moisture (as suggested by Figure 7.1) but on the close link between soil moisture and surface water, and soil moisture and groundwater (see Figure 7.7 and Figure 8.5).

◁ The correlation of ASCAT time series to precipitation is high for most parts of the study area (correlation coefficients are above 0.7 as shown in Figure 8.5 and the 90% confidence interval ranges from 0.6 to 0.9). This is reasonable as near-surface soil moisture variations seen by ASCAT are directly triggered by the precipitation dynamics. Nevertheless, the correlation tends to decrease toward the southeastern downstream parts of the basin, whereas the correlation of ASCAT with WGHM simulation-based surface water storage simultaneously increases. In this region the groundwater recharge is high (> 100 mm) (Frappart et al, 2013b). This implies that the relevance of local rainfall-induced soil moisture variations decreases in favor of soil moisture variations caused by allochthonous processes at the regional scale, i.e., surface water inflow from upstream areas of the river basin. ▷ (Abelen et al, 2015)

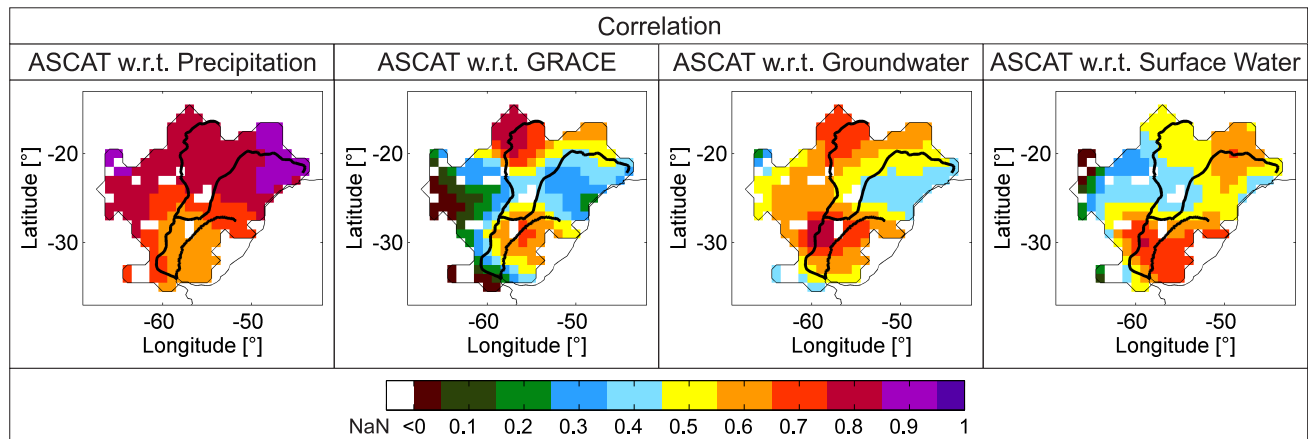


Figure 8.5: Correlation after data harmonization for soil moisture from ASCAT with respect to precipitation from GPCC (column 1), terrestrial water storage from GRACE (column 2), groundwater from WGHM (column 3), and surface water storage from WGHM (column 4) (as shown in Abelen et al, 2015).

8.4 Hydrological Extremes and Natural Disasters

The previous two chapters have shown that the various soil moisture data sets are over large parts of the La Plata Basin consistent and that soil moisture is closely linked to TWS in the northern wetland Pantanal (which is regulating the river flow of the basin) and in the southern Pampas region (where the anomaly of the signal is very high). Furthermore previous maps have shown that there is specifically in the La Plata Basin a high correlation between the anomalies of the soil moisture products and GRACE (see Figure 7.4). This information is the basis for analyzing variations in soil moisture and changes in TWS from GRACE with respect to natural disasters, which happened in this basin over the observed time span.

◁ The comparison of the anomalies of different hydrological parameters in the La Plata Basin is shown in Figure 8.6. The time series reflect the close connection between soil moisture and precipitation in most parts of the basin (as also shown in Figure 8.4 and Figure 8.5). Furthermore, the anomalies are in agreement with time variations of water levels at different locations in the La Plata Basin, as presented by Frappart et al (2013b). The comparatively smooth GRACE time series is an expression of the integrative nature of TWS that, to some extent, balances out short-time variations in individual storage components. Furthermore, anomalies of GRACE TWS tend to be shifted by a few months with respect to soil moisture and precipitation, as it takes time until precipitation extremes accumulate within surface and ground water storage. A drastic decrease in soil moisture can therefore be an indicator for an upcoming deficit or surplus in TWS.

One example is the La Plata drought in 2009, wherein soil moisture was lowest between December 2008 and January 2009, and TWS reached its minimum in May 2009. The minimum soil moisture in December 2008 agrees with the fact that the drought was declared and registered in January 2009 as a natural disaster within the International Disaster Database EM-DAT. Furthermore, the local minima for soil moisture in May 2009 and the decrease in TWS until May 2009 illustrate that the drought lasted for several months until approximately November, 2009. The clear signal of the La Plata drought of 2008/2009 in GRACE TWS was also observed by Chen et al (2010b). The flood period in the boreal winter of 2009/2010 as supported by Pereira and Pacino (2012) and the flood

period in the beginning of 2011 are also visible in the GRACE data. Apart from these events, it was not possible to link anomalies of GRACE TWS directly to the listed natural disasters. This is due to the coarse spatial resolution of the GRACE sensor and its low sensitivity to small mass changes. Also short-time events such as storms might not affect all water storage components contained in TWS.

In contrast, almost all droughts and floods could be identified as single events or as accumulated events (e.g. winter 2009/2010 and March and April 2011) in at least one of the soil moisture data sets from ASCAT, AMSR-E, or WGHM. The only exception is the flood in Brazil in November 2010, which affected the northeastern fringe area of the basin, including parts of Minas Gerais, São Paulo, and Rio de Janeiro. Furthermore, some meteorological events (storms and cyclones) could be linked to anomalies in the soil moisture data, e.g., the storm in Paraguay in August 2008. During this month, precipitation data from GPCC and the two soil moisture data sets from AMSR-E and ASCAT show local maxima.

Figure 8.7 emphasizes that specific extreme events can be identified more clearly when focusing on smaller regions. For example, the flood in Bolivia from December 2007 to February 2008 is clearly visible in all soil moisture signatures when averaging over the western sub-region in the Chaco only. At the same time, it became clear that the minima of the AMSR-E signal in June 2010, as seen in the basin average in Figure 5, is not associated with the drought in Bolivia. Thus, a differentiation into hydrological extreme events of basin-wide character or of regional extent is only possible with the given data sets.

Figure 8.6 does not show the expected below average precipitation in the La Plata Basin during the moderate La Niña period of 2007/2008. However, atypical precipitation patterns during this La Niña period were also observed in southeastern Australia (Gallant and Karoly, 2009). From the summer of 2008 onward, there is a strong relationship between variations in soil moisture and the ONI (Figure 8.6). The first phase of the La Plata drought in 2009 fell into the weak La Niña period during the boreal winter of 2008/2009, which is also supported by Chen et al (2010b). Furthermore, the moderate El Niño period in the boreal winter of 2009/2008 coincides with the very high soil moisture values in December 2009 and several floods affecting Argentina, Brazil, Bolivia, and Uruguay. The anomaly is also visible in TWS from GRACE and initiated by high precipitation during November and December 2009. The strong La Niña period during the boreal winter of 2010/2011 is shown as local minima during November 2010 for all parameters (except for AMSR-E).

The dominant spatial patterns of the various data sets and the major differences among them were further analyzed by PCA. The first, second, and third modes explain approximately 60%, 25%, and 5% of the TWS signal from GRACE and the soil moisture signals from ASCAT and WGHM, respectively. For AMSR-E, the first three modes account for 50%, 25%, and 10% of the signal. The first mode mainly represents the seasonal part of the signal (Figure 8.8, row 1). In the PCs, no time shift between the seasonal cycles of the different soil moisture products is visible. For GRACE, the phase of the seasonal signal is approximately two months later. The EOFs of the first mode show a characteristic opposing pattern in the northern part of the La Plata Basin versus in the southeastern part (Figure 8.9, row 1). The inverse annual signal for AMSR-E visible in Figure 8.4 (column 1, rows 3-4) in the western and northern parts of the basin is reflected by the inverse signs of the EOFs of AMSR-E compared with the EOFs of the other soil moisture products in this region. The nonconformity between AMSR-E and other soil moisture data sets is also reflected in the PCs and EOFs of the second mode.

The PCs of the second and third modes show secondary minima for soil moisture from ASCAT and WGHM during the La Plata drought in 2009 (Figure 8.8, rows 2-3). This indicates that the southern, central (Figure 8.9, row 2, columns 2-3), and eastern parts (Figure 8.9, row 3, columns 2-3) of the basin were mostly affected. The described spatial pattern is in agreement with precipitation maps for

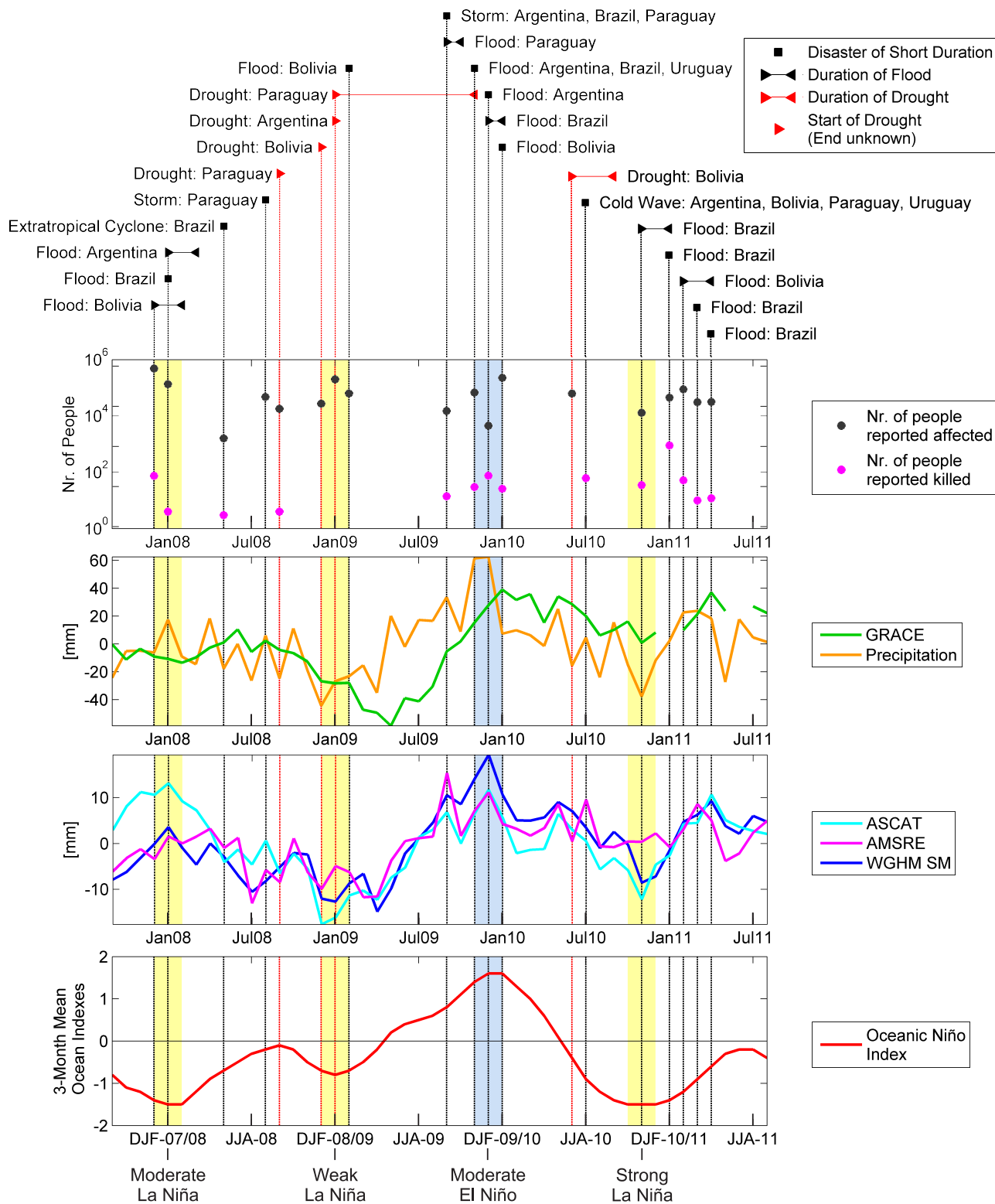


Figure 8.6: Disasters as registered by the International Disaster Database EM-DAT for the La Plata Basin (top), number of people affected and killed for each disaster (second from top), monthly anomalies as basin averages after data harmonization for TWS from GRACE, precipitation from GPCC (third from top), and soil moisture from ASCAT, AMSR-E, and WGSM (ASCAT and AMSR-E are scaled with respect to WGSM; fourth from top), and El Niño and La Niña anomalies as described by NOAA through the Oceanic Niño Index (ONI; bottom) (as shown in Abelen et al, 2015).

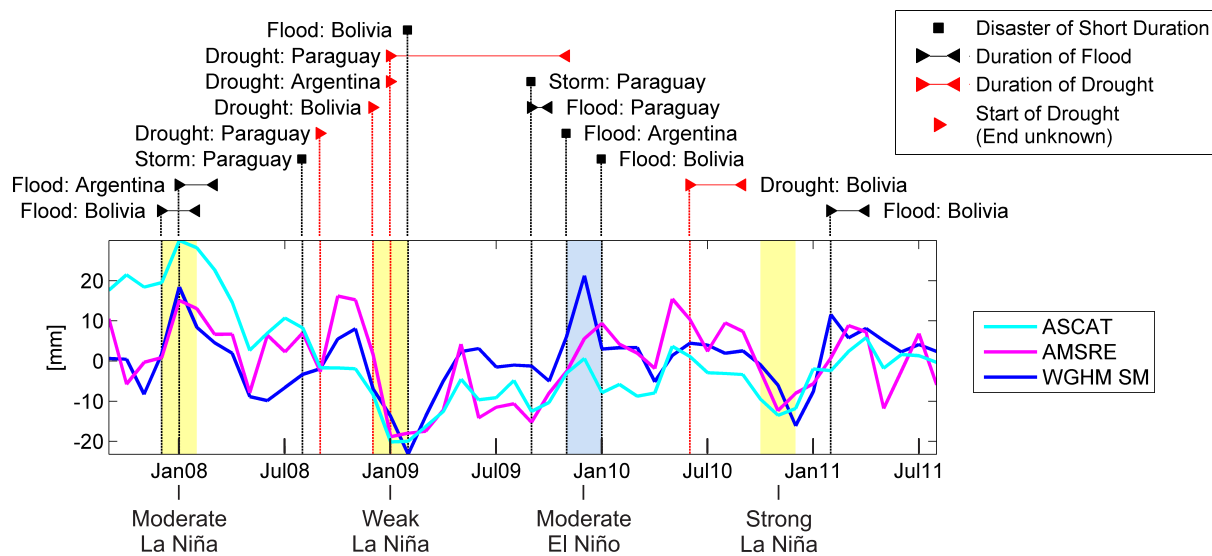


Figure 8.7: Disasters as registered by the International Disaster Database EM-DAT for the deciduous broadleaf forest (Chaco) in the western part of the La Plata Basin (see Figure 1) (top) and monthly anomalies of soil moisture from ASCAT, AMSR-E, and WGHM (ASCAT and AMSR-E are scaled with respect to WGHM; bottom) (as shown in Abelen et al, 2015).

the La Plata Basin in winter and spring 2009 from the Argentinean National Meteorological Service (SMN), as presented by Pereira and Pacino (2012). Furthermore, they are also supported by the spatial patterns of soil moisture from ASCAT in Figure 8.10.

Similarly to the La Plata drought in 2009, the flood period associated with El Niño in the boreal winter of 2009/2010 can be identified in the PCs of the third and second modes of the soil moisture data. As the anomaly in the third mode (Figure 8.8, row 3) appears before the anomaly in the second mode (Figure 8.8, row 2), the eastern part of the basin (Figure 8.9, row 3, columns 2-3) followed by the southeastern part (Figure 8.9, row 2, columns 2-3) were affected. This sequence of spatial patterns is also supported by the precipitation anomalies of SMN (Pereira and Pacino, 2012). Furthermore they are reflected in the signatures of precipitation and soil moisture in Figure 8.4 (column 2, rows 5-7).

For GRACE, the two periods of extremes are also clearly visible in the PCs of the second and third modes. For the La Plata drought in 2009, the second mode is shifted by a few months and the third mode by several months with respect to the signatures of soil moisture. The EOF of the second mode (Figure 8.9, row 2, column 4) shows that the northeastern and central parts of the basin were first affected. Then, based on the EOF of the third mode (Figure 8.9, row 3, column 4), the southern part was affected. The temporal development of the drought provided by the PCs is in agreement with Figure 8.10 and is similar to the results of Chen et al (2010b); minimum values of water storage in the entire basin occurred during the first half of 2009 followed by strong but regionally confined low water storage in the southern part in July and August. The strong decline in TWS in the northern part of the basin results according to WGHM (see Figure 8.10) from a strong decrease in surface water along the Paraguay River and decline in groundwater in the Guarani Aquifer in the northeastern part of the basin.

For the first half of 2009, the soil moisture data show that the largest anomalies were in the southern, central and eastern parts of the basin, which is also shown in Figure 8.10. However, within the International Disaster Database EM-DAT, the largest impact of the drought was registered in

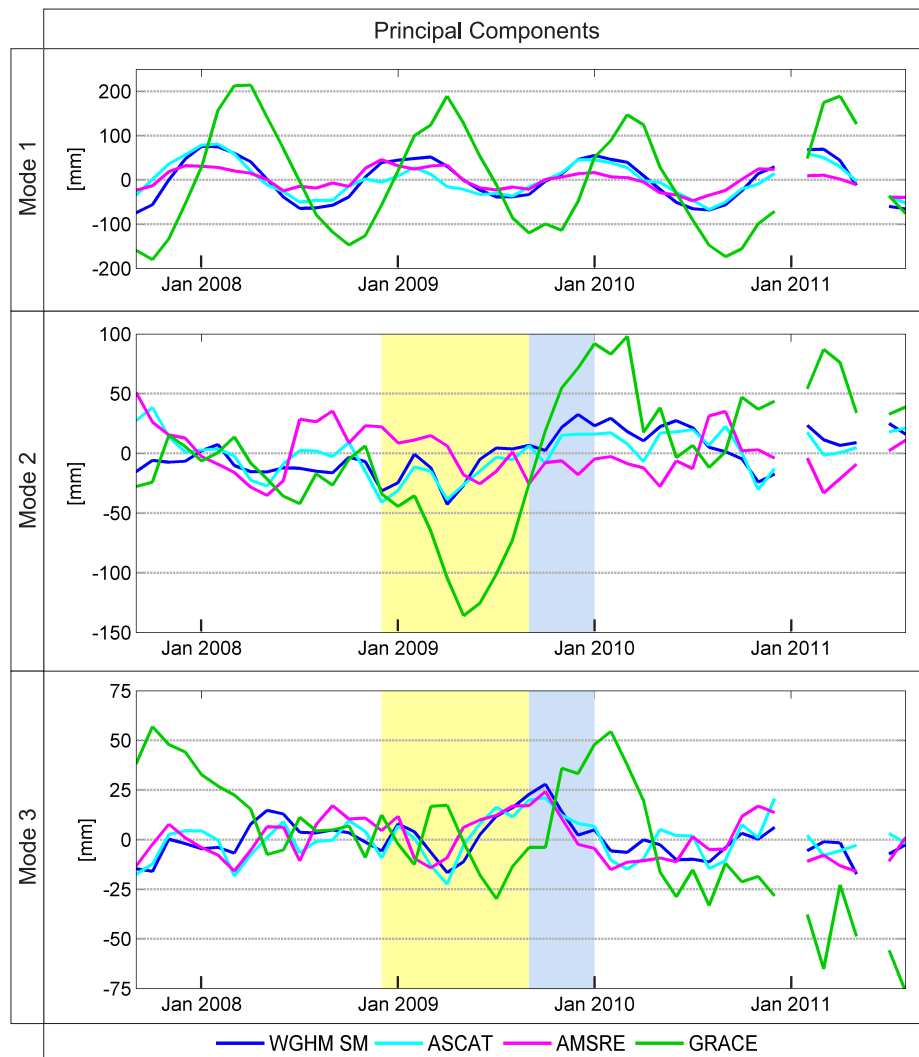


Figure 8.8: Principal components for the first, second, and third modes for soil moisture from AMSR-E, ASCAT, WGHM (AMSR-E and ASCAT data are scaled with respect to WGHM), and GRACE after data harmonization. For the second and third modes, the shaded areas indicate the La Plata drought in 2009 (yellow) and the flood period associated with El Niño in the boreal winter of 2009/2010 (blue) (as shown in Abelen et al, 2015).

the central and northwestern parts of the basin, affecting more than 227,000 people in Bolivia and Paraguay. It is possible that the International Disaster Database EM-DAT lacks information on the impact of the drought; for example, the database does not contain any information on the drought situation in Uruguay.

A situation report of the United Nations Development Program in Uruguay (dated at the beginning of the drought in January 2009) clarifies that Uruguay was affected by the drought (e.g. through food shortages and lack of water for livestock; Mandeville et al, 2009). However, the report also states that there was a lack of integral information on the impact of the drought and the economic consequences. This example shows that databases like EM-DAT might be incomplete due to the difficulty in collecting and receiving quantitative data on an international level. Moreover, it should be noted that the disaster classification given by EM-DAT explicitly considers the vulnerability of the

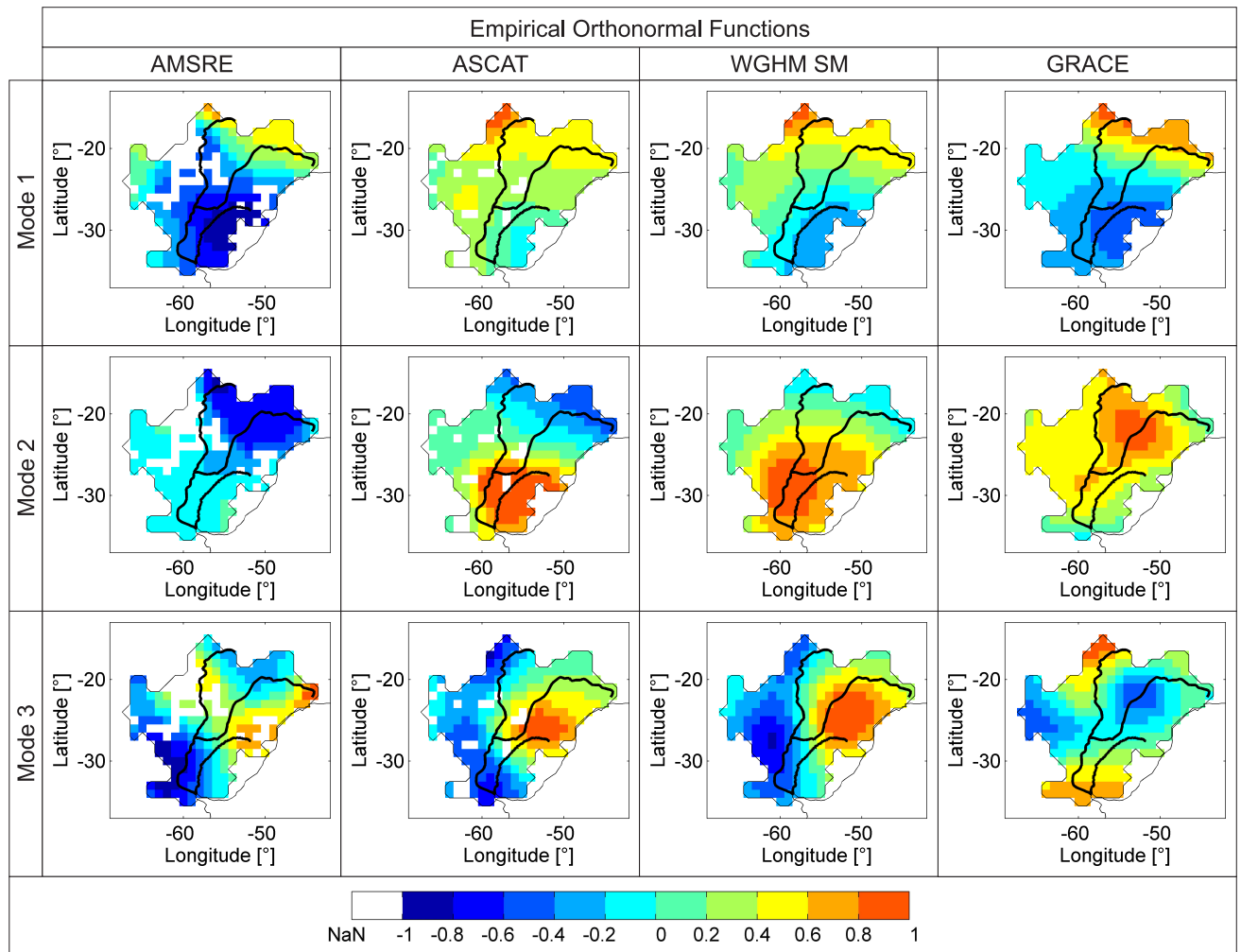


Figure 8.9: Empirical orthonormal functions for the first, second, and third modes for soil moisture from AMSR-E (column 1), ASCAT (column 2), and WGHM (column 3) (AMSR-E and ASCAT data are scaled with respect to WGHM) and terrestrial water storage from GRACE (column 4) after data harmonization (as shown in Abelen et al, 2015).

region, which is defined by demographic factors such as population density (which is relatively low in Uruguay; Encyclopedia Britannica, 2011), environmental factors (e.g. state of resource degradation and depletion), social factors (e.g. traditional knowledge systems), and economic factors (e.g. economic status of individuals, communities, and nations) as described by the United Nations Office for Disaster Risk Reduction (UNISDR, 2004). In contrast, the soil moisture and TWS products only reflect the physical factors in terms of a subset of hydrometeorological hazards. ▷ (Abelen et al, 2015)

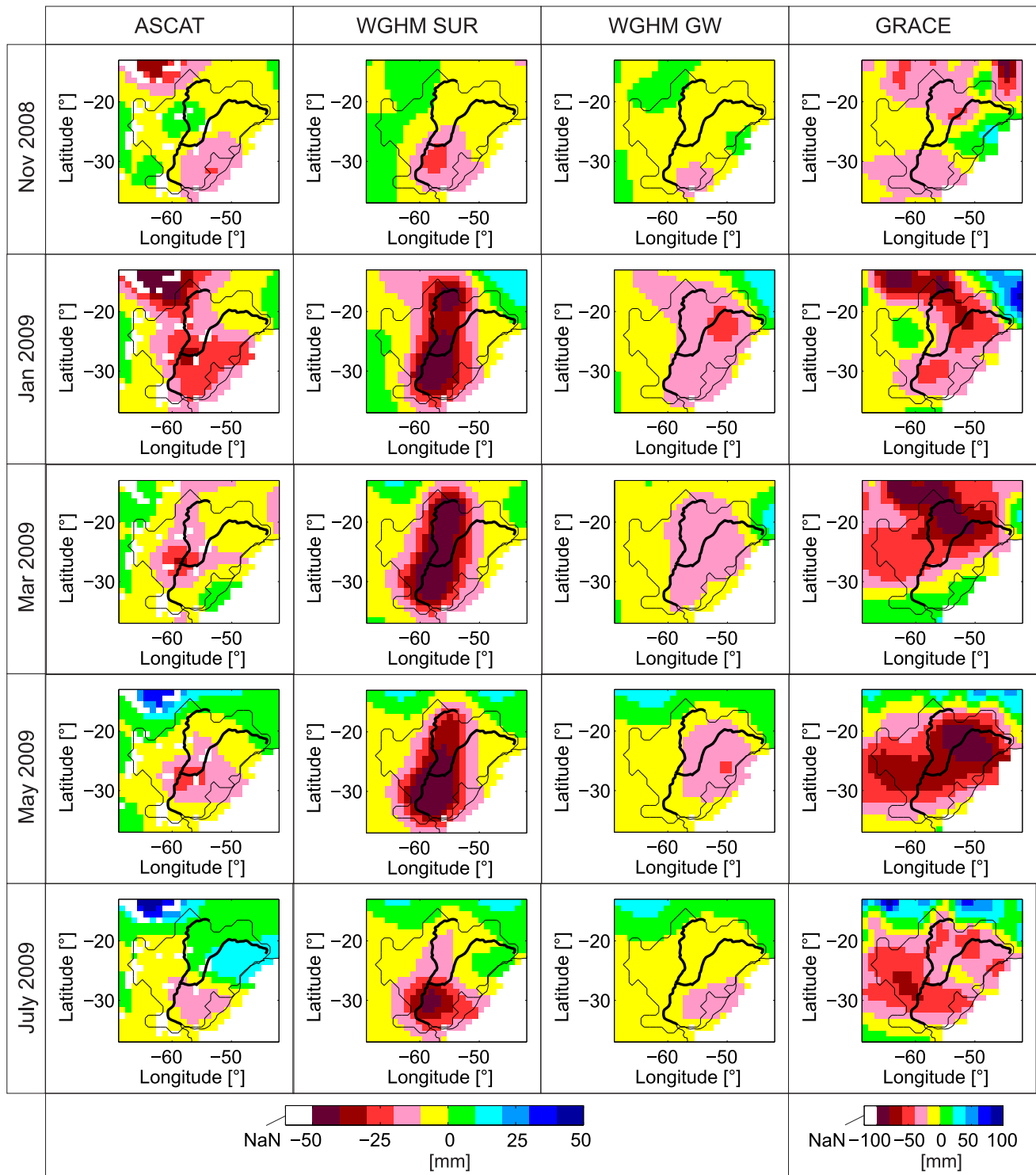


Figure 8.10: The evolution of the 2009 La Plata drought from January to July 2009 (advancing in time in two months steps from row 1 to row 5) for surface soil moisture from ASCAT (scaled with respect to root zone soil moisture from WGHM herein, column 1), surface water from WGHM (column 2), groundwater from WGHM (column 3) and TWS from GRACE (column 4).

8.5 Summary

This chapter dealt with the question whether the combination of soil moisture and TWS data is useful to understand hydrological extremes and associated natural disasters (RQ 3). As study area the La Plata Basin in South America was chosen, as in this region anomalies of soil moisture and TWS agree well and prior studies have shown that GRACE data were able to capture hydrological extreme events. Furthermore, the basin has a very large size (which is favorable for GRACE data) and low topographic complexity (which is favorable for soil moisture data).

◁ First, the various soil moisture data sets were compared. The results indicate that soil moisture products from ASCAT and WGHM are strongly correlated (correlation coefficients above 0.7) in the majority of the sub-regions of the La Plata Basin. For AMSR-E, the correlation coefficients take values above 0.6. However, in the eastern deciduous broadleaf forest, the western evergreen broadleaf forest, and the wetland Pantanal, signatures of AMSR-E differ strongly from those of both WGHM and ASCAT. In the eastern forested region, neither ASCAT nor AMSR-E correlate well with soil moisture from WGHM, possibly due to signal disturbance by the topographic complexity and dense vegetation in this region.

Second, interdependencies between the dynamics in soil moisture and the dynamics in TWS were brought into focus. A close link between soil moisture and TWS was identified in regions where groundwater or inflow of surface water from upstream areas influences the dynamics of soil moisture. Those regions include in the La Plata Basin the northern wetland Pantanal and the south eastern part of the basin, where specifically the anomalies of soil moisture and TWS are highly correlated.

Third, extreme meteorological and hydrological conditions, specifically those that have been classified as natural disasters within the International Disaster Database EM-DAT, were brought into focus. Thus, two independent data sources were linked. On the one hand, signatures of hydrological variables were analyzed to gather information on hydrometeorological extremes. On the other hand, natural disasters that affected the La Plata Basin during the analyzed time period were identified to include information on the number of people affected or killed by extreme events. The analysis of both data sets showed that most of the strong variations in soil moisture match temporally with natural disasters (droughts, floods, or storms). For two hydrologic extreme periods that led to several natural disasters (the La Plata drought in 2009 and the flood period in the winter of 2009/2010), it could be observed that soil moisture first changes drastically followed by TWS from GRACE with a delay of a few months. In these two cases, soil moisture serves as an indicator for the later deficit or surplus in TWS. Furthermore, results (of the PCA) indicate that hydrological extremes first affect large parts of the basin (for TWS especially the northern parts) before they concentrate in the southern parts as for example during the 2009 La Plata drought.

Out of four El Niño and La Niña events during the analyzed time period, three events match with extreme soil moisture and TWS conditions. These events include the weak La Niña event in 2008/2009, the moderate El Niño event in 2009/2010, and the strong La Niña event in 2010/2011. The most meteorologically and hydrologically affected areas were the southern, central, and eastern parts of the La Plata Basin. However, based on the International Disaster Database, the main impacts were registered in the central and northwestern parts of the basin. This reveals that several limitations have to be considered when linking extremes in soil moisture or TWS to natural disasters.

On the one hand, not all extreme hydrologic events have large impacts on society. This might be due to the fact that the destructiveness of a disaster not only depends on the magnitude of the hydrometeorological extreme indicated by GRACE, WGHM, ASCAT or AMSR-E but also on the

vulnerability of the region considered in EM-DAT, which largely depends on other factors such as the preparedness of the population and the population density. On the other hand, the collection of quantitative information on the impacts of disasters is challenging on an international level. Therefore, limited data availability in the EM-DAT database for the southern parts of the study area cannot be excluded. Analyzing the hydrological signals as basin averages and with a temporal resolution of only one month makes the identification of regional or short-term events difficult. Nevertheless, it could be shown that the remote sensing products used here allow for differentiating hydrological extreme events of basin wide character or of local to regional extents. ▷ (Abelen et al, 2015)

9 Conclusion

The introduction to this study has pointed out that the understanding and large-scale mapping of soil moisture and terrestrial water storage are of great importance to various sectors including those which deal with agricultural production, water supply management and Earth system science (see Section 1.1). Both hydrological parameters have been extensively analyzed in previous studies on an individual basis or in combination with other data sets, for example with data on river runoff (Chapter 2 and Chapter 3). However, studies which directly link both parameters were lacking.

This study investigated interrelations of soil moisture and TWS, making use of global satellite products, which have just emerged in the last 15 years for soil moisture and TWS. Although soil moisture is usually considered to be a “small” water storage component (with a low signal amplitude), in this study it is assumed that variations in soil moisture and TWS can be related if soil moisture significantly influences changes in TWS (the variations in soil moisture are much larger than the variations of the other storage components) or if it changes proportionally with another dominant storage component. Storage components, which sum up together with soil moisture to equal TWS, were limited in this study to groundwater and surface water to reduce the complexity of interrelations. Consequently, regions which receive snowfall or are covered with ice were excluded from the analysis (see Section 5.1).

The main data sets, which were used in this study include two surface soil moisture products from the active microwave sensor ASCAT (Section 4.1) and the passive microwave sensor AMSR-E (Section 4.2), the outputs of WGHM on root zone soil moisture, surface water, groundwater and TWS (Section 4.4), and measurements of TWS dynamics from the satellite gravity mission GRACE (Section 4.3).

As GRACE data have very distinct characteristics (they are provided in spherical harmonics and require special filtering) it is not straight forward to compare the various data sets. Also the quality of each data set differs around the globe. From a hydrological point of view interrelations between soil moisture and TWS are complex because the contribution of each storage component to TWS varies in space and time and interrelations among all storage components exist. From an application perspective, investigations were needed to show if the combined analysis of both parameters creates added value, for example, in the field of natural disaster monitoring.

Based on these challenges this study followed a three step approach (see Section 1.2 and Section 1.3). First, it was investigated if and in which way it is feasible to compare the used data sets (especially the soil moisture data sets and GRACE data) in terms of their different data structures (how can the data sets be processed in a harmonious way and what is the impact of such a process?) and in terms of their data quality (e.g. are the various soil moisture data sets consistent? Which regions of the world need to be excluded due to poor data quality?). The investigation showed (see Chapter 6) that it is feasible to bring global soil moisture products in relation with TWS from GRACE if:

- All data sets are processed in a harmonious way and therefore the structures (e.g. temporal and spatial resolution, spatial smoothness) of all data sets are comparable. In this study, the

main steps of the harmonized processing (see Section 5.2) include the conversion into spherical harmonics (of degree and order 70), the application of a Gauss filter (of 300 km half-wavelength), the projection back onto a $1^\circ \times 1^\circ$ grid and the aggregation to a monthly data set. Additionally, a least-squares polynomial filter was applied to the GRACE data.

- Regions are excluded where the harmonious processing alters the signal artificially (see Section 6.1). In this study it is proposed to exclude pixels where correlation coefficients between the original and the harmoniously processed signal are less than a certain threshold, which was set to 0.7 herein. By setting this threshold, mainly desert regions with low signal variability (equal or close to zero) were excluded. In those regions the signal is artificially altered in the course of the conversion into spherical harmonics. Also spatial leakage, which is associated with the Gauss filtering, is especially dominant in arid environments, which are surrounded by regions with high signal variability.
- Regions are excluded where the quality of the used soil moisture or TWS data products is low (see Sections 6.2 and Sections 6.3, respectively and also the description of the data products in Chapter 4). Those are mainly regions which:
 - Experienced earthquakes of magnitude 8 or higher or are affected by PGR for GRACE.
 - Regions with dense vegetation cover, high topographic complexity, high fraction of open water, snow or ice cover, desert regions, or regions affected by RFI for satellite based soil moisture products.
 - Regions with high hydrological complexity (e.g. low seasonal signal and highly fluctuating anomalies) or low in-situ data coverage (because in-situ data are needed as input to the model or for calibration and validation) for hydrological models.
- Only anomalies with respect to some reference value (e.g. long-term or seasonal mean) are analyzed as GRACE only delivers information on changes in TWS.
- The focus is on large-scale patterns which are for example related to meteorological or climate events (and not on small-scale patterns which are e.g. related to the soil type and the topography of the region). This is due to the fact that GRACE data have a low temporal (monthly) and spatial resolution and are smooth as they require spatial filtering.
- The focus is not on the absolute contribution of soil moisture to TWS but on relative relations (e.g. correlation and time shifts, see Section 5.4 and Section 5.5) between both parameters (this is specifically relevant for studies which use information on surface soil moisture from remote sensing and not information on root zone soil moisture).

On the basis of these findings, as a second step interrelations between soil moisture and TWS, and soil moisture and other storage components were investigated, using correlation and time shift analysis (see Sections 5.4 to Section 5.5). The following conclusions can be made from this second part of the analysis (Chapter 7):

- Time shifts between soil moisture and TWS, or soil moisture and groundwater or surface water are similar and range between zero and two months.
- Patterns of correlation between soil moisture and TWS can be related to the soil moisture regime map published by NRCS-USDA (1997). In the following the term “humid” refers to udic and xeric soil moisture regimes and “arid” refers to ustic and aridic soil moisture regimes.

- In general soil moisture and TWS show a higher agreement in humid areas (e.g. in the Amazonas) than in arid areas (this observation is only based on the analysis of the root zone soil moisture from WGHM in combination with GRACE data, as satellite soil moisture data are not available over densely vegetated regions).
- In extremely arid areas like the Kalahari Desert and the deserts of Australia there is no agreement between variations of soil moisture and TWS, probably because the variation in TWS lies below the accuracy of GRACE (which is around 40 mm for GRACE data as processed in this study).
- In the remaining semi-arid (e.g. India) and humid (e.g. Southern China and Myanmar) regions soil moisture and TWS correlate well if soil moisture is also interrelated with groundwater and/or surface water (as regions with snow and ice are masked those two storage components sum-up together with soil moisture to TWS in all analyzed regions).
- An exception is the Sahel Zone where the dynamics of soil moisture are in high agreement with TWS from GRACE but not necessarily with the dynamics of groundwater or surface water. The high agreement with TWS from GRACE is due to the fact that in this region soil moisture has a large seasonal amplitude (between 40 and 140 mm according to WGHM), which dominates the seasonal amplitudes of the other two water storage components (the seasonal amplitude of soil moisture is larger than the sum of the seasonal amplitudes of groundwater and surface water). This indicates that the TWS signal can only be understood in this region if it is related to the dynamics of soil moisture. Soil moisture in this region is not a “small” but a significant water storage component and has a seasonal amplitude which can be mapped by GRACE.

Having found interrelations between soil moisture and TWS over wide areas of the globe, the third part of the analysis focused on an application of the combined analysis of soil moisture and TWS data. Therefore, exemplarily the use of large-scale data sets of soil moisture and TWS for the analysis of hydrological extreme events in the La Plata Basin in South America was investigated. The focus was on highly destructive events that have been classified as natural disasters within the International Disaster Database EM-DAT (see Section 5.7). The combined analysis of soil moisture and TWS in the La Plata Basin (see Chapter 8) showed that:

- Hydrometeorological extremes, which are reflected in soil moisture and TWS data, largely match with natural disasters which are registered due to their destructiveness within EM-DAT (e.g. due to high economic damage, or the number of people affected or killed by an event). While soil moisture data rather reflects single disasters (like droughts, floods and storms), TWS variation from GRACE tends to be related to longer drought and flood periods such as those which are associated with El Niño and La Niña.
- When linking extremes in soil moisture or TWS to natural disasters several limitations exist:
 - There is not necessarily a link between hydrological extremes and natural disasters as the destructiveness of an event (which is only considered in EM-DAT) does not only depend on the magnitude of the hydrometeorological extreme but also on the vulnerability of the region, which largely depends on other factors such as the preparedness of the population and the population density.
 - Anomalies which are reflected in the basin average can originate from different parts of the basin. Therefore, links between e.g. soil moisture anomalies and certain regionally confined disasters need to be analyzed at smaller scales.
 - The collection of quantitative and reliable information on the impacts of disasters is challenging on an international level. Therefore, EM-DAT data may be incomplete or flawed.

- Soil moisture and TWS data can provide complementary information on the temporary development of hydrological extremes: soil moisture rather provides information on the start of an event and TWS on its duration (an example is the La Plata drought of 2009).
- Soil moisture can serve as indicator for upcoming lack in water storage (examples are the La Plata drought of 2009 and the El Niño flooding period of 2009/2010).

By summarizing the findings of the three step analysis, it can be finally concluded that it is possible to bring soil moisture and TWS products into comparable formats, that the harmoniously analyzed data sets show strong interrelations between both parameters in various parts of the world, and that those links can be used for the analysis and mapping of natural disasters, that had a large impact on society.

10 Outlook

This study described basic steps for the combined analysis of variations in soil moisture and TWS, using large-scale products from satellites and one hydrological model. The results highlight that interrelations of soil moisture and TWS can increase our understanding on the data quality of the used data products (see Section 7.2), that they highlight complex interrelations between various storage components on global scale (see Section 7.2 and Section 7.3) and over large river basins (see Section 8.3), and that they have the potential to contribute to a better understanding and mapping of natural disasters (see Section 8.4). However, as this field of research has hardly been explored so far, many open questions and challenges remain, and various fields of research and application are still untouched.

The following list shall highlight remaining open questions, which have not been addressed in this study yet, show some new possibilities for the combination of various emerging data sets and give incentives for upcoming research.

Data:

- To increase the data coverage and data quality of satellite based information on soil moisture, the latest soil moisture products from SMOS, SMAP and Sentinel-1 could be integrated into the study. Alternatively, merged satellite soil moisture products as described by Liu et al (2011) could be used. The comparison of TWS from GRACE with multi-decadal merged satellite soil moisture products (see Liu et al, 2012) would allow to increase the observed time span (which is in this study limited to four years). However, the identification of errors or error sources of merged data sets is more complex.
- In order to simplify the use of satellite based soil moisture data, the thresholds for the flags (see Section 4.1 for ASCAT and Section 4.2 for AMSR-E) could be increased to exclude more strictly data with low data quality. With it the data can be interpreted more easily but at the same time the data coverage decreases. The decrease in coverage might be compensable by the use of additional soil moisture data sets from satellites and hydrological models. (In this thesis the thresholds of the flags are set low to get a better understanding of the data quality and to increase data coverage which is essential for the global approach of converting data into spherical harmonics.)
- In order to gain more profound knowledge on the magnitude of root zone soil moisture, in-situ measurements and outputs of other global hydrological models could be integrated into the study. The quantitative analysis of soil moisture data would provide new information on the share of soil moisture in TWS. This information would also be helpful to quantify the portion of soil moisture within the total water balance and the percentage of soil moisture in fresh water. The satellite or model based estimates could replace previous simpler estimations of the Earth's soil moisture storage as for example the ones presented by Shiklomanov (1993).
- Instead of using GFZ GRACE solutions only, the assemble GRACE solution of all three processing centers (GFZ, JPL, and CSR) as described by Sakumura et al (2014) and suggested on the official data distribution website of NASA (grace.jpl.nasa.gov/data/choosing-a-solution/)

could be integrated into the study. According to Sakumura et al (2014) this reduces the noise for the TWS solutions (however, this is based on the assumption that no systematic errors are contained in any of the merged solutions).

Methods:

- The analyzed time span should be increased, in order to analyze if observed interrelations are also visible over other or longer time intervals (this is however limited by the overlap in time between the analyzed data sets).
- In this study GRACE data are represented in spherical harmonics and processed by using mainly a least-squares and a Gauss filter. Several alternatives exist to this widely used procedure as for example described by Kusche (2007) and Werth et al (2009). Therefore, it could be tested if other GRACE processing techniques can also be implemented for soil moisture data to receive harmoniously processed data sets. Specifically the use of regional approaches, such as spherical scaling functions and wavelets (Schmidt et al, 2008a), are promising to avoid artifacts in regions with poor data availability, because they do not require global data coverage and are highly localized with respect to space and time. Another recent approach is the use of spherical cap mascons, which do not necessitate empirical filters to remove north-south stripes and suffer less from leakage errors (Watkins et al, 2015). After implementing alternative processing approaches, the results could then be compared to those shown in this study for example with respect to their impact on the data structure and information content (e.g. due to varying characteristics with respect to spatial leakage, spatial resolution, and time shift effects). By this means the harmonious processing of all data sets could be optimized.
- Dirmeyer et al (2004) suggested that when being aggregated to monthly time scales, surface soil moisture data show similar variations (in relative terms) to root zone soil moisture data. By using in-situ data, which are collected at different soil depths in daily intervals or by using modeled data for different soil depths with a temporal resolution of one day, this hypothesis could be tested. The results would improve our understanding on the different dynamics of surface and root zone soil moisture for larger time intervals and facilitate the interpretation of the results of this study (because in this study root zone and surface soil moisture are compared in monthly time intervals).
- In this study the seasonal amplitudes of various hydrological storage components have been compared to identify regions where the seasonal signal of soil moisture dominates the sum of all other seasonal signals (see Section 7.1). The case study on the La Plata Basin has shown that this information is not sufficient to define whether soil moisture dominates other storage components with respect to their entire signal. In regions where the seasonal anomaly is similar or larger in magnitude than the seasonal signal, soil moisture might still be dominated by other storage components, even if the seasonal signal is high in amplitude with respect to other storage components. Therefore, future studies should investigate in which regions of the world soil moisture dominates other water storage components with respect to the entire signal.
- This study has shown that variations of soil moisture precede variations of TWS by about one month in large parts of the world (see Figure 7.3). This phenomenon could be further analyzed to find out whether soil moisture can serve over large areas and over long time spans as an indicator for upcoming shortage or surplus in TWS (the case study of the La Plata Basin needs to be expanded to further regions and longer time periods to obtain a global view).

Study Area:

- In India correlations between soil moisture and TWS are exceptionally high for the seasonal signal and in some parts also for the anomaly. A detailed case study of this region (similar to the one of the La Plata Basin) could give answer to the question why this is case and what this strong interrelation tells about the hydrological processes in this region.
- Another interesting study region is Australia. While the seasonal signals of soil moisture and TWS do not show high correlations, there is a stronger relation between the anomalies of both parameters (see Figure 7.4). A detailed analysis would reveal if this is a result (as in the case of the La Plata Basin) of the strong influence of El Niño and La Niña in this region.

Application:

- In this study hydrometeorological data have been linked to information on the social impacts of natural disasters. Potential links to economical impacts still need to be investigated. Therefore, economical information on the direct (e.g. destruction of property and infrastructure) and indirect (e.g. through business interruption) losses which result from natural disasters need to be integrated into the analysis of weather extremes. Such an approach is one example of giving future studies a more interdisciplinary character.
- The monitoring of weather extremes and related natural disasters is one field of application for the combined analysis of soil moisture and TWS data. Future studies could exploit other potential fields of application such as agricultural monitoring and the prediction of ignition and spread of fire. These fields of research would address the challenge of expanding and diversifying the application possibilities of scientific findings in order to create added value to society.
- The increasing amount of data from satellites and models opens up new possibilities of linking various data sets in order to address interdisciplinary fields of research. The exploitation and application of those information sources could be supported by increasing the comparability of the various data sets and by pooling the expertise and resources of the scientific community.

Twenty years ago the global mapping of soil moisture and TWS via satellites was still in its infancy. Recent and future satellite missions and the development of new processing algorithms will create new challenges and opportunities to address open research questions such as those which are listed above.

“The important thing is not to stop questioning. Curiosity has its own reason for existing.”
(Albert Einstein)

Bibliography

- A G, Wahr J, Zhong S (2012) Computations of the viscoelastic response of a 3-D compressible Earth to surface loading: an application to Glacial Isostatic Adjustment in Antarctica and Canada. *Geophysical Journal International* 192(2):557–572, DOI 10.1093/gji/ggs030
- Abelen S, Seitz F, Schmidt M, Güntner A (2011) Analysis of regional variations in soil moisture by means of remote sensing, satellite gravimetry and hydrological modelling. In: *GRACE, Remote Sensing and Ground-Based Methods in Multi-Scale Hydrology*, IAHS Red Book Series, Nr. 343, International Association of Hydrological Sciences: Oxford, UK, pp 9–15
- Abelen S, Seitz F (2013) Relating satellite gravimetry data to global soil moisture products via data harmonization and correlation analysis. *Remote Sensing of Environment* 136:89–98, DOI 10.1016/j.rse.2013.04.012
- Abelen S, Seitz F, Abarca-del Rio R, Güntner A (2015) Droughts and Floods in the La Plata Basin in Soil Moisture Data and GRACE. *Remote Sensing* 7(6):7324–7349, DOI 10.3390/rs70607324
- Al-Yaari A, Wigneron JP, Ducharne A, Kerr Y, de Rosnay P, de Jeu R, Govind A, Al Bitar A, Albergel C, Muñoz-Sabater J, Richaume P, Mialon A (2014) Global-scale evaluation of two satellite-based passive microwave soil moisture data sets (SMOS and AMSR-E) with respect to modelled estimates. *Remote Sensing of Environment* 149:181–195, DOI doi:10.1016/j.rse.2014.04.006
- Albergel C, Rüdiger C, Carrer D, Calvet JC, Fritz N, Naeimi V, Bartalis Z, Hasenauer S (2008a) An evaluation of ASCAT surface soil moisture products with in-situ observations in southwestern France. *Hydrology and Earth System Sciences Discussions* 5(4):2221–2250, DOI 10.5194/hessd-5-2221-2008
- Albergel C, Rüdiger C, Pellarin T, Calvet JC, Fritz N, Froissard F, Suquia D, Petitpa A, Piguet B, Martin E (2008b) From near-surface to root-zone soil moisture using an exponential filter: an assessment of the method based on in-situ observations and model simulations. *Hydrology and Earth System Sciences Discussions* 5(3):1603–1640, DOI 10.5194/hessd-5-1603-2008
- Albergel C, de Rosnay P, Balsamo G, Isaksen L, Muñoz-Sabater J (2012) Soil Moisture Analyses at ECMWF: Evaluation Using Global Ground-Based In Situ Observations. *Journal of Hydrometeorology* 13(5):1442–1460, DOI 10.1175/JHM-D-11-0107.1
- Albergel C, Dorigo W, Balsamo G, Muñoz-Sabater J, de Rosnay P, Isaksen L, Brocca L, de Jeu R, Wagner W (2013a) Monitoring multi-decadal satellite earth observation of soil moisture products through land surface reanalyses. *Remote Sensing of Environment* 138:77–89, DOI 10.1016/j.rse.2013.07.009
- Albergel C, Dorigo W, Reichle RH, Balsamo G, de Rosnay P, Muñoz-Sabater J, Isaksen L, de Jeu R, Wagner W (2013b) Skill and Global Trend Analysis of Soil Moisture from Reanalyses and Microwave Remote Sensing. *Journal of Hydrometeorology* 14(4):1259–1277, DOI 10.1175/JHM-D-12-0161.1
- Alkama R, Decharme B, Douville H, Becker M, Cazenave A, Sheffield J, Voldoire A, Tyteca S, Le Moigne P (2010) Global Evaluation of the ISBA-TRIP Continental Hydrological System. Part I:

- Comparison to GRACE Terrestrial Water Storage Estimates and In Situ River Discharges. *Journal of Hydrometeorology* 11(3):583–600, DOI 10.1175/2010JHM1211.1
- Anderson WB, Zaitchik BF, Hain CR, Anderson MC, Yilmaz MT, Mecikalski J, Schultz L (2012) Towards an integrated soil moisture drought monitor for East Africa. *Hydrology and Earth System Sciences* 16(8):2893–2913, DOI 10.5194/hess-16-2893-2012
- Arendt AA, Luthcke SB, Larsen CF, Abdalati W, Krabill WB, Beedle MJ (2008) Validation of high-resolution GRACE mascon estimates of glacier mass changes in the St. Elias Mountains, Alaska, USA, using aircraft laser altimetry. *Journal of Glaciology* 54(188):778–787, DOI 10.3189/002214308787780067
- Bartalis Z, Scipal K, Wagner W (2006) Azimuthal anisotropy of scatterometer measurements over land. *IEEE Transactions on Geoscience and Remote Sensing* 44(8):2083–2092, DOI 10.1109/TGRS.2006.872084
- Bartalis Z, Wagner W, Naeimi V, Hasenauer S, Scipal K, Bonekamp H, Figa J, Anderson C (2007) Initial soil moisture retrievals from the METOP-A Advanced Scatterometer (ASCAT). *Geophysical Research Letters* 34(20), DOI 10.1029/2007GL031088
- Bartalis Z, Naeimi V, Hasenauer S, Wagner W (2008) ASCAT Soil Moisture Product Handbook. Tech. Rep. ASCAT Soil Moisture Report Series, No. 15, Institute of Photogrammetry and Remote Sensing, Vienna University of Technology, Austria
- Batjes NH (1996) Development of a world data set of soil water retention properties using pedotransfer rules. *Geoderma* 71(1-2):31–52, DOI 10.1016/0016-7061(95)00089-5
- Berbery EH, Barros VR (2002) The Hydrologic Cycle of the La Plata Basin in South America. *Journal of Hydrometeorology* 3(6):630–645, DOI 10.1175/1525-7541(2002)003<0630:THCOTL>2.0.CO;2
- Bettadpur S (2007) Level-2 gravity field product user handbook, GRACE 327-734, Revision 3.0. Tech. rep., Center for Space Research, The University of Texas at Austin, USA
- Bevis M, Businger S, Herring TA, Rocken C, Anthes RA, Ware RH (1992) GPS meteorology - Remote sensing of atmospheric water vapor using the Global Positioning System. *Journal of Geophysical Research: Atmosphere* 97(D14):15787–15801, DOI 10.1029/92JD01517
- Bevis M, Alsdorf D, Kendrick E, Fortes LP, Forsberg B, Smalley R, Becker J (2005) Seasonal fluctuations in the mass of the Amazon River system and Earth's elastic response. *Geophysical Research Letters* 32(16), DOI 10.1029/2005GL023491
- Biemans H, Hutjes RWA, Kabat P, Strengers BJ, Gerten D, Rost S (2009) Effects of Precipitation Uncertainty on Discharge Calculations for Main River Basins. *Journal of Hydrometeorology* 10(4):1011–1025, DOI 10.1175/2008JHM1067.1
- Bolten JD, Crow WT, Zhan X, Jackson TJ, Reynolds CA (2010) Evaluating the Utility of Remotely Sensed Soil Moisture Retrievals for Operational Agricultural Drought Monitoring. *IEEE Journal of Selected Topics in Applied Earth Observations and Remote Sensing* 3(1):57–66, DOI 10.1109/JSTARS.2009.2037163
- Bouman J, Fuchs M, Ivins E, van der Wal W, Schrama E, Visser P, Horwath M (2014) Antarctic outlet glacier mass change resolved at basin scale from satellite gravity gradiometry. *Geophysical Research Letters* 41(16):5919–5926, DOI 10.1002/2014GL060637
- Box GEP, Jenkins GM, Reinsel GC (1994) *Time Series Analysis: Forecasting and Control*, 3rd edn. Prentice Hall: Englewood Cliff, NJ, USA

- Brocca L, Melone F, Moramarco T, Wagner W, Naeimi V, Bartalis Z, Hasenauer S (2010) Improving runoff prediction through the assimilation of the ASCAT soil moisture product. *Hydrology and Earth System Sciences* 14(10):1881–1893, DOI 10.5194/hess-14-1881-2010
- Brocca L, Hasenauer S, Lacava T, Melone F, Moramarco T, Wagner W, Dorigo W, Matgen P, Martínez-Fernández J, Llorens P, Latron J, Martin C, Bittelli M (2011) Soil moisture estimation through ASCAT and AMSR-E sensors: An intercomparison and validation study across Europe. *Remote Sensing of Environment* 115(12):3390–3408, DOI 10.1016/j.rse.2011.08.003
- Brocca L, Moramarco T, Melone F, Wagner W, Hasenauer S, Hahn S (2012) Assimilation of Surface- and Root-Zone ASCAT Soil Moisture Products Into Rainfall-Runoff Modeling. *IEEE Transactions on Geoscience and Remote Sensing* 50(7):2542–2555, DOI 10.1109/TGRS.2011.2177468
- Caffera RM, Berbery EH (2006) La Plata Basin Climatology. In: Barros V, Clarke R, Días PS (eds) *Climate Change in the La Plata Basin*, Research Centre for Sea and Atmosphere (CIMA), Buenos Aires, Argentina, pp 16–34
- Calmant S, Seyler F, Cretaux JF (2008) Monitoring continental surface waters by satellite altimetry. *Surveys in Geophysics* 29(4-5):247–269, DOI 10.1007/s10712-008-9051-1
- Cazenave A, Chen J (2010) Time-variable gravity from space and present-day mass redistribution in the Earth system. *Earth and Planetary Science Letters* 298(3-4):263–274, DOI 10.1016/j.epsl.2010.07.035
- Champagne C, McNairn H, Berg AA (2011) Monitoring agricultural soil moisture extremes in Canada using passive microwave remote sensing. *Remote Sensing of Environment* 115(10):2434–2444, DOI 10.1016/j.rse.2011.04.030
- Chen JL, Wilson CR, Famiglietti JS, Rodell M (2007) Attenuation effect on seasonal basin-scale water storage changes from GRACE time-variable gravity. *Journal of Geodesy* 81(4):237–245, DOI 10.1007/s00190-006-0104-2
- Chen JL, Wilson CR, Tapley BD, Yang ZL, Niu GY (2009) 2005 drought event in the Amazon River basin as measured by GRACE and estimated by climate models. *Journal of Geophysical Research: Solid Earth* 114(B5), DOI 10.1029/2008JB006056
- Chen JL, Wilson CR, Tapley BD (2010a) The 2009 exceptional Amazon flood and interannual terrestrial water storage change observed by GRACE. *Water Resources Research* 46(12), DOI 10.1029/2010WR009383
- Chen JL, Wilson CR, Tapley BD, Longuevergne L, Yang ZL, Scanlon BR (2010b) Recent La Plata basin drought conditions observed by satellite gravimetry. *Journal of Geophysical Research: Atmosphere* 115(D22), DOI 10.1029/2010JD014689
- Climate Prediction Center of NOAA (2014) Historical El Niño/ La Niña episodes. URL http://www.cpc.ncep.noaa.gov/products/analysis_monitoring/ensostuff/ensoyears.shtml, date of access 2014-09-06
- Coronel G, Menéndez Á, Chamorro L (2006) Physiography and Hydrology. In: Barros V, Clarke R, Días PS (eds) *Climate Change in the La Plata Basin*, Research Centre for Sea and Atmosphere (CIMA), Buenos Aires, Argentina, pp 44–60
- Cosh M (2004) Watershed scale temporal and spatial stability of soil moisture and its role in validating satellite estimates. *Remote Sensing of Environment* 92(4):427–435, DOI 10.1016/j.rse.2004.02.016

- Cosh MH, Jackson TJ, Starks P, Heathman G (2006) Temporal stability of surface soil moisture in the Little Washita River watershed and its applications in satellite soil moisture product validation. *Journal of Hydrology* 323(1-4):168–177, DOI 10.1016/j.jhydrol.2005.08.020
- Crossley D, de Linage C, Hinderer J, Boy JP, Famiglietti J (2012) A comparison of the gravity field over Central Europe from superconducting gravimeters, GRACE and global hydrological models, using EOF analysis. *Geophysical Journal International* 189(2):877–897, DOI 10.1111/j.1365-246X.2012.5404.x
- Dahle C, Flechtner F, Gruber C, König D, König R, Michalak G, Neumayer KH (2012) GFZ GRACE Level-2 Processing Standards Document for Level-2 Product Release 0005, (Scientific Technical Report STR12/02 Data, Revised Edition, January 2013). Tech. rep., Deutsches GeoForschungsZentrum GFZ, Potsdam, DOI 10.2312/GFZ.b103-1202-25
- Dahle C, Flechtner F, Gruber C, König D, König R, Michalak G, Neumayer KH (2014) GFZ RL05: An Improved Time-Series of Monthly GRACE Gravity Field Solutions. In: Flechtner F, Sneeuw N, Schuh WD (eds) *Observation of the System Earth from Space - CHAMP, GRACE, GOCE, and Future Missions*, Springer, Berlin Heidelberg, Germany, chap 4, pp 29–39
- De Viron O, Panet I, Mikhailov V, Van Camp M, Diament M (2008) Retrieving earthquake signature in grace gravity solutions. *Geophysical Journal International* 174(1):14–20, DOI 10.1111/j.1365-246X.2008.03807.x
- Dharssi I, Bovis KJ, Macpherson B, Jones CP (2011) Operational assimilation of ASCAT surface soil wetness at the Met Office. *Hydrology and Earth System Sciences* 15(8):2729–2746, DOI 10.5194/hess-15-2729-2011
- Dirmeyer PA (2000) Using a global soil wetness dataset to improve seasonal climate simulation. *Journal of Climate* 13:2900–2922, DOI 10.1175/1520-0442(2000)013<2900:UAGSWD>2.0.CO;2
- Dirmeyer PA, Guo Z, Gao X (2004) Comparison, Validation, and Transferability of Eight Multi-year Global Soil Wetness Products. *Journal of Hydrometeorology* 5(6):1011–1033, DOI 10.1175/JHM-388.1
- Döll P, Kaspar F, Lehner B (2003) A global hydrological model for deriving water availability indicators: model tuning and validation. *Journal of Hydrology* 270(1-2):105–134, DOI 10.1016/S0022-1694(02)00283-4
- Döll P, Hoffmann-Dobrev H, Portmann FT, Siebert S, Eicker A, Rodell M, Strassberg G, Scanlon BR (2012) Impact of water withdrawals from groundwater and surface water on continental water storage variations. *Journal of Geodynamics* 59-60:143–156, DOI 10.1016/j.jog.2011.05.001
- Dorigo WA, Scipal K, Parinussa RM, Liu YY, Wagner W, de Jeu RAM, Naeimi V (2010) Error characterisation of global active and passive microwave soil moisture datasets. *Hydrology and Earth System Sciences* 14(12):2605–2616, DOI 10.5194/hess-14-2605-2010
- Dorigo WA, van Oevelen P, Wagner W, Drusch M, Mecklenburg S, Robock A, Jackson T (2011a) A New International Network for in Situ Soil Moisture Data. *Eos, Transactions American Geophysical Union* 92(17):141–142, DOI 10.1029/2011EO170001
- Dorigo WA, Wagner W, Hohensinn R, Hahn S, Paulik C, Xaver A, Gruber A, Drusch M, Mecklenburg S, van Oevelen P, Robock A, Jackson T (2011b) The International Soil Moisture Network: A data hosting facility for global in situ soil moisture measurements. *Hydrology and Earth System Sciences* 15(5):1675–1698, DOI 10.5194/hess-15-1675-2011

- Dorigo WA, de Jeu R, Chung D, Parinussa R, Liu Y, Wagner W, Fernández-Prieto D (2012) Evaluating global trends (1988–2010) in harmonized multi-satellite surface soil moisture. *Geophysical Research Letters* 39(18), DOI 10.1029/2012GL052988
- Draper CS, Walker JP, Steinle PJ, de Jeu RAM, Holmes TRH (2009) An evaluation of AMSRE derived soil moisture over Australia. *Remote Sensing of Environment* 113(4):703–710, DOI 10.1016/j.rse.2008.11.011
- Draper CS, Reichle RH, De Lannoy GJM, Liu Q (2012) Assimilation of passive and active microwave soil moisture retrievals. *Geophysical Research Letters* 39(4), DOI 10.1029/2011GL050655
- Drusch M (2007) Initializing numerical weather prediction models with satellite-derived surface soil moisture: Data assimilation experiments with ECMWF's integrated forecast system and the TMI soil moisture data set. *Journal of Geophysical Research: Atmospheres* 112(3), DOI 10.1029/2006JD007478
- Encyclopedia Britannica (2011) South America: population density. URL <http://kids.britannica.com/comptons/art-160672>, date of access 2014-10-31
- Escorihuela MJ, Chanzy A, Wigneron JP, Kerr YH (2010) Effective soil moisture sampling depth of L-band radiometry: A case study. *Remote Sensing of Environment* 114(5):995–1001, DOI 10.1016/j.rse.2009.12.011
- Famiglietti JS, Rodell M (2013) Water in the balance. *Science* 340(6138):1300–1301, DOI 10.1126/science.1236460
- Famiglietti JS, Cazenave A, Eicker A, Reager JT, Rodell M, Velicogna I (2015) Satellites provide the big picture. *Science* 349(6249):684–685, DOI 10.1126/science.aac9238
- Fan X, Thompson B (2001) Confidence Intervals for Effect Sizes. *Educational and Psychological Measurement* 61(4):517–531, DOI 10.1177/0013164401614001
- Fernández LI, Schuh H, Schmidt M, Seitz F (2007) Effects of inter-annual water storage variations on polar motion. *Geophysical Journal International* 169(1):12–18, DOI 10.1111/j.1365-246X.2006.03304.x
- Ferrazzoli P, Rahmoune R, Moccia F, Grings F, Salvia M, Barber M, Douna V, Karszenbaum H, Soldano A, Goniadzki D, Parmuchi G, Montenegro C, Kandus P, Borro M (2010) The Effect of Rain and Flooding Events on AMSR-E Signatures of La Plata Basin, Argentina. *IEEE Journal of Selected Topics in Applied Earth Observations and Remote Sensing* 3(1):81–90, DOI 10.1109/JSTARS.2010.2040584
- Flechtner F, Bettadpur S, Watkins M, Kruizinga G (2015) GRACE Science Data System Monthly Report May 2015. Tech. rep.
- Forman BA, Reichle RH, Rodell M (2012) Assimilation of terrestrial water storage from GRACE in a snow-dominated basin. *Water Resources Research* 48(1):1–14, DOI 10.1029/2011WR011239
- Forootan E, Kusche J (2012) Separation of global time-variable gravity signals into maximally independent components. *Journal of Geodesy* 86(7):477–497, DOI 10.1007/s00190-011-0532-5
- Forootan E, Awange JL, Kusche J, Heck B, Eicker A (2012) Independent patterns of water mass anomalies over Australia from satellite data and models. *Remote Sensing of Environment* 124:427–443, DOI 10.1016/j.rse.2012.05.023
- Frappart F, Ramillien G, Biancamaria S, Mognard NM, Cazenave A (2006) Evolution of high-latitude snow mass derived from the GRACE gravimetry mission (2002–2004). *Geophysical Research Letters* 33(2), DOI 10.1029/2005GL024778

- Frappart F, Ramillien G, Leblanc M, Tweed SO, Bonnet MP, Maisongrande P (2011) An independent component analysis filtering approach for estimating continental hydrology in the GRACE gravity data. *Remote Sensing of Environment* 115(1):187–204, DOI 10.1016/j.rse.2010.08.017
- Frappart F, Ramillien G, Ronchail J (2013a) Changes in terrestrial water storage versus rainfall and discharges in the Amazon basin. *International Journal of Climatology* 33(14):3029–3046, DOI 10.1002/joc.3647
- Frappart F, Seoane L, Ramillien G (2013b) Validation of GRACE-derived terrestrial water storage from a regional approach over South America. *Remote Sensing of Environment* 137:69–83, DOI 10.1016/j.rse.2013.06.008
- Fuchs MJ, Bouman J, Broerse T, Visser P, Vermeersen B (2013) Observing coseismic gravity change from the Japan Tohoku-Oki 2011 earthquake with GOCE gravity gradiometry. *Journal of Geophysical Research: Solid Earth* 118(10):5712–5721, DOI 10.1002/jgrb.50381
- Gallant AJE, Karoly DJ (2009) Atypical influence of the 2007 La Niña on rainfall and temperature in southeastern Australia. *Geophysical Research Letters* 36(14), DOI 10.1029/2009GL039026
- Gao BC (1996) NDWI - A normalized difference water index for remote sensing of vegetation liquid water from space. *Remote Sensing of Environment* 58(3):257–266, DOI 10.1016/S0034-4257(96)00067-3
- Gao Y, Xie H, Lu N, Yao T, Liang T (2010) Toward advanced daily cloud-free snow cover and snow water equivalent products from Terra-Aqua MODIS and Aqua AMSR-E measurements. *Journal of Hydrology* 385(1-4):23–35, DOI 10.1016/j.jhydrol.2010.01.022
- Garcia NO (1996) The spatial variability of runoff and precipitation in the Rio de la Plata basin. *Hydrological Sciences Journal* 41(3):279–300, DOI 10.1080/02626669609491503
- Golden Gate Weather Service (2014) El Niño and La Niña Years and Intensities Based on Oceanic Niño Index (ONI). URL <http://ggweather.com/enso/oni.htm>, date of access 2014-09-06
- Grimm AM, Barros VR, Doyle ME (2000) Climate Variability in Southern South America Associated with El Niño and La Niña Events. *Journal of Climate* 13(1):35–58, DOI 10.1175/1520-0442(2000)013<0035:CVISSA>2.0.CO;2
- Gudmundsson L, Tallaksen LM, Stahl K, Clark DB, Dumont E, Hagemann S, Bertrand N, Gerten D, Heinke J, Hanasaki N, Voss F, Koirala S (2012) Comparing large-scale hydrological model simulations to observed runoff percentiles in Europe. *Journal of Hydrometeorology* 13(2):604–620, DOI 10.1175/JHM-D-11-083.1
- Guha-Sapir D, Below R, Hoyois P (2009) EM-DAT The International Disaster Database / Centre for Research on the Epidemiology of Disasters - CRED. URL www.emdat.be, date of access 2014-10-16
- Güntner A, Stuck J, Werth S, Döll P, Verzano K, Merz B (2007) A global analysis of temporal and spatial variations in continental water storage. *Water Resources Research* 43(5), DOI 10.1029/2006WR005247
- Güntner A (2008) Improvement of Global Hydrological Models Using GRACE Data. *Surveys in Geophysics* 29(4-5):375–397, DOI 10.1007/s10712-008-9038-y
- Guo Z, Dirmeyer PA (2006) Evaluation of the Second Global Soil Wetness Project soil moisture simulations: 1. Intermodel comparison. *Journal of Geophysical Research: Atmospheres* 111(22), DOI 10.1029/2006JD007233

- Haddeland I, Clark DB, Franssen W, Ludwig F, Voß F, Arnell NW, Bertrand N, Best M, Folwell S, Gerten D, Gomes S, Gosling SN, Hagemann S, Hanasaki N, Harding R, Heinke J, Kabat P, Koirala S, Oki T, Polcher J, Stacke T, Viterbo P, Weedon GP, Yeh P (2011) Multimodel estimate of the global terrestrial water balance: setup and first results. *Journal of Hydrometeorology* 12:869–884, DOI 10.1175/2011JHM1324.1
- Hamilton SK (2002) Human impacts on hydrology in the Pantanal wetland of South America. *Water Science and Technology* 45(11):35–44
- Harding R, Best M, Blyth E, Hagemann S, Kabat P, Tallaksen LM, Warnaars T, Wiberg D, Weedon GP, van Lanen H, Ludwig F, Haddeland I (2011) WATCH: current knowledge of the terrestrial global water cycle. *Journal of Hydrometeorology* 12:1149–1156, DOI 10.1175/JHM-D-11-024.1
- Heathman GC, Starks PJ, Ahuja LR, Jackson TJ (2003) Assimilation of surface soil moisture to estimate profile soil water content. *Journal of Hydrology* 279(1-4):1–17, DOI 10.1016/S0022-1694(03)00088-X
- Heiskanen WA, Moritz H (1967) *Physical geodesy*. Freeman and Co., San Francisco, USA and London, UK
- Hillel D (1998) *Environmental Soil Physics*. Academic Press, San Diego, USA
- Hornacek M, Wagner W, Sabel D, Truong HL, Snoeij P, Hahmann T, Diedrich E, Doubkova M (2012) Potential for High Resolution Systematic Global Surface Soil Moisture Retrieval via Change Detection Using Sentinel-1. *IEEE Journal of Selected Topics in Applied Earth Observations and Remote Sensing* 5(4):1303–1311, DOI 10.1109/JSTARS.2012.2190136
- Hornbuckle BK, England AW, Anderson MC (2007) The Effect of Intercepted Precipitation on the Microwave Emission of Maize at 1.4 GHz. *IEEE Transactions on Geoscience Remote Sensing* 45(7):1988–1995, DOI 10.1109/TGRS.2007.894057
- Houborg R, Rodell M, Li B, Reichle R, Zaitchik BF (2012) Drought indicators based on model-assimilated Gravity Recovery and Climate Experiment (GRACE) terrestrial water storage observations. *Water Resources Research* 48(7), DOI 10.1029/2011WR011291
- Huang J, Halpenny J, van der Wal W, Klatt C, James TS, Rivera A (2012) Detectability of groundwater storage change within the Great Lakes Water Basin using GRACE. *Journal of Geophysical Research* 117(B8), DOI 10.1029/2011JB008876
- Jackson TJ, Schmugge TJ (1991) Vegetation Effects on the Microwave Emission of Soils. *Remote Sensing of Environment* 212(3):203–212, DOI 10.1016/0034-4257(91)90057-D
- Jackson TJ (2005) Remote Sensing Soil Moisture. In: Hillel D (ed) *Encyclopedia of Soils in the Environment*, vol 3, Elsevier, Ltd., Oxford, UK, pp 392–398
- Jackson TJ, Cosh MH, Bindlish R, Starks PJ, Bosch DD, Seyfried M, Goodrich DC, Moran MS, Du J (2010) Validation of advanced microwave scanning radiometer soil moisture products. *IEEE Transactions on Geoscience and Remote Sensing* 48(12):4256–4272, DOI 10.1109/TGRS.2010.2051035
- Jackson TJ, Bindlish R, Cosh MH, Zhao T, Starks PJ, Bosch DD, Seyfried M, Moran MS, Goodrich DC, Kerr YH, Leroux D (2012) Validation of soil moisture and Ocean Salinity (SMOS) soil moisture over watershed networks in the U.S. *IEEE Transactions on Geoscience and Remote Sensing* 50(5):1530–1543, DOI 10.1109/TGRS.2011.2168533

- Jajarmizadeh M, Harun S, Mohsen S (2012) A Review on Theoretical Consideration and Types of Models in Hydrology. *Journal of Environmental Science and Technology* 5(5):249–261, DOI <http://dx.doi.org/10.3923/jest.2012.249.261>
- de Jeu RAM, Wagner W, Holmes TRH, Dolman AJ, van de Giesen NC, Friesen J (2008) Global Soil Moisture Patterns Observed by Space Borne Microwave Radiometers and Scatterometers. *Surveys in Geophysics* 29(4):399–420, DOI 10.1007/s10712-008-9044-0
- Jiang D, Wang J, Huang Y, Zhou K, Ding X, Fu J (2014) The review of GRACE data applications in terrestrial hydrology monitoring. *Advances in Meteorology* 2014, DOI 10.1155/2014/725131
- Jin S, Feng G (2013) Large-scale variations of global groundwater from satellite gravimetry and hydrological models, 2002–2012. *Global and Planetary Change* 106:20–30, DOI 10.1016/j.gloplacha.2013.02.008
- Joseph G (2005) *Fundamentals of Remote Sensing*, 2nd edn. University Press, India
- JPL (2015) JPL, CSR or GFZ-which solution should I use? URL <http://grace.jpl.nasa.gov/data/choosing-a-solution/>, date of access 2015-10-16
- Kato H, Rodell M, Beyrich F, Cleugh H, Gorsel EV (2007) Sensitivity of Land Surface Simulations to Model Physics, Land Characteristics, and Forcings, at Four CEOP Sites. *Journal of the Meteorological Society of Japan* 85A:187–204, DOI 10.2151/jmsj.85A.187
- Kerr YH, Waldteufel P, Wigneron JP, Delwart S, Cabot F, Boutin J, Escorihuela MJ, Font J, Reul N, Gruhier C, Juglea SE, Drinkwater MR, Hahne A, Martin-Neira M, Mecklenburg S (2010) The SMOS Mission: New Tool for Monitoring Key Elements of the Global Water Cycle. *Proceedings of the IEEE* 98(5):666–687, DOI 10.1109/JPROC.2010.2043032
- Kim G, Barros AP (2002) Downscaling of remotely sensed soil moisture with a modified fractal interpolation method using contraction mapping and ancillary data. *Remote Sensing of Environment* 83(3):400–413, DOI 10.1016/S0034-4257(02)00044-5
- Klaes KD, Cohen M, Buhler Y, Schlüssel P, Munro R, Luntama JP, von Engeln A, Clerigh EO, Bonekamp H, Ackermann J, Schmetz J (2007) An introduction to the Eumetsat polar system. *Bulletin of the American Meteorological Society* 88(July):1085–1096, DOI 10.1175/BAMS-88-7-1085
- Klees R, Zapreeva EA, Winsemius HC, Savenije HHG (2006) The bias in GRACE estimates of continental water storage variations. *Hydrology and Earth System Sciences Discussions* 3(6):3557–3594, DOI 10.5194/hessd-3-3557-2006
- Klees R, Liu X, Wittwer T, Gunter BC, Revtova EA, Tenzer R, Ditmar P, Winsemius HC, Savenije HHG (2008) A Comparison of Global and Regional GRACE Models for Land Hydrology. *Surveys in Geophysics* 29(4-5):335–359, DOI 10.1007/s10712-008-9049-8
- Klink CA, Machado RB (2005) Conservation of the Brazilian Cerrado. *Conservation Biology* 19(3):707–713, DOI 10.1111/j.1523-1739.2005.00702.x
- Koster RD, Suarez MJ (2001) Soil Moisture Memory in Climate Models. *Journal of Hydrometeorology* 2(6):558–570, DOI 10.1175/1525-7541(2001)002<0558:SMMICM>2.0.CO;2
- Koster RD, Guo Z, Yang R, Dirmeyer PA, Mitchell K, Puma MJ (2009) On the nature of soil moisture in land surface models. *Journal of Climate* 22(16):4322–4335, DOI 10.1175/2009JCLI2832.1
- Kravtsova VI, Tarasenko TV (2010) Space monitoring of Aral Sea degradation. *Water Resources* 37(3):285–296, DOI 10.1134/S0097807810030036

- Kumar DN, Reshmidevi TV (2013) Remote Sensing Applications in Water Resources. *Journal of the Indian Institute of Science* 93(2):164–187
- Kurtenbach E, Mayer-Gürr T, Eicker A (2009) Deriving daily snapshots of the Earth's gravity field from GRACE LIB data using Kalman filtering. *Geophysical Research Letters* 36(17):1–5, DOI 10.1029/2009GL039564
- Kusche J (2007) Approximate decorrelation and non-isotropic smoothing of time-variable GRACE-type gravity field models. *Journal of Geodesy* 81(11):733–749, DOI 10.1007/s00190-007-0143-3
- Lacava T, Cuomo V, Di Leo EV, Pergola N, Romano F, Tramutoli V (2005) Improving soil wetness variations monitoring from passive microwave satellite data: The case of April 2000 Hungary flood. *Remote Sensing of Environment* 96(2):135–148, DOI 10.1016/j.rse.2005.01.015
- Landerer FW, Swenson SC (2012) Accuracy of scaled GRACE terrestrial water storage estimates. *Water Resources Research* 48(4):1–11, DOI 10.1029/2011WR011453
- Larkin NK (2005) Global seasonal temperature and precipitation anomalies during El Niño autumn and winter. *Geophysical Research Letters* 32(16), DOI 10.1029/2005GL022860
- Lawrimore J, Heim Jr RR, Svoboda M, Swail V, Englehart PJ (2002) Beginning a New Era of Drought Monitoring Across North America. *Bulletin of the American Meteorological Society* 83:1191–1192
- Leese J, Jackson T, Pitman A, Dirmeyer P (2001) Meeting summary: GEWEX/BAHC International Workshop on Soil Moisture Monitoring, Analysis, and Prediction for Hydrometeorological and Hydroclimatological Applications. *Bulletin of the American Meteorological Society* 82(7):1423–1430
- Lemoine JM, Bruinsma S, Loyer S, Biancale R, Marty JC, Perosanz F, Balmino G (2007) Temporal gravity field models inferred from GRACE data. *Advances in Space Research* 39(10):1620–1629, DOI 10.1016/j.asr.2007.03.062
- Leroux DJ, Kerr YH, Richaume P, Fieuzal R (2013) Spatial distribution and possible sources of SMOS errors at the global scale. *Remote Sensing of Environment* 133:240–250, DOI 10.1016/j.rse.2013.02.017
- Liang S, Li X, Wang J (2012) *Advanced Remote Sensing: Terrestrial Information Extraction and Applications*. Academic Press, USA
- Liu YY, Parinussa RM, Dorigo WA, de Jeu RAM, Wagner W, van Dijk AIJM, McCabe MF, Evans JP (2011) Developing an improved soil moisture dataset by blending passive and active microwave satellite-based retrievals. *Hydrology and Earth System Sciences* 15:425–436, DOI 10.5194/hess-15-425-2011
- Liu YY, Dorigo WA, Parinussa RM, de Jeu RAM, Wagner W, McCabe MF, Evans JP, van Dijk AIJM (2012) Trend-preserving blending of passive and active microwave soil moisture retrievals. *Remote Sensing of Environment* 123:280–297, DOI 10.1016/j.rse.2012.03.014
- Loew A, Stacke T, Dorigo W, de Jeu R, Hagemann S (2013) Potential and limitations of multidecadal satellite soil moisture observations for selected climate model evaluation studies. *Hydrology and Earth System Sciences* 17(9):3523–3542, DOI 10.5194/hess-17-3523-2013
- Long D, Scanlon BR, Longuevergne L, Sun AY, Fernando DN, Save H (2013) GRACE satellite monitoring of large depletion in water storage in response to the 2011 drought in Texas. *Geophysical Research Letters* 40(13):3395–3401, DOI 10.1002/grl.50655

- Longuevergne L, Wilson CR, Scanlon BR, Crétaux JF (2013) GRACE water storage estimates for the middle east and other regions with significant reservoir and lake storage. *Hydrology and Earth System Sciences* 17(12):4817–4830, DOI 10.5194/hess-17-4817-2013
- Lundin LC, Bergström S, Eriksson E, Seibert J (2000) Hydrological models and modelling. In: Lundin LC (ed) *Sustainable Water Management 1: The Waterscape*, Uppsala University, Sweden, chap 11, pp 129–140
- Mahfouf JF (2010) Assimilation of satellite-derived soil moisture from ASCAT in a limited-area NWP model. *Quarterly Journal of the Royal Meteorological Society* 136(648):784–798, DOI 10.1002/qj.602
- Mandeville P, Campagnoni R, Bernardi R (2009) Informe de estado de situación - SITREP Sequía e incendios en Uruguay. Tech. rep., URL <http://reliefweb.int/report/uruguay/informe-de-estado-de-situacion-sequia-e-incendios-en-uruguay>, date of access 2014-11-05
- Milly PCD, Shmakin AB (2002) Global Modeling of Land Water and Energy Balances. Part I: The Land Dynamics (LaD) Model. *Journal of Hydrometeorology* 3(3):283–299, DOI 10.1175/1525-7541(2002)003<0283:GMOLWA>2.0.CO;2
- Miralles DG, Crow WT, Cosh MH (2010) Estimating Spatial Sampling Errors in Coarse-Scale Soil Moisture Estimates Derived from Point-Scale Observations. *Journal of Hydrometeorology* 11(6):1423–1429, DOI 10.1175/2010JHM1285.1
- Mueller B, Hirschi M, Seneviratne SI (2011) New diagnostic estimates of variations in terrestrial water storage based on ERA-Interim data. *Hydrological Processes* 25(7):996–1008, DOI 10.1002/hyp.7652
- Müller Schmied H, Eisner S, Franz D, Wattenbach M, Portmann FT, Flörke M, Döll P (2014) Sensitivity of simulated global-scale freshwater fluxes and storages to input data, hydrological model structure, human water use and calibration. *Hydrology and Earth System Sciences Discussions* 11:1583–1649, DOI 10.5194/hessd-11-1583-2014
- Musy A, Hingray B, Picouet C (2015) *Hydrology: A Science for Engineers*. CRC Press, Boca Raton, USA
- Ngo-Duc T, Laval K, Ramillien G, Polcher J, Cazenave A (2007) Validation of the land water storage simulated by Organising Carbon and Hydrology in Dynamic Ecosystems (ORCHIDEE) with Gravity Recovery and Climate Experiment (GRACE) data. *Water Resources Research* 43(4):1–8, DOI 10.1029/2006WR004941
- Njoku EG, Li L (1999) Retrieval of Land Surface Parameters Using Passive Microwave Measurements at 6 to 18 GHz. *IEEE Transactions on Geoscience and Remote Sensing* 37(1):79–93, DOI 10.1109/36.739125
- Njoku EG, Jackson TJ, Lakshmi V, Member S, Chan TK, Nghiem SV (2003) Soil Moisture Retrieval From AMSR-E. *IEEE Transactions on Geoscience and Remote Sensing* 41(2):215–229, DOI 10.1109/TGRS.2002.808243
- Nolin AW (2010) Recent advances in remote sensing of seasonal snow. *Journal of Glaciology* 56(200):1141–1150, DOI 10.3189/002214311796406077
- NRCS-USDA (1997) Soil Climate Map. URL http://www.nrcs.usda.gov/wps/portal/nrcs/detail/soils/use/?cid=nrcs142p2_054017, date of access 2016-01-19

- Ochsner TE, Cosh MH, Cuenca RH, Dorigo WA, Draper CS, Hagimoto Y, Kerr YH, Njoku EG, Small EE, Zreda M (2013) State of the Art in Large-Scale Soil Moisture Monitoring. *Soil Science Society of America Journal* 77(6):1888–1919, DOI 10.2136/sssaj2013.03.0093
- Oliva R, Daganzo-Eusebio E, Kerr YH, Mecklenburg S, Nieto S, Richaume P, Gruhier C (2012) SMOS radio frequency interference scenario: Status and actions taken to improve the RFI environment in the 1400-1427-MHZ passive band. *IEEE Transactions on Geoscience and Remote Sensing* 50(5):1427–1439, DOI 10.1109/TGRS.2012.2182775
- O'Neill P, Entekhabi D, Njoku E, Kellogg K (2010) The NASA Soil Moisture Active Passive (SMAP) mission: Overview. In: 2010 IEEE International Geoscience and Remote Sensing Symposium, IEEE, pp 3236–3239, DOI 10.1109/IGARSS.2010.5652291
- Overgaard J, Rosbjerg D, Butts MB (2005) Land-surface modelling in hydrological perspective. *Bio-geosciences Discussions* 2(6):1815–1848, DOI 10.5194/bgd-2-1815-2005
- Owe M, de Jeu R, Walker J (2001) A Methodology for Surface Soil Moisture and Vegetation Optical Depth Retrieval Using the Microwave Polarization Difference Index. *IEEE Transactions on Geoscience and Remote Sensing* 39(8):1643–1654
- Owe M, de Jeu R, Holmes T (2008) Multisensor historical climatology of satellite-derived global land surface moisture. *Journal of Geophysical Research* 113(F1), DOI 10.1029/2007JF000769
- Pallarés OR, Berretta EJ, Maraschin GE (2005) The South American Campos ecosystem. In: Suttie JM, Reynolds SG, Batello C (eds) *Grasslands of the World*, Food and Agricultural Organization of the United Nations, Rome, pp 171–219
- Papa F, Güntner A, Frappart F, Prigent C, Rossow WB (2008) Variations of surface water extent and water storage in large river basins: A comparison of different global data sources. *Geophysical Research Letters* 35(11), DOI 10.1029/2008GL033857
- Parinussa RM, Holmes TRH, Yilmaz MT, Crow WT (2011) The impact of land surface temperature on soil moisture anomaly detection from passive microwave observations. *Hydrology and Earth System Sciences* 15(10):3135–3151, DOI 10.5194/hess-15-3135-2011
- Pereira A, Pacino MC (2012) Annual and seasonal water storage changes detected from GRACE data in the La Plata Basin. *Physics of the Earth and Planetary Interiors* 212-213:88–99, DOI 10.1016/j.pepi.2012.09.005
- Pereira A, Miranda S, Pacino MC, Forsberg R (2012) Water Storage Changes from GRACE Data in the La Plata Basin. In: Kenyon S, Pacino MC, Marti U (eds) *Geodesy for Planet Earth*, International Association of Geodesy Symposia, vol 136, Springer-Verlag Berlin Heidelberg, Germany, pp 613–618, DOI 10.1007/978-3-642-20338-1_75
- Petropoulos GP (2014) *Remote Sensing of Energy Fluxes and Soil Moisture Content*. CRC Press, Boca Raton, USA
- Pielke RA, Liston GE, Eastman JL, Lu L, Coughenour M (1999) Seasonal weather prediction as an initial value problem. *Journal of Geophysical Research* 104(D16):19,463–19,479, DOI 10.1029/1999JD900231
- Piles M, Camps A, Vall-Llossera M, Corbella I, Panciera R, Rudiger C, Kerr YH, Walker J (2011) Downscaling SMOS-derived soil moisture using MODIS visible/infrared data. *IEEE Transactions on Geoscience and Remote Sensing* 49(9):3156–3166, DOI 10.1109/TGRS.2011.2120615
- Politis G (2008) The Pampas and Campos of South America. In: Silverman H, Isbell WH (eds) *The Handbook of South American Archaeology*, Springer-Verlag New York, USA, pp 235–260

- Preisendorfer RW, Mobley C (1988) *Principal Component Analysis in Meteorology and Oceanography*. Elsevier, Amsterdam, Netherlands, DOI 10.1029/JD093iD09p10815
- Purcell A, Dehecq A, Tregoning P, Potter EK, McClusky SC, Lambeck K (2011) Relationship between glacial isostatic adjustment and gravity perturbations observed by GRACE. *Geophysical Research Letters* 38(18), DOI 10.1029/2011GL048624
- Ramillien G, Frappart F, Güntner A, Ngo-Duc T, Cazenave A, Laval K (2006a) Time variations of the regional evapotranspiration rate from Gravity Recovery and Climate Experiment (GRACE) satellite gravimetry. *Water Resources Research* 42(10), DOI 10.1029/2005WR004331
- Ramillien G, Lombard A, Cazenave A, Ivins E, Llubes M, Remy F, Biancale R (2006b) Interannual variations of the mass balance of the Antarctica and Greenland ice sheets from GRACE. *Global and Planetary Change* 53(3):198–208, DOI 10.1016/j.gloplacha.2006.06.003
- Ramillien G, Famiglietti JS, Wahr J (2008) Detection of Continental Hydrology and Glaciology Signals from GRACE: A Review. *Surveys in Geophysics* 29(4-5):361–374, DOI 10.1007/s10712-008-9048-9
- Rangelova E, van der Wal W, Braun A, Sideris MG, Wu P (2007) Analysis of Gravity Recovery and Climate Experiment time-variable mass redistribution signals over North America by means of principal component analysis. *Journal of Geophysical Research: Earth Surface* 112(3), DOI 10.1029/2006JF000615
- Reager J, Thomas A, Sproles E, Rodell M, Beaudoin H, Li B, Famiglietti J (2015) Assimilation of GRACE Terrestrial Water Storage Observations into a Land Surface Model for the Assessment of Regional Flood Potential. *Remote Sensing* 7(11):14,663–14,679, DOI 10.3390/rs71114663
- Rees WG (2013) *Physical Principles of Remote Sensing*, 3rd edn. Cambridge University Press, New York, USA
- Reichle R, Koster R, Dong J, Berg A (2004) Global soil moisture from satellite observations, land surface models, and ground data: Implications for data assimilation. *Journal of Hydrometeorology* 5:430–442, DOI 10.1175/1525-7541(2004)005<0430:GSMFSO>2.0.CO;2
- Reigber C, Schwintzer P, Lühr P (1999) The CHAMP geopotential mission. *Bollettino di Geofisica Teorica ed Applicata* 40(3–4):285–289
- Reigber C, Schwintzer P, Neumayer KH, Barthelmes F, König R, Förste C, Balmino G, Biancale R, Lemoine JM, Loyer S, Bruinsma S, Perosanz F, Fayard T (2003) The CHAMP-only earth gravity field model EIGEN-2. *Advances in Space Research* 31(8):1883–1888, DOI 10.1016/S0273-1177(03)00162-5
- Ribeiro MC, Metzger JP, Martensen AC, Ponzoni FJ, Hirota MM (2009) The Brazilian Atlantic Forest: How much is left, and how is the remaining forest distributed? Implications for conservation. *Biological Conservation* 142(6):1141–1153, DOI 10.1016/j.biocon.2009.02.021
- Rodell M, Famiglietti JS (2001) An analysis of terrestrial water storage variations in Illinois with implications for the Gravity Recovery and Climate Experiment (GRACE). *Water Resources Research* 37(5):1327–1339, DOI 10.1029/2000WR900306
- Rodell M, Famiglietti JS, Chen J, Seneviratne SI, Viterbo P, Holl S, Wilson CR (2004a) Basin scale estimates of evapotranspiration using GRACE and other observations. *Geophysical Research Letters* 31(20), DOI 10.1029/2004GL020873
- Rodell M, Houser PR, Jambor U, Gottschalck J, Mitchell K, Meng CJ, Arsenault K, Cosgrove B, Radakovich J, Bosilovich M, Entin JK, Walker JP, Lohmann D, Toll D (2004b) The Global Land

- Data Assimilation System. *Bulletin of the American Meteorological Society* 85(3):381–394, DOI 10.1175/BAMS-85-3-381
- Rodell M, Chao BF, Au AY, Kimball JS, McDonald KC (2005) Global Biomass Variation and Its Geodynamic Effects: 198298. *Earth Interactions* 9:1–19, DOI 10.1175/EI126.1
- Rodell M, Velicogna I, Famiglietti JS (2009) Satellite-based estimates of groundwater depletion in India. *Nature* 460(7258):999–1002, DOI 10.1038/nature08238
- Rodgers JL, Nicewander WA (2008) Thirteen Ways to Look at the Correlation Coefficient. *The American Statistician* 42(1):59–66
- Rummel R, Balmino G, Johannessen J, Visser P, Woodworth P (2002) Dedicated gravity field missions - principles and aims. *Journal of Geodynamics* 33(1-2):3–20, DOI 10.1016/S0264-3707(01)00050-3
- Rummel R (2005) Geoid and Gravity in Earth Sciences - An Overview. *Earth, Moon, and Planets* 94(1-2):3–11, DOI 10.1007/s11038-005-3755-8
- Rummel R, Yi W, Stummer C (2011) GOCE gravitational gradiometry. *Journal of Geodesy* 85:777–790, DOI 10.1007/s00190-011-0500-0
- Sakumura C, Bettadpur S, Bruinsma S (2014) Ensemble prediction and intercomparison analysis of GRACE time-variable gravity field models. *Geophysical Research Letters* 41(5):1389–1397, DOI 10.1002/2013GL058632.1.
- Sawaya K (2003) Extending satellite remote sensing to local scales: land and water resource monitoring using high-resolution imagery. *Remote Sensing of Environment* 88(1):144–156, DOI 10.1016/j.rse.2003.04.0006
- Scanlon BR, Longuevergne L, Long D (2012) Ground referencing GRACE satellite estimates of groundwater storage changes in the California Central Valley, USA. *Water Resources Research* 48(4):1–9, DOI 10.1029/2011WR011312
- Schanda E (1986) *Physical Fundamentals of Remote Sensing*. Springer-Verlag Berlin, Germany
- Schmidt M, Fengler M, Mayer-Gürr T, Eicker A, Kusche J, Sánchez L, Han SC (2006a) Regional gravity modeling in terms of spherical base functions. *Journal of Geodesy* 81(1):17–38, DOI 10.1007/s00190-006-0101-5
- Schmidt M, Han SC, Kusche J, Sanchez L, Shum CK (2006b) Regional high-resolution spatiotemporal gravity modeling from GRACE data using spherical wavelets. *Geophysical Research Letters* 33(8), DOI 10.1029/2005GL025509
- Schmidt R, Schwintzer P, Flechtner F, Reigber C, Günter A, Döll P, Ramillien G, Cazenave A, Petrovic S, Jochmann H (2006c) GRACE observations of changes in continental water storage. *Global and Planetary Change* 50(1-2):112–126, DOI 10.1016/j.gloplacha.2004.11.018
- Schmidt M, Seitz F, Shum CK (2008a) Regional four-dimensional hydrological mass variations from GRACE, atmospheric flux convergence, and river gauge data. *Journal of Geophysical Research* 113(B10), DOI 10.1029/2008JB005575
- Schmidt R, Flechtner F, Meyer U, Neumayer KH, Dahle C, König R, Kusche J (2008b) Hydrological Signals Observed by the GRACE Satellites. *Surveys in Geophysics* 29(4-5):319–334, DOI 10.1007/s10712-008-9033-3

- Schmidt R, Petrovic S, Güntner A, Barthelmes F, Wunsch J, Kusche J (2008c) Periodic components of water storage changes from GRACE and global hydrology models. *Journal of Geophysical Research* 113(B8), DOI 10.1029/2007JB005363
- Schneeberger K, Stamm C, Mätzler C, Flüher H (2004) Ground-based dual-frequency radiometry of bare soil at high temporal resolution. *IEEE Transactions on Geoscience and Remote Sensing* 42(3):588–595, DOI 10.1109/TGRS.2003.821058
- Schneider U, Becker A, Finger P, Meyer-Christoffer A, Rudolf B, Ziese M (2011) GPCC Monitoring Product: Near Real-Time Monthly Land-Surface Precipitation from Rain-Gauges based on SYNOP and CLIMAT data. DOI 10.5676/DWD_GPCC/MP_M_V4_100
- Schnitzer S, Seitz F, Eicker A, Güntner A, Wattenbach M, Menzel A (2013) Estimation of soil loss by water erosion in the Chinese Loess Plateau using Universal Soil Loss Equation and GRACE. *Geophysical Journal International* 193(3):1283–1290, DOI 10.1093/gji/ggt023
- Schwatke C, Dettmering D, Bosch W, Seitz F (2015) DAHITI – an innovative approach for estimating water level time series over inland waters using multi-mission satellite altimetry. *Hydrology and Earth System Sciences* 19:4345–4364, DOI 10.5194/hess-19-4345-2015
- Scipal K, Scheffler C, Wagner W (2005) Soil moisture-runoff relation at the catchment scale as observed with coarse resolution microwave remote sensing. *Hydrology and Earth System Sciences* 9(3):173–183, DOI 10.5194/hess-9-173-2005
- Scipal K, Holmes T, de Jeu R, Naeimi V, Wagner W (2008) A possible solution for the problem of estimating the error structure of global soil moisture data sets. *Geophysical Research Letters* 35(24), DOI 10.1029/2008GL035599
- Seitz F, Schmidt M, Shum C (2008) Signals of extreme weather conditions in Central Europe in GRACE 4-D hydrological mass variations. *Earth and Planetary Science Letters* 268(1-2):165–170, DOI 10.1016/j.epsl.2008.01.001
- Seneviratne SI, Viterbo P, Lüthi D, Schär C (2004) Inferring changes in terrestrial water storage using ERA-40 reanalysis data: The Mississippi River basin. *Journal of Climate* 17(11):2039–2057, DOI 10.1175/1520-0442(2004)017<2039:ICITWS>2.0.CO;2
- Seneviratne SI, Corti T, Davin EL, Hirschi M, Jaeger EB, Lehner I, Orlowsky B, Teuling AJ (2010) Investigating soil moisture-climate interactions in a changing climate: A review. *Earth-Science Reviews* 99(3-4):125–161, DOI 10.1016/j.earscirev.2010.02.004
- Seo KW, Wilson CR, Famiglietti JS, Chen JL, Rodell M (2006) Terrestrial water mass load changes from Gravity Recovery and Climate Experiment (GRACE). *Water Resources Research* 42(5), DOI 10.1029/2005WR004255
- Shepherd A, Ivins ER, A G, Barletta V, Bentley MJ, Bettadpur S, Briggs KH, Bromwich DH, Forsberg R, Galin N, Horwath M, Jacobs S, Joughin I, King MA, Lenaerts JT, Li J, Ligtenberg SR, Luckman A, Luthcke SB, McMillan M, Meister R, Milne G, Mouginot J, Muir A, Nicolas JP, Paden J, Payne AJ, Pritchard H, Rignot E, Rott H, Srensen LS, Scambos TA, Scheuchl B, Schrama EJ, Smith B, Sundal AV, van Angelen JH, van de Berg WJ, van den Broeke MR, Vaughan DG, Velicogna I, Wahr J, Whitehouse PL, Wingham DJ, Yi D, Young D, Zwally HJ (2012) A Reconciled Estimate of Ice-Sheet Mass Balance. *Science* 338(6111), DOI 10.1126/science.1228102
- Shiklomanov IA (1993) World fresh water resources. In: Gleick PH (ed) *Water in Crisis: A Guide to the World's Fresh Water Resources*, Oxford University Press, New York, USA

- Singh A, Seitz F, Schwatke C (2012) Inter-annual water storage changes in the Aral Sea from multi-mission satellite altimetry, optical remote sensing, and GRACE satellite gravimetry. *Remote Sensing of Environment* 123:187–195, DOI 10.1016/j.rse.2012.01.001
- Singh A, Seitz F, Schwatke C (2013) Application of multi-sensor satellite data to observe water storage variations. *IEEE Journal of Selected Topics in Applied Earth Observations and Remote Sensing* 6(3):1502–1508, DOI 10.1109/JSTARS.2013.2258326
- Sood A, Smakhtin V (2015) Global hydrological models: a review. *Hydrological Sciences Journal* 60(4):549–565, DOI 10.1080/02626667.2014.950580
- Sperry JS, Hacke UG, Oren R, Comstock JP (2002) Water deficits and hydraulic limits to leaf water supply. *Plant, Cell and Environment* 25(2):251–263, DOI 10.1046/j.0016-8025.2001.00799.x
- Stephen H, Long DG (2005) Modeling microwave emissions of erg surfaces in the sahara desert. *IEEE Transactions on Geoscience and Remote Sensing* 43(12):2822–2830, DOI 10.1109/TGRS.2005.857899
- Strassberg G, Scanlon BR, Rodell M (2007) Comparison of seasonal terrestrial water storage variations from GRACE with groundwater-level measurements from the High Plains Aquifer (USA). *Geophysical Research Letters* 34(14), DOI 10.1029/2007GL030139
- Su F, Lettenmaier DP (2009) Estimation of the Surface Water Budget of the La Plata Basin. *Journal of Hydrometeorology* 10(4):981–998, DOI 10.1175/2009JHM1100.1
- Su CH, Ryu D, Young RI, Western AW, Wagner W (2013) Inter-comparison of microwave satellite soil moisture retrievals over the Murrumbidgee Basin, southeast Australia. *Remote Sensing of Environment* 134:1–11, DOI 10.1016/j.rse.2013.02.016
- Swenson S, Wahr J (2006) Post-processing removal of correlated errors in GRACE data. *Geophysical Research Letters* 33(8), DOI 10.1029/2005GL025285
- Swenson SC, Milly PCD (2006) Climate model biases in seasonally of continental water storage revealed by satellite gravimetry. *Water Resources Research* 42(3), DOI 10.1029/2005WR004628
- Syed TH, Famiglietti JS, Chen J, Rodell M, Seneviratne SI, Viterbo P, Wilson CR (2005) Total basin discharge for the Amazon and Mississippi River basins from GRACE and a land-atmosphere water balance. *Geophysical Research Letters* 32(24), DOI 10.1029/2005GL024851
- Syed TH, Famiglietti JS, Rodell M, Chen J, Wilson CR (2008) Analysis of terrestrial water storage changes from GRACE and GLDAS. *Water Resources Research* 44(2), DOI 10.1029/2006WR005779
- Tang Q, Gao H, Lu H, Lettenmaier DP (2009) Remote sensing: hydrology. *Progress in Physical Geography* 33(4):490–509, DOI 10.1177/0309133309346650
- Tapley BD, Bettadpur S, Ries JC, Thompson PF, Watkins MM (2004) GRACE Measurements of Mass Variability in the Earth System. *Science* 305(5683):503–505, DOI 10.1126/science.1099192
- Taylor RG, Scanlon B, Döll P, Rodell M, van Beek R, Wada Y, Longuevergne L, Leblanc M, Famiglietti JS, Edmunds M, Konikow L, Green TR, Chen J, Taniguchi M, Bierkens MFP, MacDonald A, Fan Y, Maxwell RM, Yechieli Y, Gurdak JJ (2013) Ground water and climate change. *Nature Climate Change* 3(4):322–329, DOI 10.1038/NCLIMATE1744
- Ulaby FT, Moore RK, Fung AK (1982) Physical mechanisms and empirical models for scattering and emission. In: *Microwave Remote Sensing: Active and Passive (vol. II)*, Addison-Wealey, Reading, USA, chap 11, pp 816–921

- Ulaby FT, Long DG (2014) *Microwave Radar and Radiometric Remote Sensing*. The University of Michigan Press, USA
- UNEP (2008) *Vital Water Graphics: An Overview of the State of the World's Fresh and Marine Waters - 2nd Edition*. URL <http://www.unep.org/dewa/vitalwater/article26.html>, date of access 2015-05-5
- UNISDR (2004) *Living with risk: a global review of disaster reduction initiatives*. United Nations Inter-Agency Secretariat of the International Strategy for Disaster Reduction, Geneva, Switzerland
- USGS (2012) Moderate-resolution Imaging Spectroradiometer (MODIS) Land Cover Type Climate Modeling Grid product (MCD12C1) with IGBP (International Geosphere-Biosphere Programme) land cover classification. URL <https://lpdaac.usgs.gov>, date of access 2015-05-23
- USGS (2015) *Historic World Earthquakes*. URL <http://earthquake.usgs.gov/earthquakes/world/historical.php>, date of access 2015-10-23
- Van Camp M, Williams SDP, Francis O (2005) Uncertainty of absolute gravity measurements. *Journal of Geophysical Research: Solid Earth* 110(B5), DOI 10.1029/2004JB003497
- Velicogna I, Wahr J (2006) Measurements of Time-Variable Gravity Show Mass Loss in Antarctica. *Science* 311(5768):1754–1756, DOI 10.1126/science.1123785
- Velicogna I (2009) Increasing rates of ice mass loss from the Greenland and Antarctic ice sheets revealed by GRACE. *Geophysical Research Letters* 36(19), DOI 10.1029/2009GL040222
- Viglizzo EF, Frank FC (2006) Land-use options for Del Plata Basin in South America: Tradeoffs analysis based on ecosystem service provision. *Ecological Economics* 57(1):140–151, DOI 10.1016/j.ecolecon.2005.03.025
- Vrugt JA, Diks CGH, Gupta HV, Bouten W, Verstraten JM (2005) Improved treatment of uncertainty in hydrologic modeling: Combining the strengths of global optimization and data assimilation. *Water Resources Research* 41(1), DOI 10.1029/2004WR003059
- Wagner W (1998) *Soil Moisture Retrieval from ERS Scatterometer Data*. PhD thesis, Technische Universität Wien, Austria
- Wagner W, Lemoine G, Rott H (1999) A Method for Estimating Soil Moisture from ERS Scatterometer and Soil Data. *Remote Sensing of Environment* 70(2):191–207, DOI 10.1016/S0034-4257(99)00036-X
- Wagner W, Blöschl G, Pampaloni P, Calvet JC, Bizzarri B, Wigneron JP, Kerr Y (2007) Operational readiness of microwave remote sensing of soil moisture for hydrologic applications. *Hydrology Research* 38(1):1–20, DOI 10.2166/nh.2007.029
- Wagner W, Hahn S, Kidd R, Melzer T, Bartalis Z, Hasenauer S, Figa-Saldaña J, de Rosnay P, Jann A, Schneider S, Komma J, Kubu G, Brugger K, Aubrecht C, Züger J, Gangkofner U, Kienberger S, Brocca L, Wang Y, Blöschl G, Eitzinger J, Steinnocher K, Zeil P, Rubel F (2013) The ASCAT soil moisture product: A review of its specifications, validation results, and emerging applications. *Meteorologische Zeitschrift* 22(1):5–33, DOI 10.1127/0941-2948/2013/0399
- Wagner W, Hahn S, Figa J, Albergel C, de Rosnay P, Brocca L, de Jeu R, Hasenauer S, Dorigo W (2014) Operations, Challenges, and Prospects of Satellite-Based Surface Soil Moisture Data Services. In: Petropoulos GP (ed) *Remote Sensing of Energy Fluxes and Soil Moisture Content*, CRC Press, chap 20, pp 463–487, DOI doi:10.1201/b15610-25

- Wahr J, Molenaar M, Bryan F (1998) Time variability of the Earth's gravity field: Hydrological and oceanic effects and their possible detection using GRACE. *Journal of Geophysical Research: Solid Earth* 103(B12):30,205–30,229
- Wahr J, Swenson S, Velicogna I (2006) Accuracy of GRACE mass estimates. *Geophysical Research Letters* 33(6), DOI 10.1029/2005GL025305
- Walker JP, Houser PR (2004) Requirements of a global near-surface soil moisture satellite mission: Accuracy, repeat time, and spatial resolution. *Advances in Water Resources* 27(8):785–801, DOI 10.1016/j.advwatres.2004.05.006
- Wang X, Xie H, Guan H, Zhou X (2007) Different responses of MODIS-derived NDVI to root-zone soil moisture in semi-arid and humid regions. *Journal of Hydrology* 340(1-2):12–24, DOI 10.1016/j.jhydrol.2007.03.022
- Watkins MM, Wiese DN, Yuang DN, Boening C, Landerer FW (2015) Improved methods for observing Earth's time variable mass distribution with GRACE using spherical cap mascons. *Journal of Geophysical Research: Solid Earth* 120(4):2648–2671, DOI 10.1002/2014JB011547
- Werth S, Güntner A, Schmidt R, Kusche J (2009) Evaluation of GRACE filter tools from a hydrological perspective. *Geophysical Journal International* 179(3):1499–1515, DOI 10.1111/j.1365-246X.2009.04355.x
- Werth S (2010) Calibration of the global hydrological model WGHM with water mass variations from GRACE gravity data. PhD thesis, University of Potsdam, Germany
- Werth S, Güntner A (2010) Calibration analysis for water storage variability of the global hydrological model WGHM. *Hydrology and Earth System Sciences* 14(1):59–78, DOI 10.5194/hess-14-59-2010
- Wilhite DA, Buchanan-Smith M (2005) Drought as a Hazard: Understanding the Natural and Social Context. In: Wilhite DA (ed) *Drought and water crisis: science, technology, and management issues*, CRC Press, Boca Raton, USA, pp 3–29
- Wu X, Walker JP, Das NN, Panciera R, Rüdiger C (2014) Evaluation of the SMAP brightness temperature downscaling algorithm using active-passive microwave observations. *Remote Sensing of Environment* 155:210–221, DOI 10.1016/j.rse.2014.08.021
- Xiao X, Boles S, Liu J, Zhuang D, Liu M (2002) Characterization of forest types in Northeastern China, using multi-temporal SPOT-4 VEGETATION sensor data. *Remote Sensing of Environment* 82(2-3):335–348, DOI 10.1016/S0034-4257(02)00051-2
- Xiao R, He X, Zhang Y, Ferreira VG, Chang L (2015) Monitoring Groundwater Variations from Satellite Gravimetry and Hydrological Models: A Comparison with in-situ Measurements in the Mid-Atlantic Region of the United States. *Remote Sensing* 7(1):686–703, DOI 10.3390/rs70100686
- Xu C, Singh VP (1998) A Review on Monthly Water Balance Models for Water Resources Investigations. *Water Resources Management* 12(1):31–50, DOI 09204741
- Xu C, Weigelt M, Sideris MG, Sneeuw N (2007) Spaceborne gravimetry and gravity field recovery. *Canadian Aeronautics and Space Journal* 53(3-4):65–75, DOI 10.5589/q07-008
- Yamamoto K, Fukuda Y, Nakaegawa T, Nishijima J (2007) Landwater variation in four major river basins of the Indochina peninsula as revealed by GRACE. *Earth, Planets and Space* 59(4):193–200, DOI 10.1186/BF03353095
- Yamamoto K, Fukuda Y, Doi K, Motoyama H (2008) Interpretation of the GRACE-derived mass trend in Enderby Land, Antarctica. *Polar Science* 2(4):267–276, DOI 10.1016/j.polar.2008.10.001

- Yilmaz MT, Hunt ER, Jackson TJ (2008) Remote sensing of vegetation water content from equivalent water thickness using satellite imagery. *Remote Sensing of Environment* 112(5):2514–2522, DOI 10.1016/j.rse.2007.11.014
- Zaitchik BF, Rodell M, Reichle RH (2008) Assimilation of GRACE Terrestrial Water Storage Data into a Land Surface Model: Results for the Mississippi River Basin. *Journal of Hydrometeorology* 9(3):535–548, DOI 10.1175/2007JHM951.1
- Zhang ZZ, Chao BF, Lu Y, Hsu HT (2009) An effective filtering for GRACE time-variable gravity: Fan filter. *Geophysical Research Letters* 36(17), DOI 10.1029/2009GL039459
- Zhang A, Jia G (2013) Monitoring meteorological drought in semiarid regions using multi-sensor microwave remote sensing data. *Remote Sensing of Environment* 134:12–23, DOI 10.1016/j.rse.2013.02.023
- Zhao W, Li A (2013) A Downscaling Method for Improving the Spatial Resolution of AMSR-E Derived Soil Moisture Product Based on MSG-SEVIRI Data. *Remote Sensing* 5(12):6790–6811, DOI 10.3390/rs5126790